Contemplative Real-time Estimation in Autonomous Vehicle Applications

Jay A. Farrell
University of California-Riverside

Multiconference on Decision and Control
September 2016, Buenos Aires, Argentina

Dynamic Systems and Optimization:

- Autonomous & Connected Vehicles
- Precise and Reliable Mapping & Positioning
- Project: Results and Applications
- Interesting Directions

Intelligence & Autonomy

Increasingly capable autonomous vehicles: a worthy challenge necessitating increased ability along various dimensions of intelligence

AV

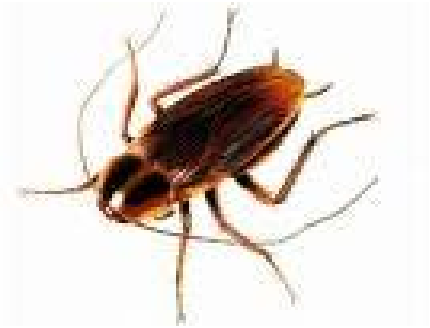

Safety of Life Applications:

- Performance
- Reliability
- Robustness

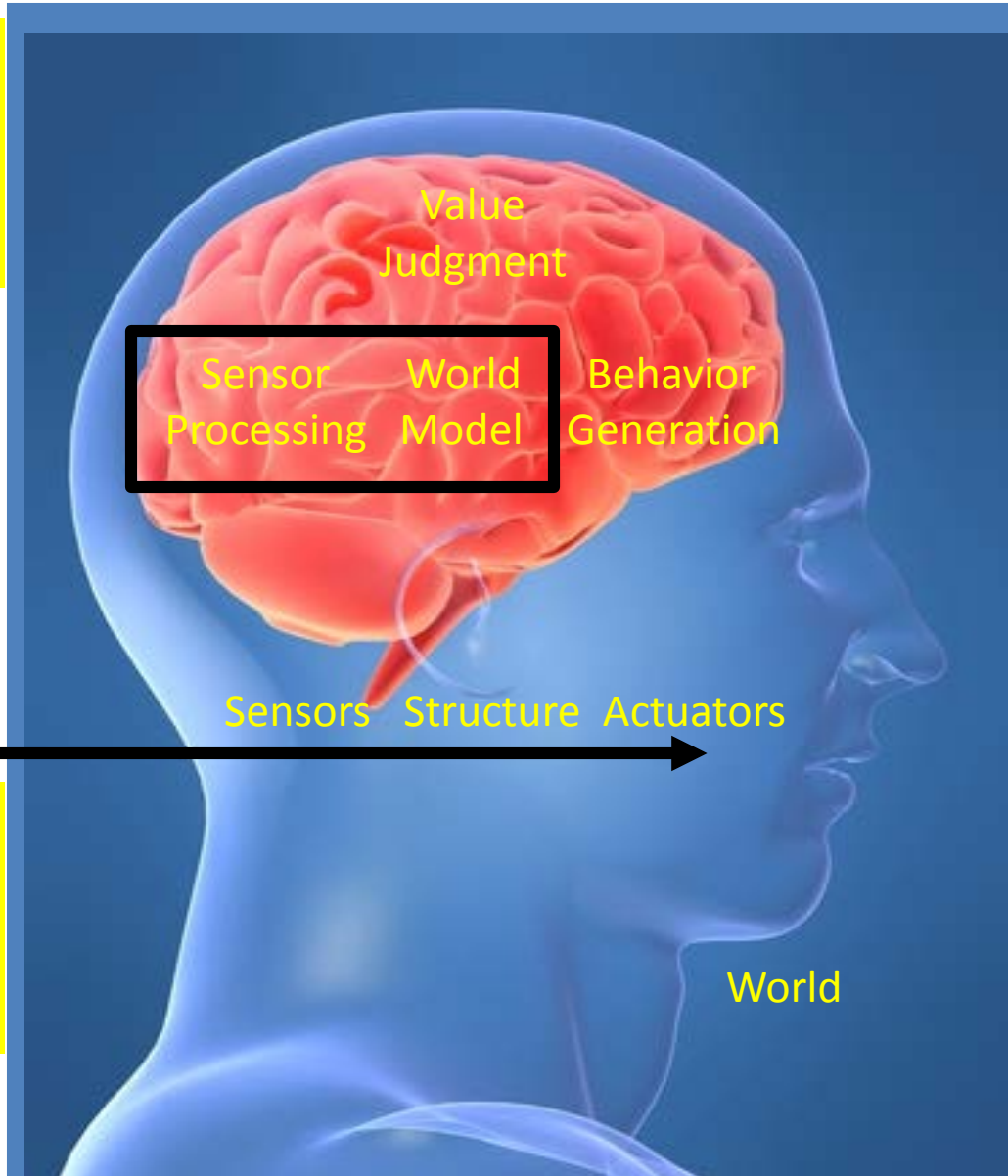

Autonomous Vehicle Examples

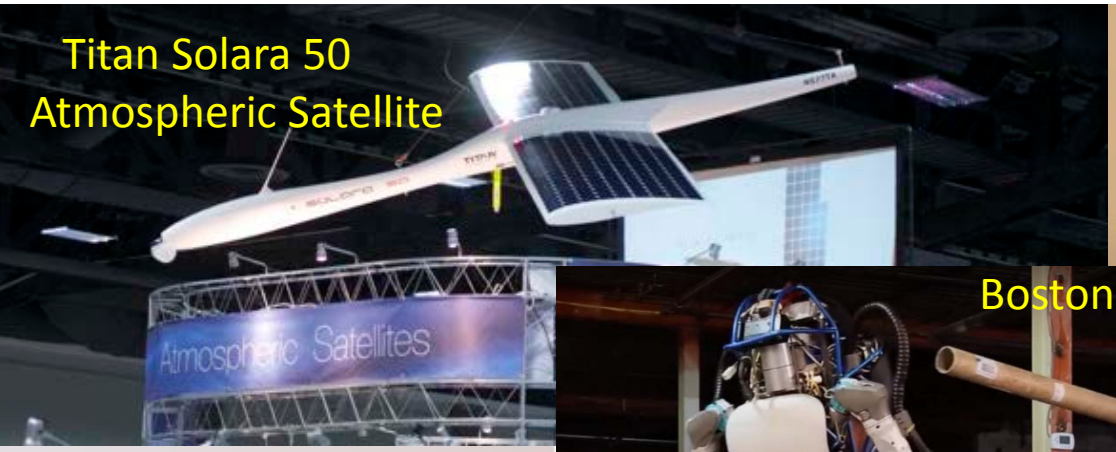

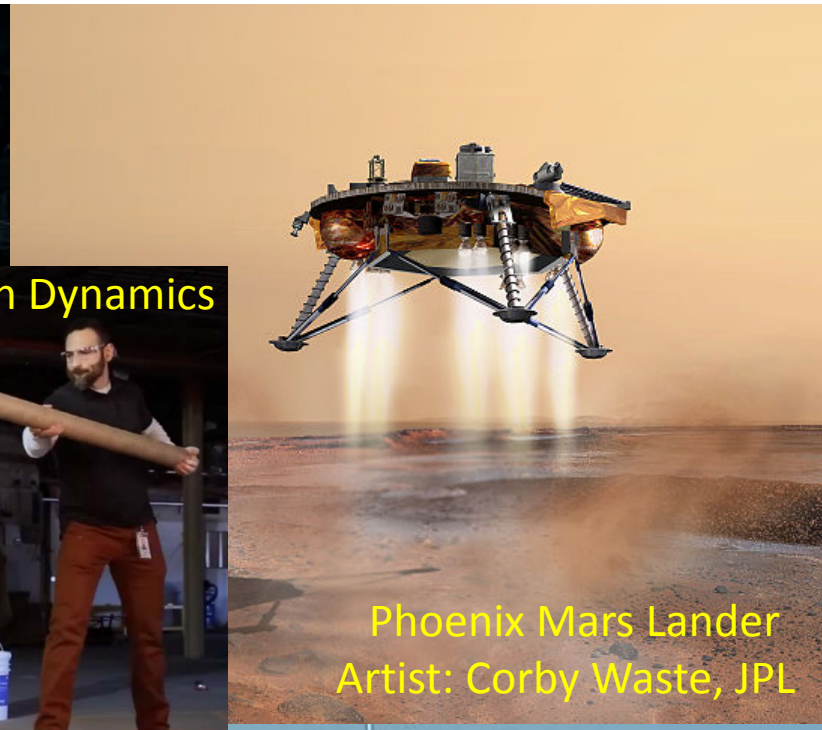

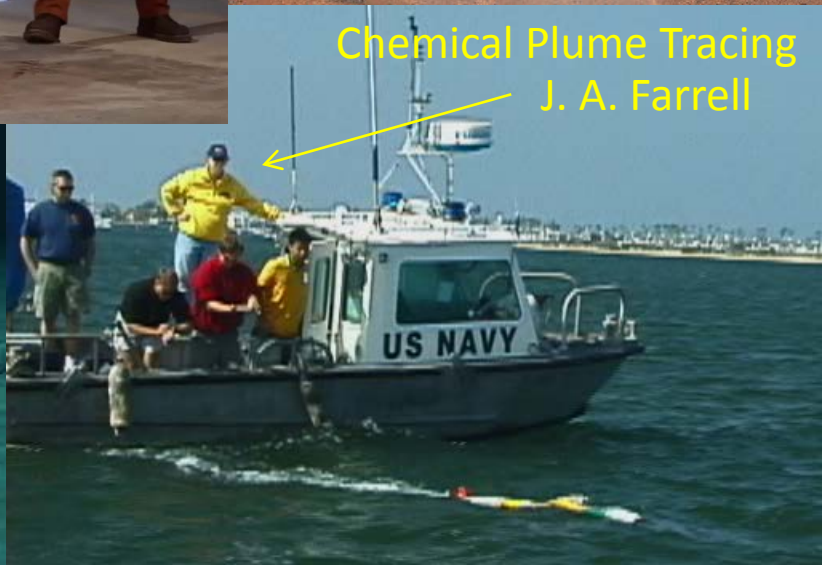

Human Driving Performance

Fatalities and Fatality Rate per 100 Million Vehicle Miles Traveled by Year

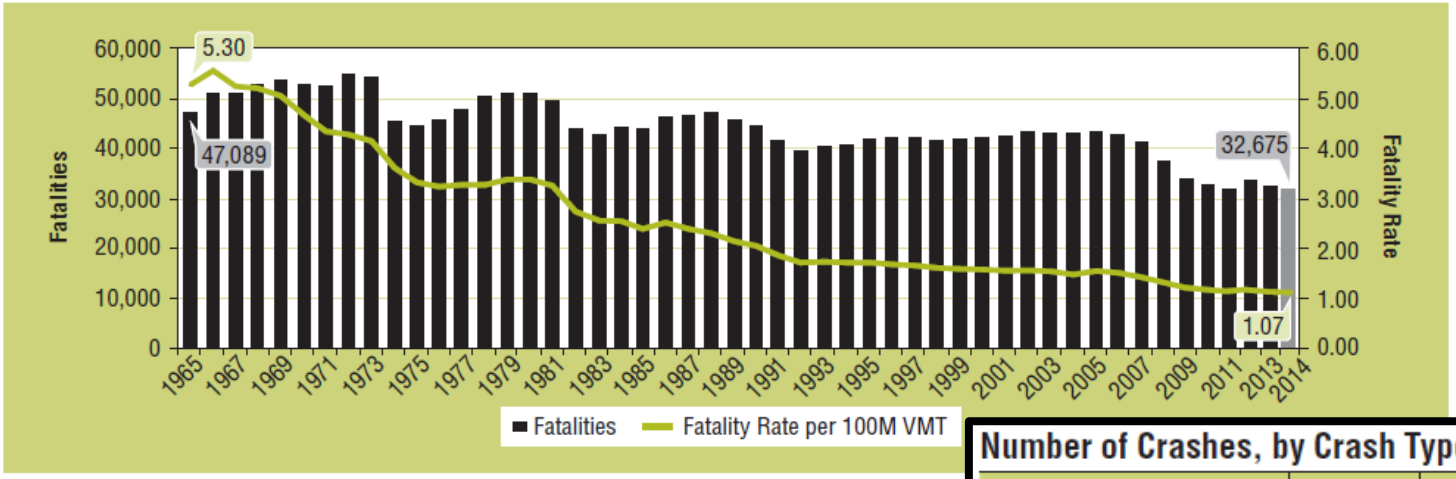

Source: 1965–1974: National Center for Health Statistics, HEW, and State Accident Summaries (Adjusted to 30-Day T
FARS 1975–2013 (Final), 2014 Annual Report File (ARF); Vehicle Miles Traveled (VMT): Federal Highway Administrati

Number of Crashes, by Crash Type

Crash Type	2013	2014	Change	% Change
Fatal Crashes	30,203	29,989	-214	-0.7%
Non-Fatal Crashes	5,657,000	6,034,000	+377,000	+6.7%
Injury Crashes	1,591,000	1,648,000	+57,000	+3.6%
Property Damage Only	4,066,000	4,387,000	+321,000	+7.9%
Total Crashes	5,687,000	6,064,000	+377,000	+6.6%

Source: FARS 2013 [Final], 2014 [ARF], NASS GES 2013, 2014

People Injured and Injury Rate per 100 Million Vehicle Miles Traveled by Year

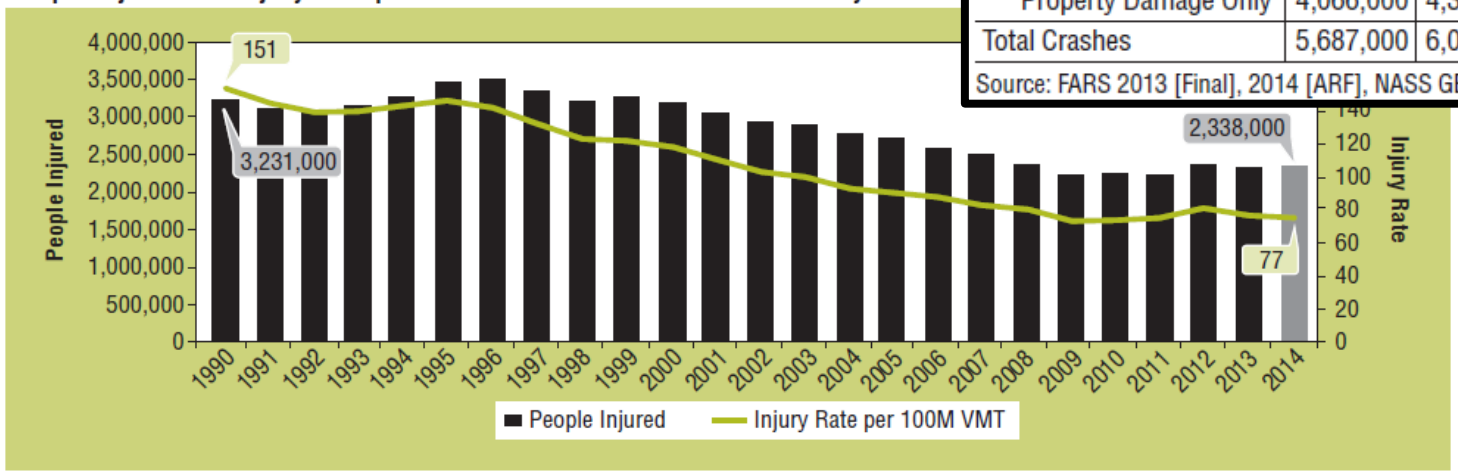

Source: NASS GES 1990–2014; VMT: FHWA.

The Survey Says ….

Consumers Desire More Automated Automobiles

Consumers Trust Driverless Cars

57% of consumers, globally, trust driverless cars—even more so in emerging markets

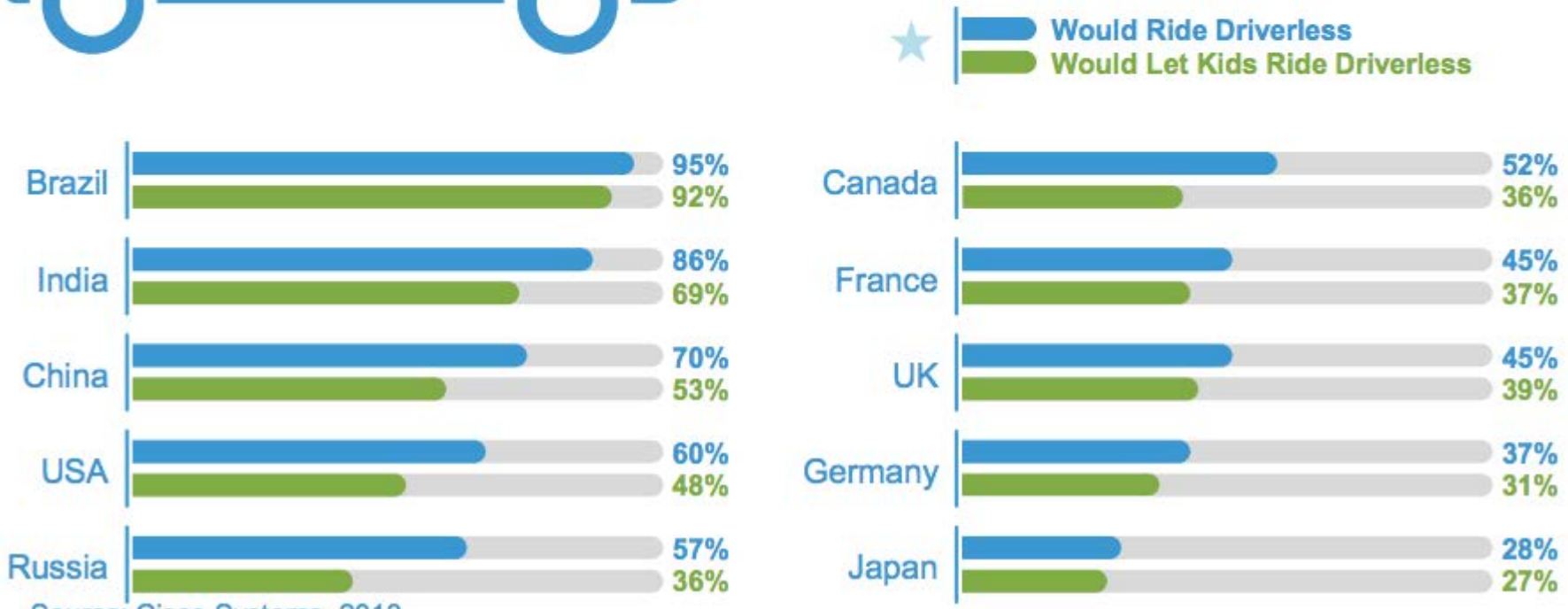

Source: Cisco Systems, 2013

Reliable Precise Positioning: AV & CV

- Autonomous & Connected Vehicles are in our future.
  - Early Phase: Commercial
  - Later: Consumer
- Vehicle Position
  - Control
  - Coordination
    - Infrastructure
    - Other vehicles
  - Sensor Fusion
- Accuracy: 10m, 1m, 0.1m
- Reliability = Trust

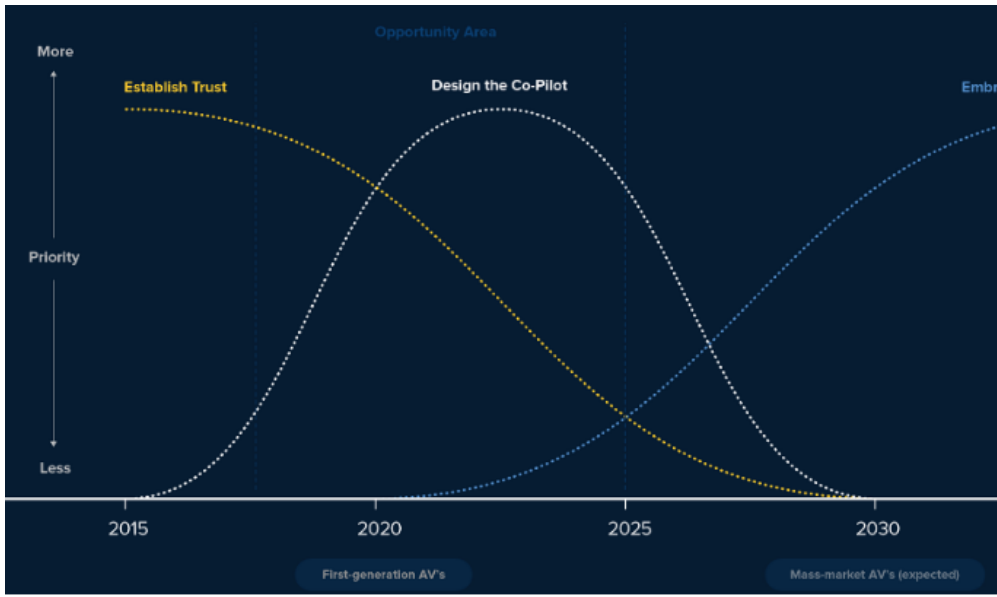

Establishing Trust ?

Tesla Model S (Beta): "Autopilot comprises multiple systems … that use cameras, radar, ultrasonic sensors and data to … automatically steer down the highway, change lanes, and adjust speed in response to traffic." (Consumer Reports)

Radar: (Tesla Press Release, Sept. 11, 2016)

- Radar added in October 2014 as a supplementary system
- Radar (10 Hz) now can be used as primary sensor without confirmation by vision system.
  - The big problem is avoiding false alarms (e.g., soda cans). …
  - Comparing several contiguous frames …
  - Fleet learning of overhead sign locations ….

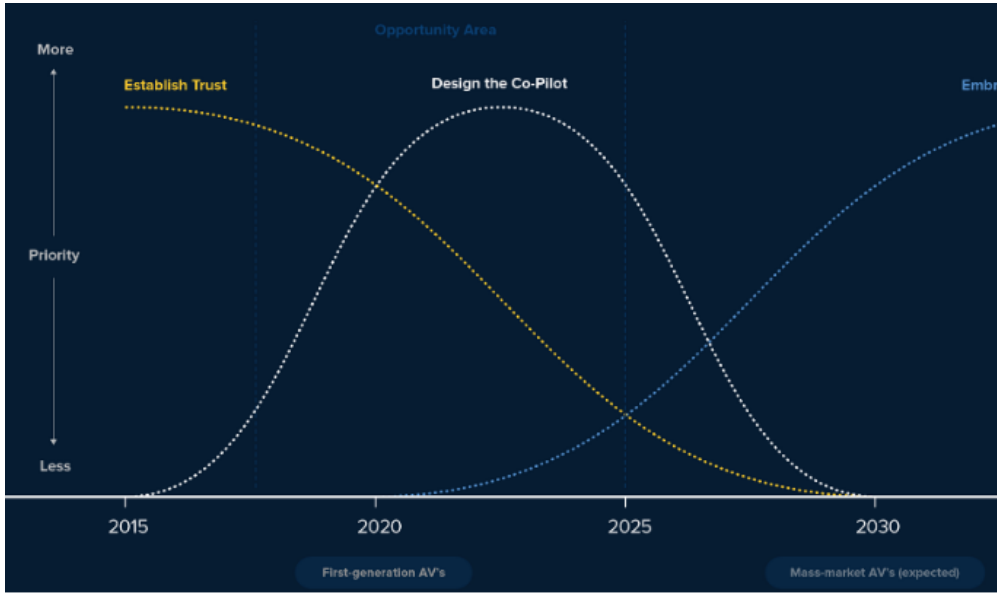

Autonomous Driving to Expo 2010

- U. of Parma (Alberto Broggi)
- 13000 km, 3 months
- Leader (human/autonomous)-follower (autonomous)
- Vision, navigation, control, planning, sensor fusion, …

Partially Autonomous Driving (Commercially Available)

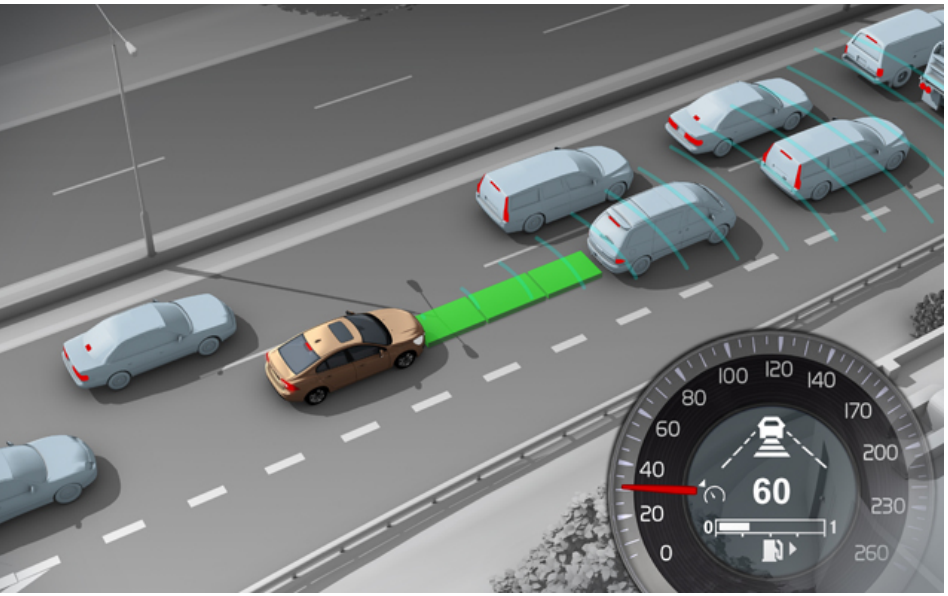

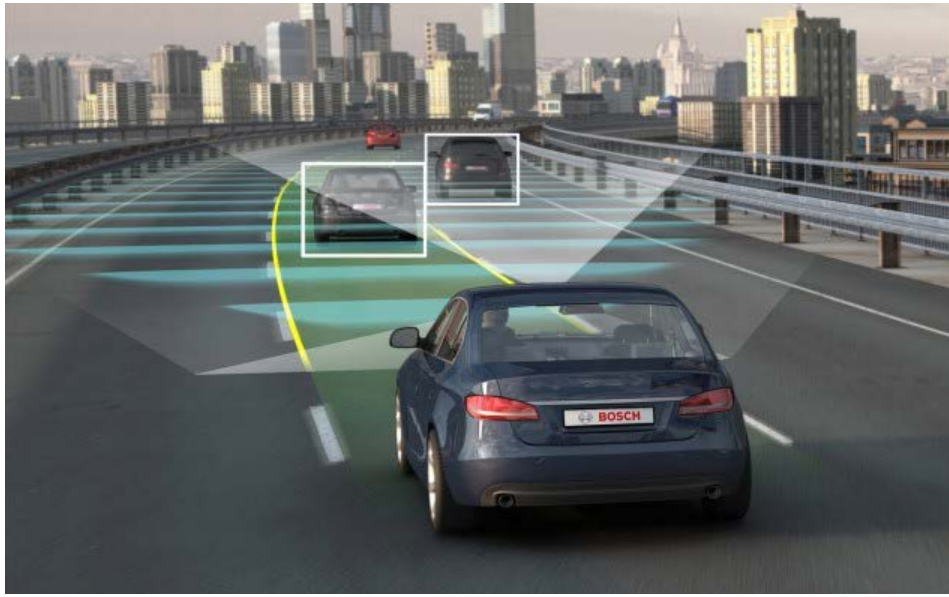

- Cruise control
- Parallel parking
- Blind spot and lane departure warning
- Intelligent cruise control w/ crash avoidance

Control is not the Limitation

Parallel Parking Demonstrations: First IEEE research papers appear in 1989

- I. E. Paromtchik, C. Laugier, “Autonomous parallel parking of a nonholonomic vehicle,” IEEE Intelligent Vehicles Symposium, 1996.
- I.E. Paromtchik, C. Laugier, “Automatic parallel parking and returning to traffic manoeuvres” IEEE IROS, 1997.
- S. Patwardhan; Han-Shue Tan; J. Guldner; M. Tomizuka, “Lane following during backward driving for front wheel steered vehicles,” American Control Conference, pp. 3348 – 3353, 1997.

Platooning Demonstrations: First IEEE research papers appear in 1994

- U. Franke, F. Bottiger, Z. Zomotor, D. Seeberger, “Truck platooning in mixed traffic,” IEEE Intelligent Vehicles Symposium, 1995.
- O. Gehring, H. Fritz, Practical results of a longitudinal control concept for truck platooning with vehicle to vehicle communication, IEEE Intelligent Transportation System, pp. 117 – 122, 1997.

US National Automated Highway System Consortium proof of technical feasibility demonstration 1997

- C. Thorpe, T. Jochem, D. Pomerleau, “The 1997 automated highway free agent demonstration,” IEEE Conference on Intelligent Transportation System, pp. 496 - 501, 1997.
- R. Sebastian, T. Kaufmann, F. Bolourchi, Han-Shue Tan, "Design of an automated highway systems steering actuator control system,” IEEE Conference on Intelligent Transportation System, pp. 254 – 259, 1997.
- D. Farkas, J. Young, B. Baertlein, U. Ozguner, Forward-looking radar navigation system for 1997 AHS demonstration, IEEE Conference on Intelligent Transportation System, pp. 672 – 675, 1997.

Autonomy: Not there yet.

- Key Insight:
  "A good state estimate, in the form of a map, is the most critical piece of information for a team of robots – and the most difficult to obtain."
- Multi-Autonomous Ground robot International Challenge (MAGIC), November 2010 in Adelaide, Australia
- Cover Story: "Exploration and Mapping with Autonomous Robot Teams" By E. Olson, J. Strom, R. Goeddel, R. Morton, P. Ranganathan, A. Richardson
  Vol. 56 No. 3, Pages 62-70,
  Communications of the ACM,
  0.1145/2428556.2428574

Connected Vehicles

Enhanced Throughput, enhanced safety, decreased emissions.

- V2V: Vehicle to vehicle
- V2I: Vehicle to Infrastructure

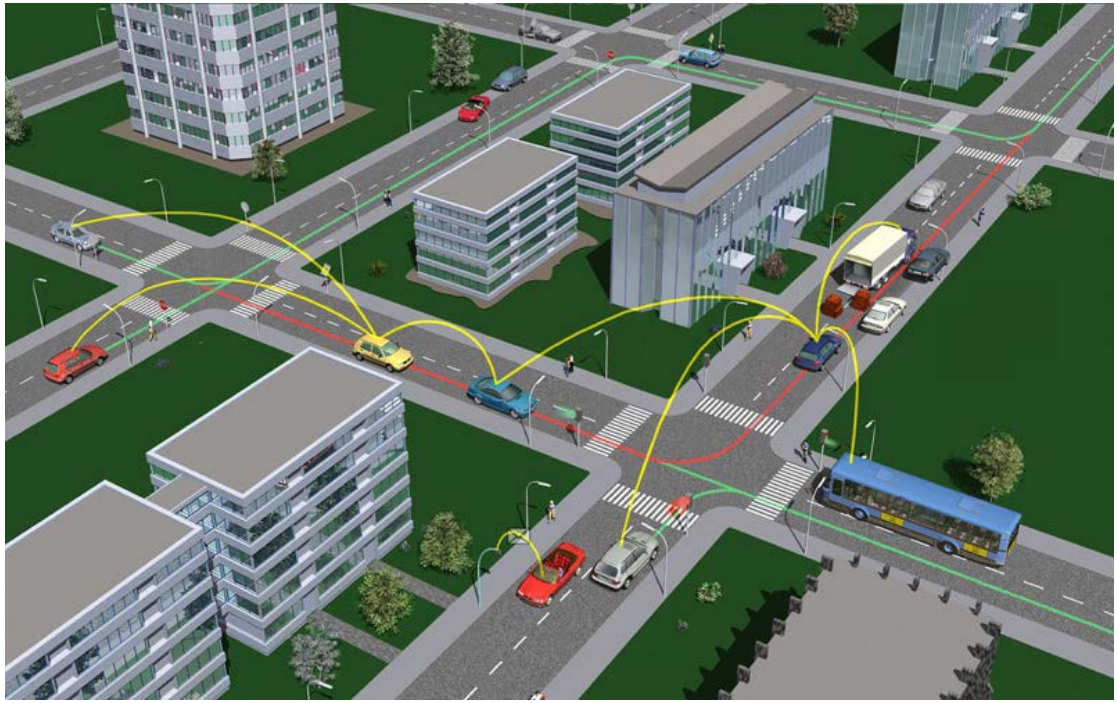

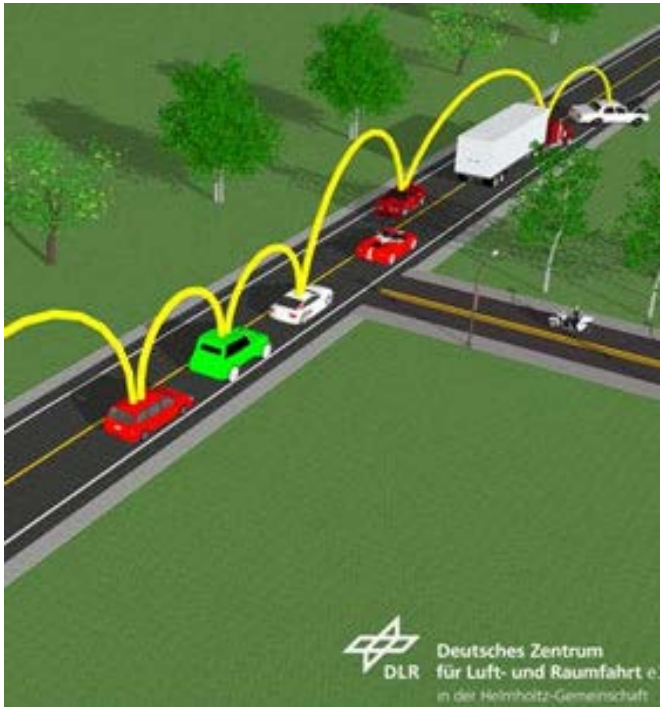

Feature Accuracy Requirements

- Required quantities: **d, S_L, S_R**
- Consider **$d = N \cdot (P_V - P_L)$** where **N** is the normal to the stop bar
- Uncertainty in **d** affected by uncertainty in both **P_V** and **P_L** : $\sigma_d^2 = \sigma_{P_V}^2 + \sigma_{P_L}^2$

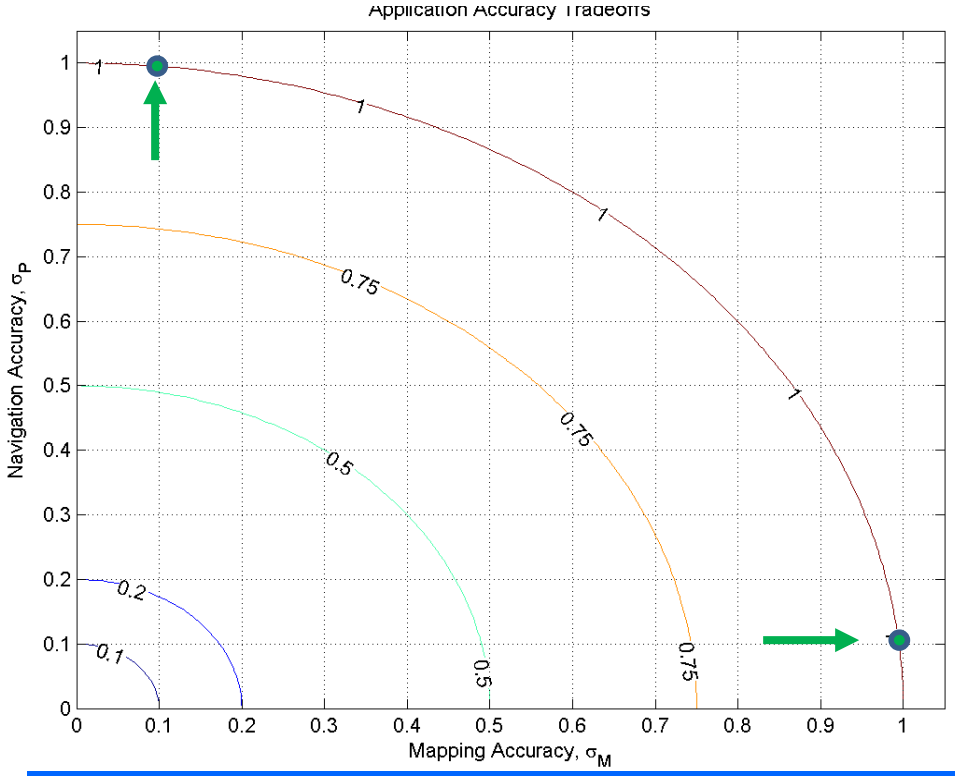

Accurate estimation is required for both:

- Map feature locations
- Real-time vehicle location

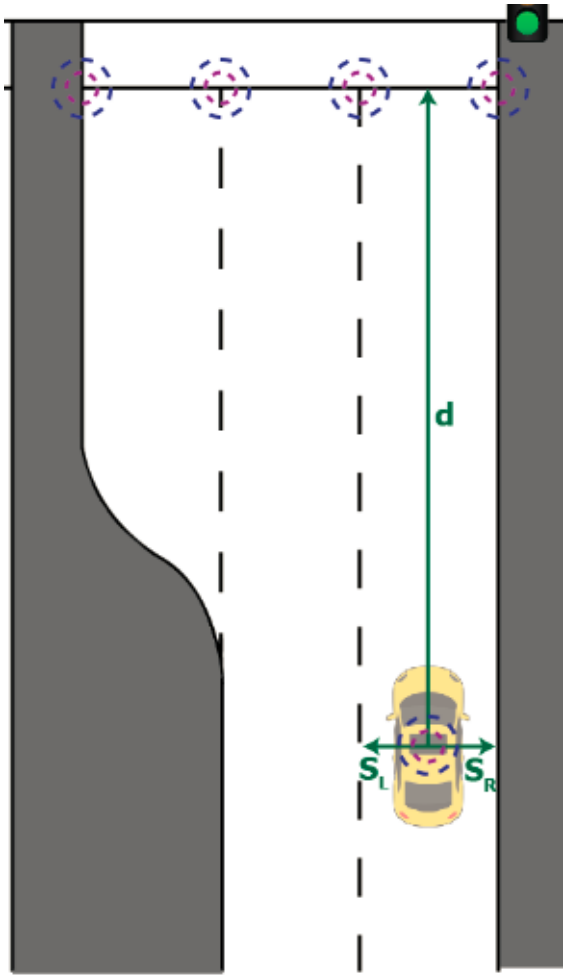

CV Positioning Specifications

- **No Positioning:** No knowledge of position is required.
- **Coarse Absolute Positioning (Which Road): O(10 m)**
  - Achieved by standard GPS *with sufficient satellite reception*
  - Possibly achievable by feature sensors with Enhanced Digital Map (EDM)
- **Lane-Level Absolute Positioning (Which Lane): O(1m)**
  - Differentially corrected GPS *with sufficient satellite reception*
  - Possibly achievable by feature sensors with EDM
- **Where-in-Lane Positioning: O(0.1m)**
  - Real Time Kinematic and/or carrier phase differentially corrected GPS *with sufficient satellite reception*
  - Already achievable in relative sense by feature sensors *under suitable conditions*

EDM's (containing features) provide the means to interconnect data between:

- vehicles and infrastructure
- feature sensors and IMU & GNSS/GPS

World Model & Sensing: Scale & Complexity

- Enhanced digital map – stores roadway features (fixed in global frame for large time-scales)
  - Facilitates feature processing
  - Knowledge of global vehicle state enables V2V and V2I sharing
- Short-range relative sensing – detects features & unmapped objects near vehicle

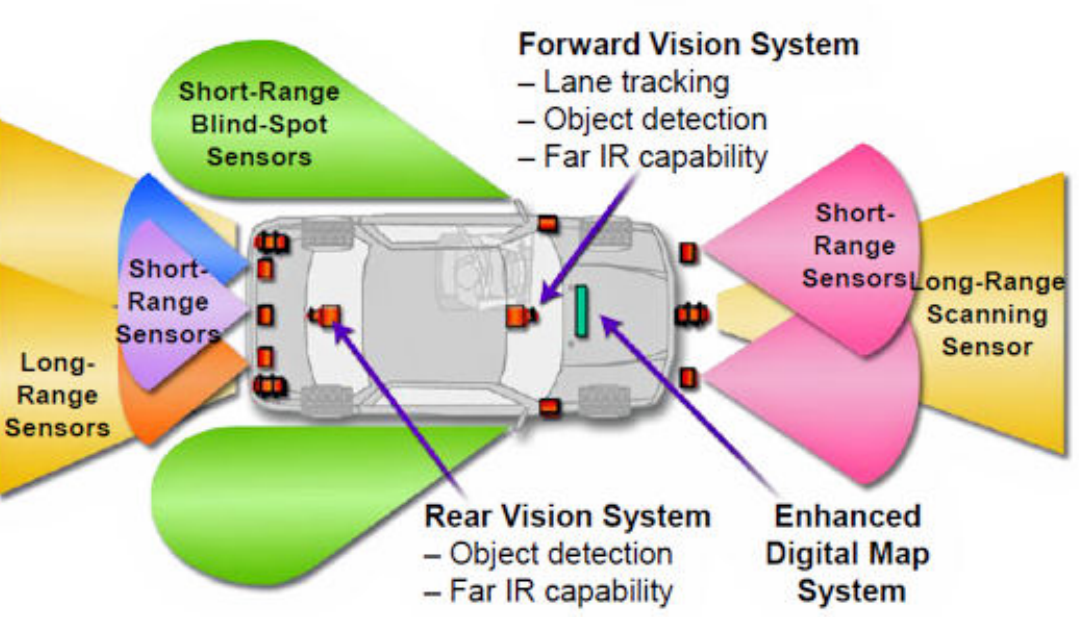

Commercial success requires EDM on a global scale

<u>In US alone:</u>

300,000 Signalized Intersections

6,000,000 miles of multilane roads

- Manual mapping is impractical.
- Independent SLAM processing by millions of vehicles on a daily basis inefficient and inconsistent

Precision Roadway Map: Data Acquisition

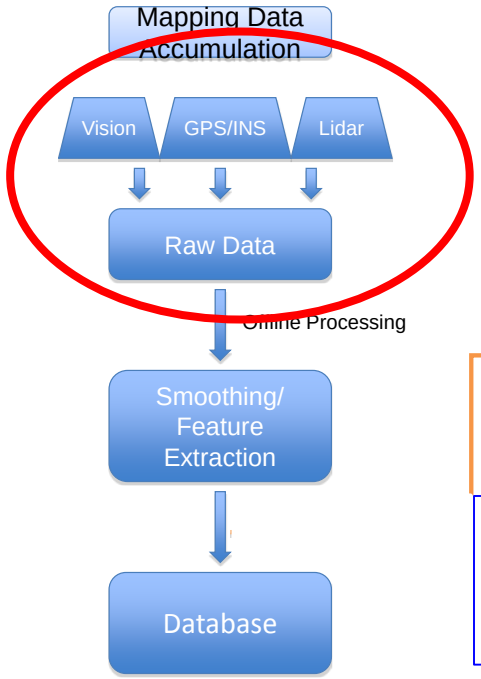

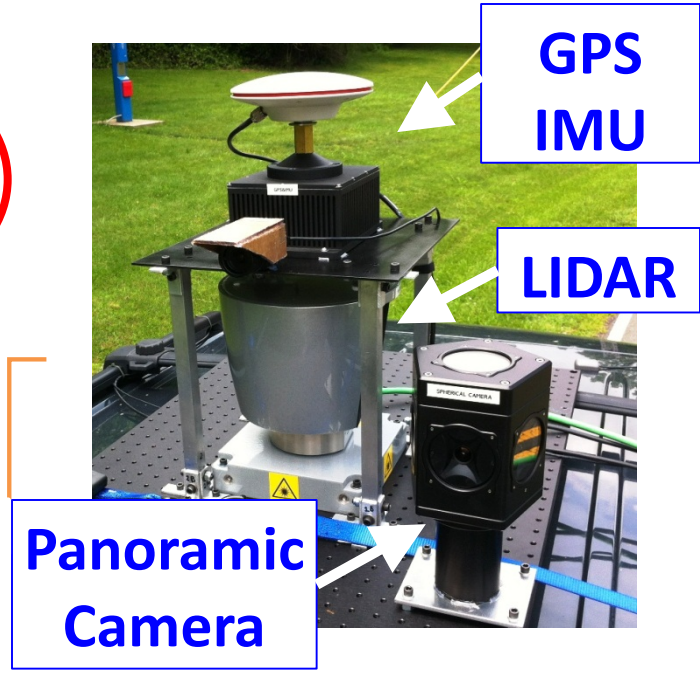

Sensor	Bytes/Msg.	Msgs./sec	Bytes/Sec	GB/Hr	GB/Hr (with timestamp overhead)
IMU	19	200	3800	0.013	0.232
LIDAR	1206	3473	4,188,438	15.08	15.278
Camera	35,836,416	7.5	268,773,120	967.583232	967.583
GPS measurement data	612	1	612	0.002	0.0374
GPS Ephemeris data	256	.002	.512	1.8432e-6	3.13344e-5
DGPS data	1071	1	1071	0.0038	0.0039
		Total:	273 MB /sec	982 GB/Hr	983 GB/Hr
		Hrs. of collection per TB:			≈1 Hr.
		Miles of coverage per TB (assuming a speed of 30 mph):			≈30 miles

Sensor Type: Comparison

- Relative: where-in-lane currently feasible; which-lane & which-road are not
  - Sensors: Camera, Radar, Ultrasound; Lidar (currently expensive)
  - Pros: Does not require map. Directly senses road relative position (locally). Many urban features. Also detects obstacles.
  - Cons: Vision can be occluded. Light sensitive performance. Instantaneous degradation with loss of vision.
  - Currently: Used for land departure warning, adaptive cruise control
- Absolute: which-lane and course positioning are currently feasible; where-in-lane is not currently *reliably* feasible
  - Sensors: GNSS (absolute position), IMU (high rate and bandwidth), Map
  - Pros: High sample rate, high bandwidth, graceful degradation to loss of GNSS
  - Cons: GPS can be occluded, challenged in urban canyons
  - Currently: Used for routing, (non-roadway) vehicle control
- Relative and Absolute Integrated with Inertial Sensors
  - Higher reliability
    - Sensor failure modes are independent
    - Abs. position & roadway feature map facilitates real time image processing
  - High rate & bandwidth
  - Graceful degradation
- Relative and Absolute Integrated with EDM
  - Facilitates data fusion
  - Facilitates collaboration: V2V and V2I

Reliable Precise Positioning: Background

Relative: obstacles & features

- Camera, Lidar, Radar, …

Absolute: Earth rel.

- GNSS
- Inertial Measurements
- EDM & Camera, Lidar, ….

Differential Carrier Phase GNSS:

- Attains 0.01m accuracy
- Used in surveying 1990's-present
- Too fragile for real-time (RT) human safety applications

Reliability by redundancy through sensor fusion

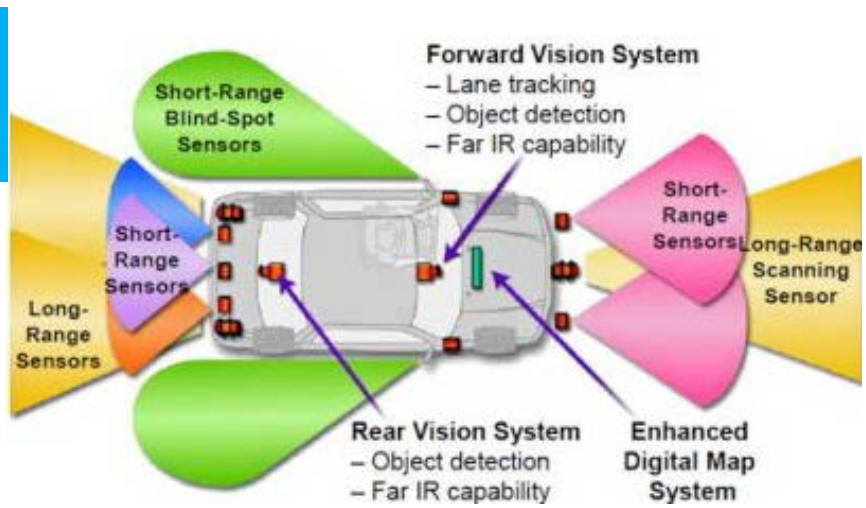

Overall Process Block Diagram

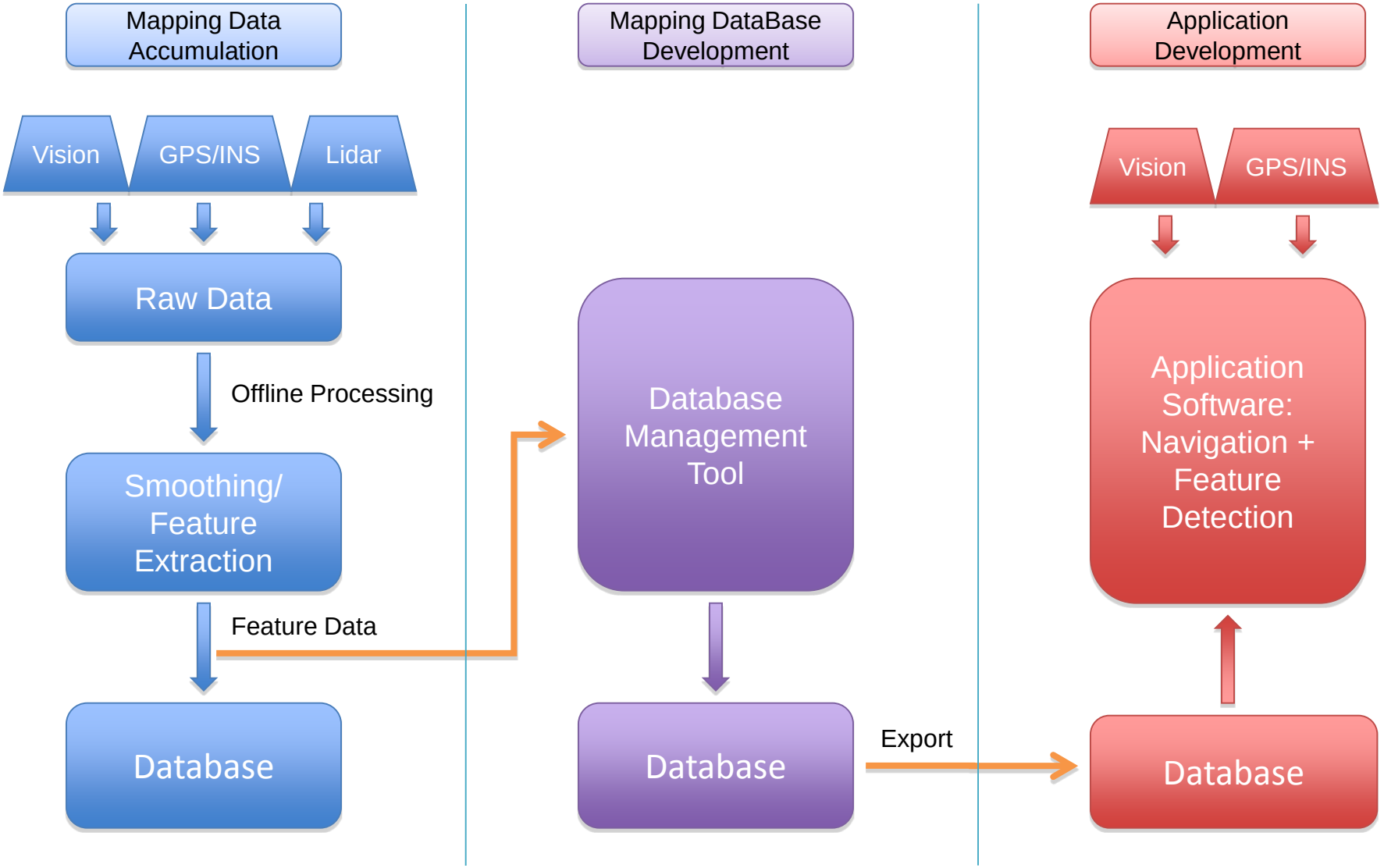

LIDAR Operation

Cost: $75,000 USD (2011)

Both size and cost are rapidly decreasing.

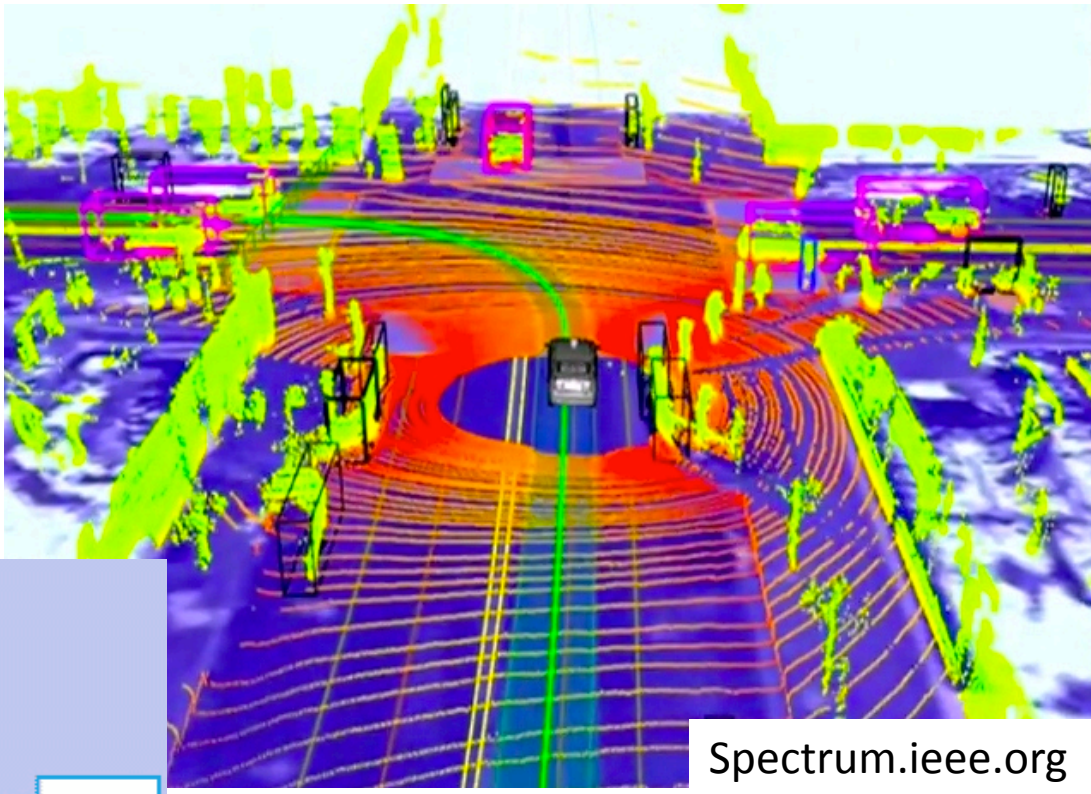

Spectrum.ieee.org

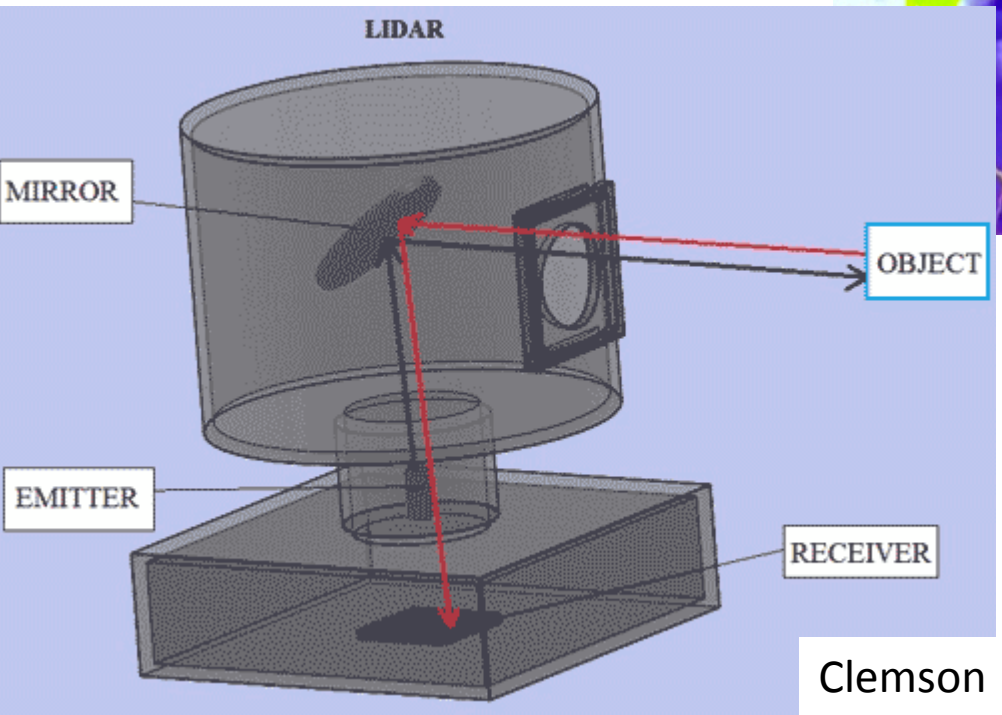

Clemson

Data: R, ψ, θ, I

- 64 samples/vertical slice
- 1000 vertical slices/revolution
- 15 revolutions/second

Driving and data collection …

Scenario:

- Instrumented vehicle driven through environment
- Recording: IMU, GNSS, LIDAR, Imagery

Velodyne LIDAR:

- 64 vertically aligned lasers
- Rotate around vertical axis at 15-20 Hz
- Measure time-of-flight and reflection intensity

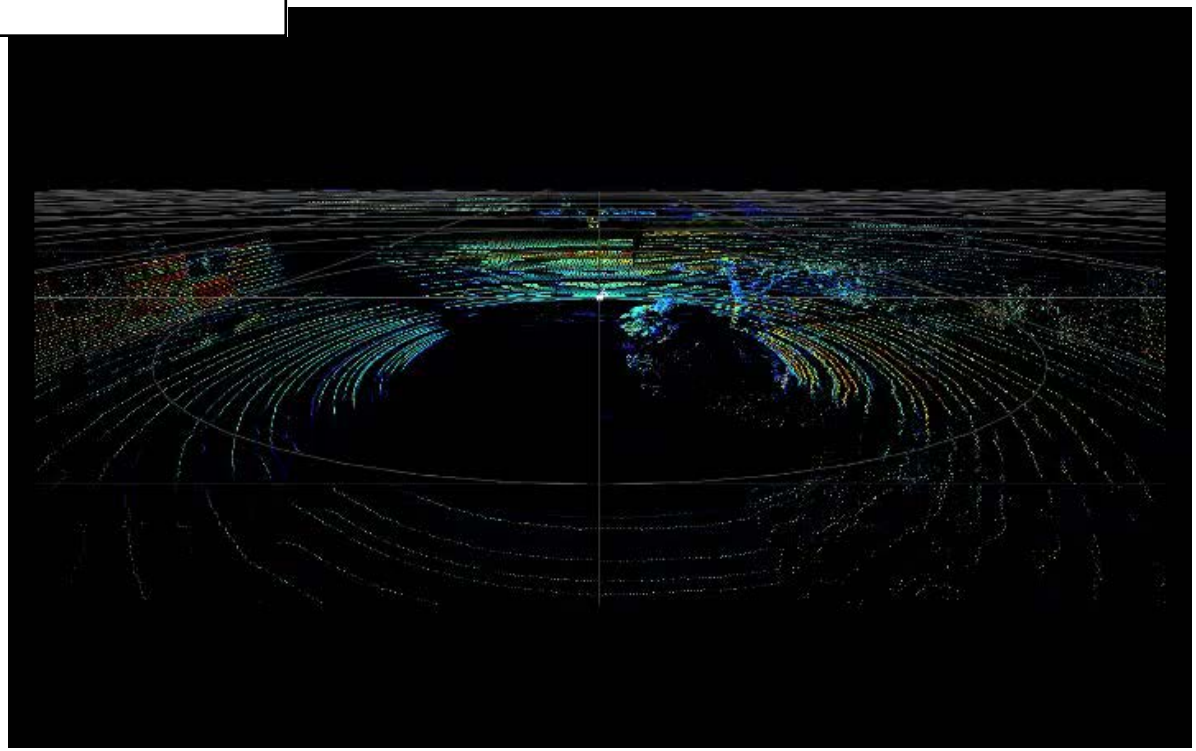

Georectification

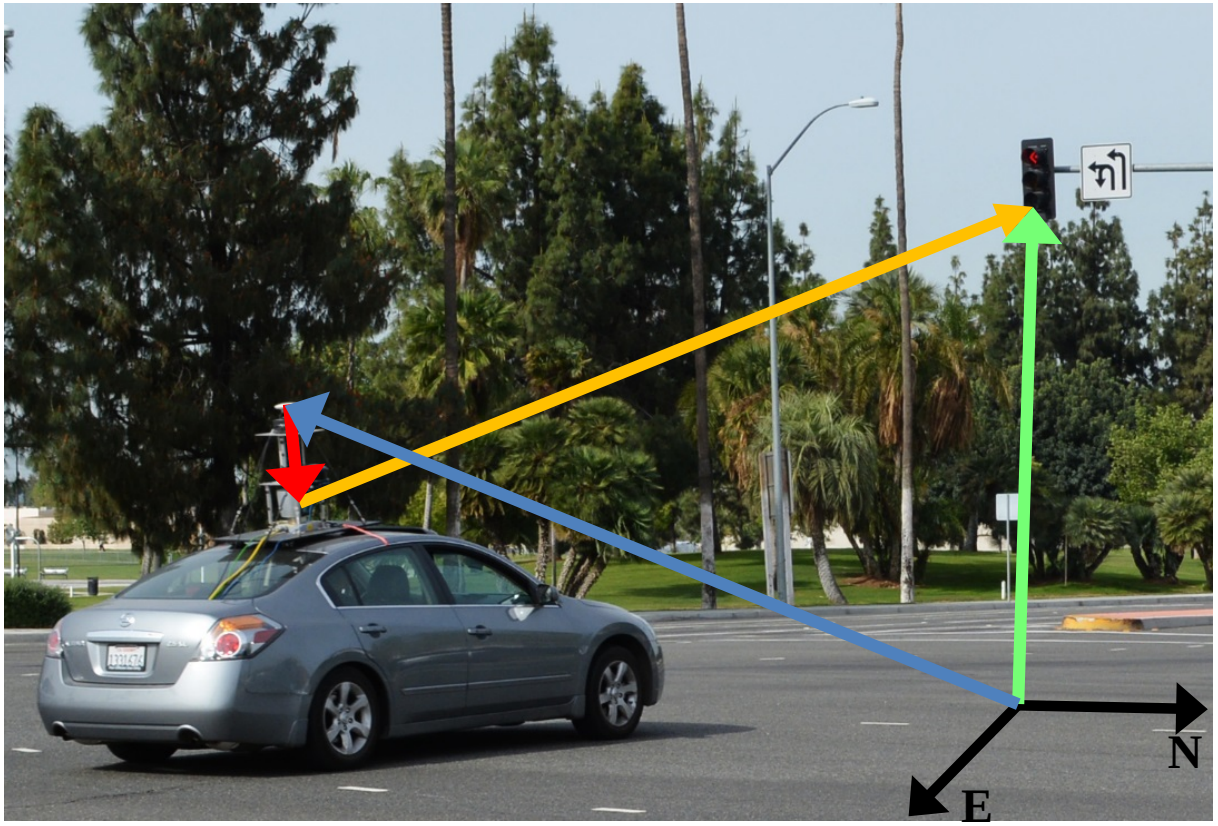

P_F^L: Position of feature in LiDAR frame, measured by LiDAR

R_{PL} & T_{PL}^P: Rotation and Translation from platform frame to LiDAR frame, constant & known from calibration

R_{WP} & T_{WP}^W: Rotation and Translation from world frame to platform frame, measured by GPS and IMU

P_F^W : Position of feature in world frame

Subscript and Superscript Definitions
- W – World
- P – Platform
- F – Feature
- L – Lidar

$$P_F^W = R_{WP}\left(R_{PL}P_F^L + T_{PL}^P\right) + T_{WP}^W$$

Reliable and Accurate estimation of vehicle state is critical
- Post-processed for Georectification
- Real-time for planning and control

The methods to be discussed apply to both.

Georectified Point Cloud: Processing

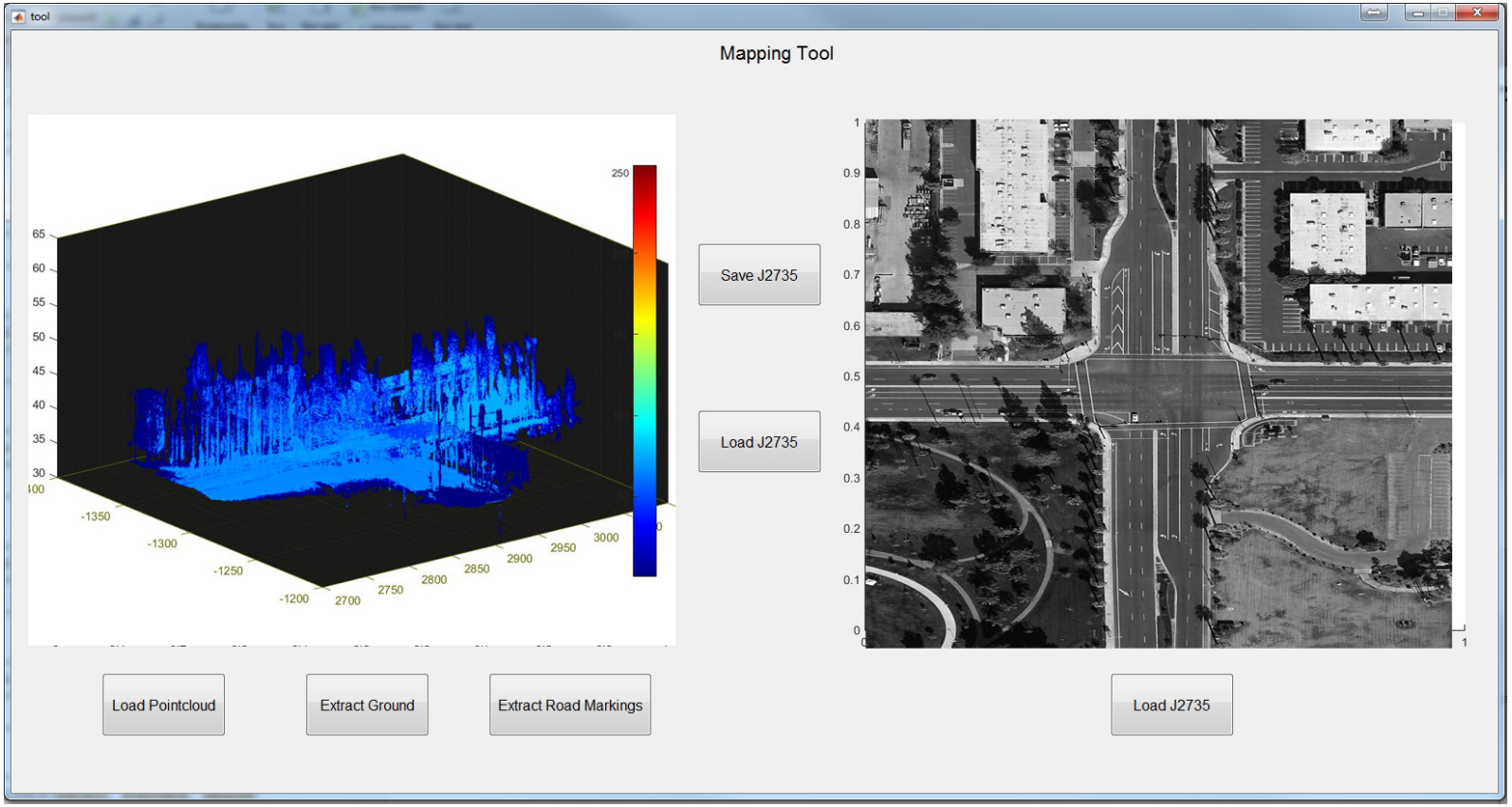

Georectified point cloud prior to processing.

Top down image of target intersection.

Road marking extraction

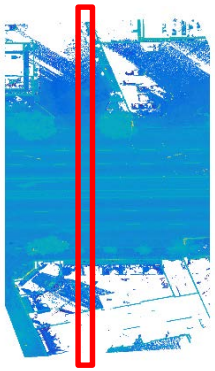

1. Roadway lateral slice

YZ
projection

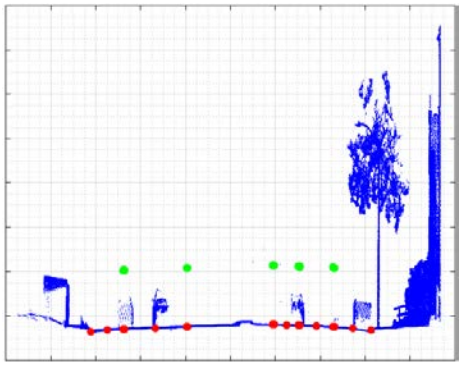

2. YZ Slice projection, with road surface seed points (red), calculated from the trajectory points (green)

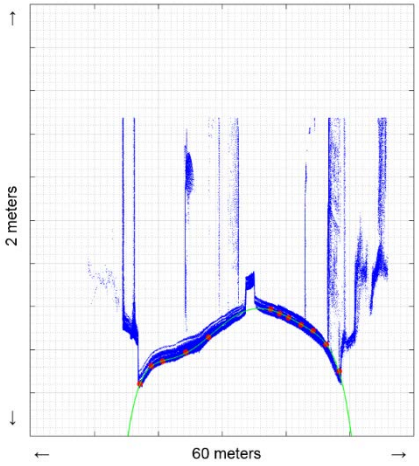

3. Seed point curve fitting

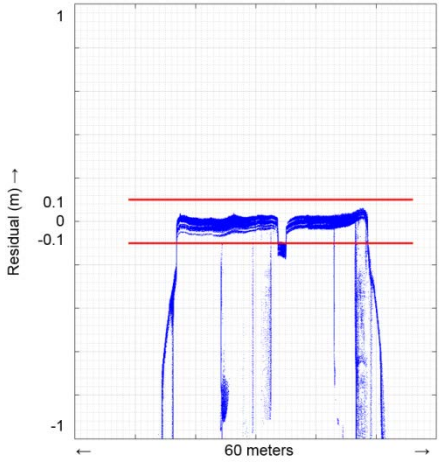

4. Residuals

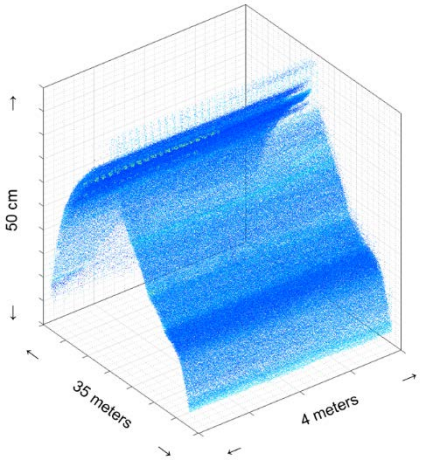

5. Extracted surface

Georectified Point Cloud: Intersection Mapping

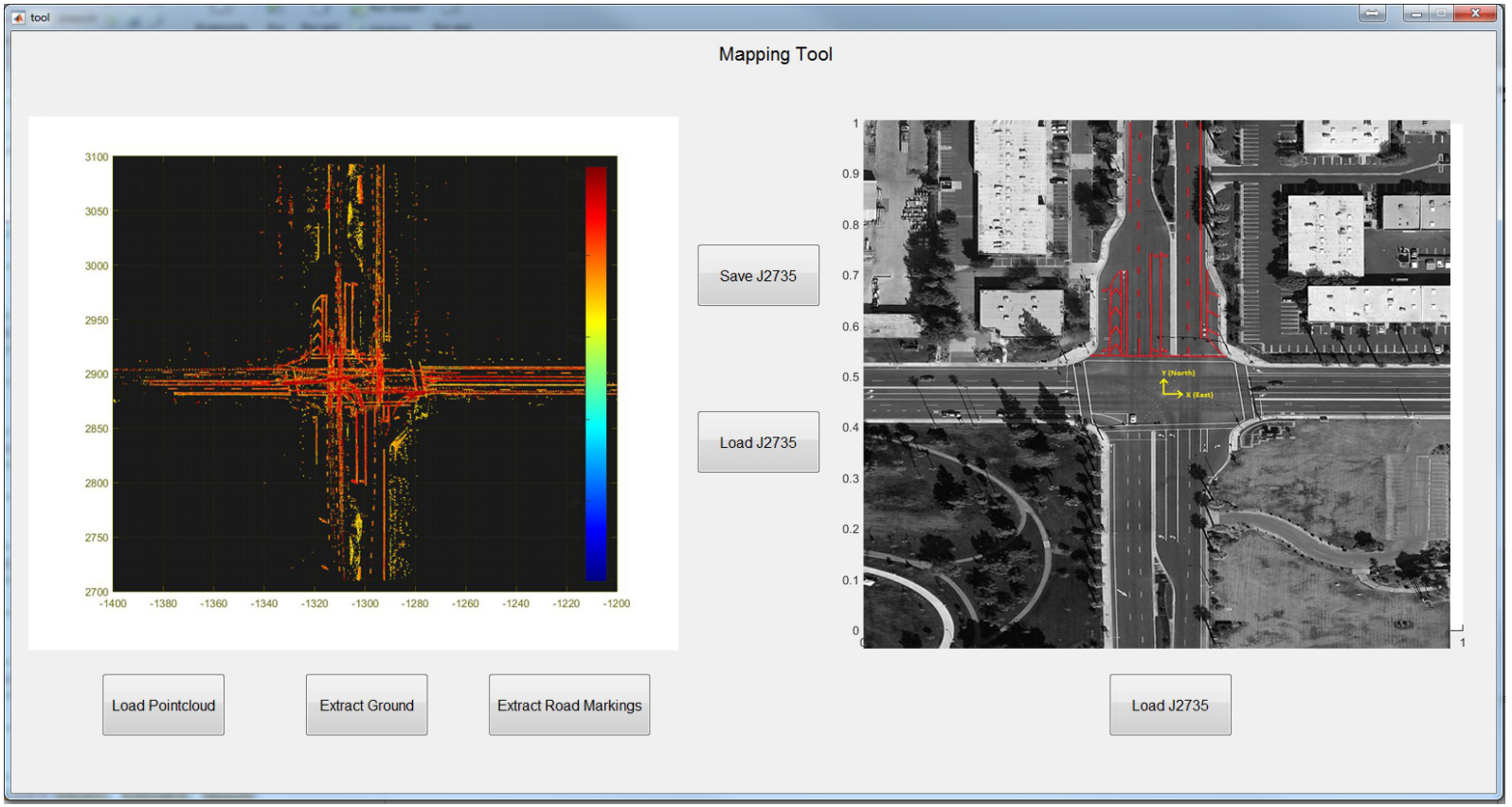

Top down view of georectified point cloud processed to extract high reflectivity points near the ground.

Top down image of target intersection with extracted J2735 data structure superimposed.

Feature types: Lane, road, meridian edges; Stop bars; signs, signals, ….

Automated Mapping Work Flow

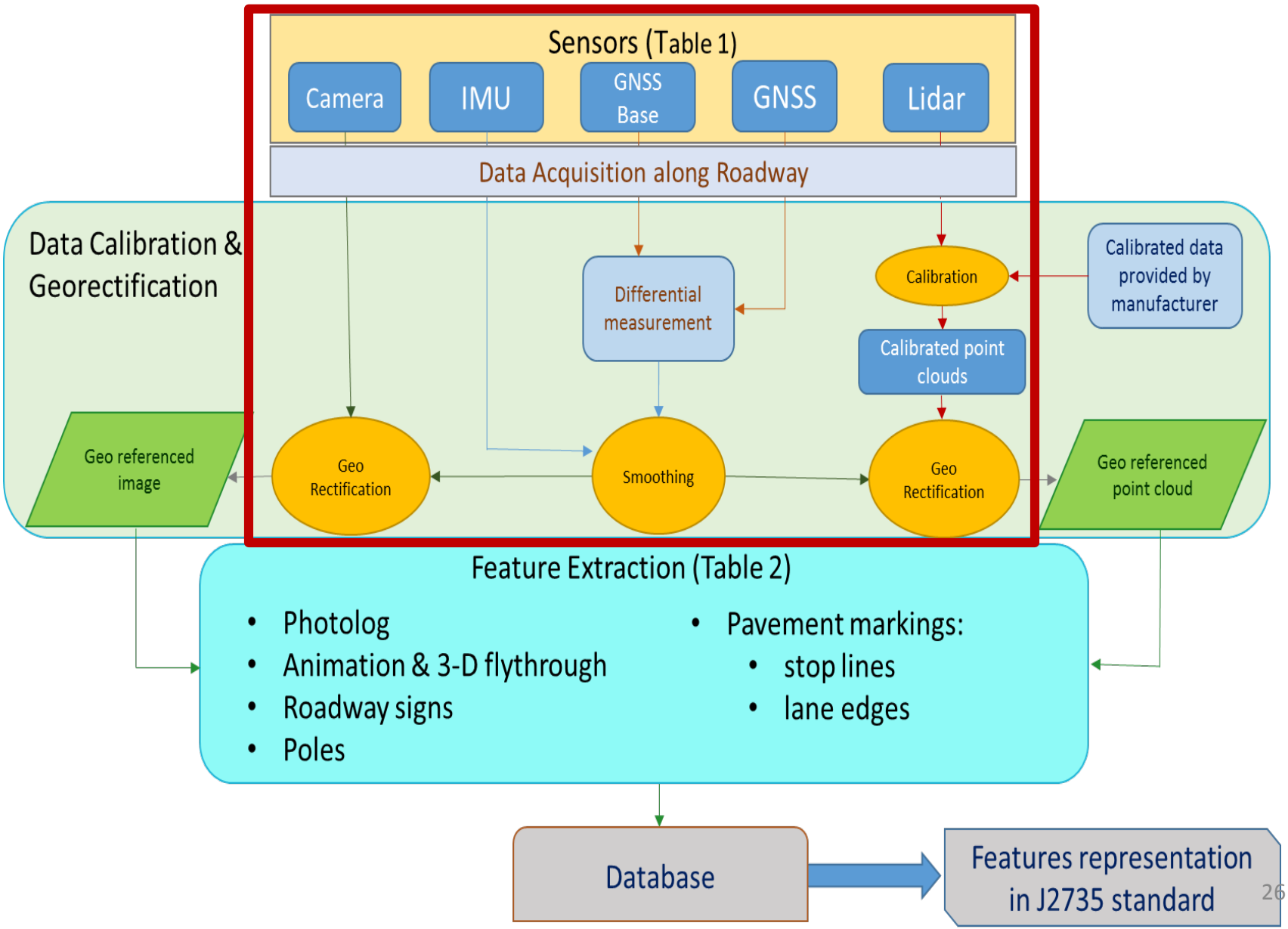

Reliable Precise Positioning: How it Works

UC RIVERSIDE UNIVERSITY OF CALIFORNIA

- Inertial Navigation:
  - High bandwidth, sampling rate, reliability
  - Slow, but unbounded, error growth
  - Used in military & commerce since 1960's
- GNSS
  - Bounded absolute position error
  - Bound is dependent on processing
  - Reliability is dependent on environment
- Feature sensors (Camera, Radar, Lidar)
  - Bounded feature relative accuracy. Abundant in urban areas.
  - No absolute accuracy (without EDM).
  - Not robust to environmental conditions (e.g. lighting)

Sensor fusion can achieve, high bandwidth, high sample rate, and accurate positioning, with reliability versus computational load tradeoff.

RTK GPS background

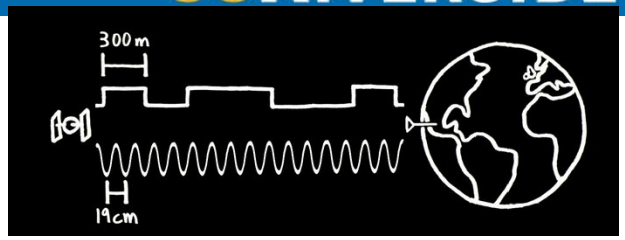

Figure from Swift Navigation

State: $\boldsymbol{x}(t) = [\boldsymbol{p}(t), \tau_r(t)] \epsilon\, R^4$

Code meas.: $\rho^i(t_k) = \boldsymbol{h}_k^i(\boldsymbol{x}(t_k)) + n_\rho^i(t_k),\ n_\rho^i \sim \mathcal{N}(0, {\sigma_\rho}^2)$

Phase meas.: $\varphi^i(t_k) = \boldsymbol{h}_k^i(\boldsymbol{x}(t_k)) + \lambda N^i(t_k) + n_\varphi^i(t_k),\ n_\varphi^i \sim \mathcal{N}(0, {\sigma_\varphi}^2)$

Real Time Kinematic (RTK):

$$\min_{\boldsymbol{p}(t_k)\in\mathbb{R}^3, \mathbf{N}\in\mathbb{Z}^m} \sum_i \left[\|h_k^i(\boldsymbol{p}(t_k)) - \rho^i(t_k)\|_{\sigma_\rho^2}^2 + \|h_k^i(\boldsymbol{p}(t_k)) + \lambda N^i - \varphi^i(t_k)\|_{\sigma_\varphi^2}^2 \right].$$

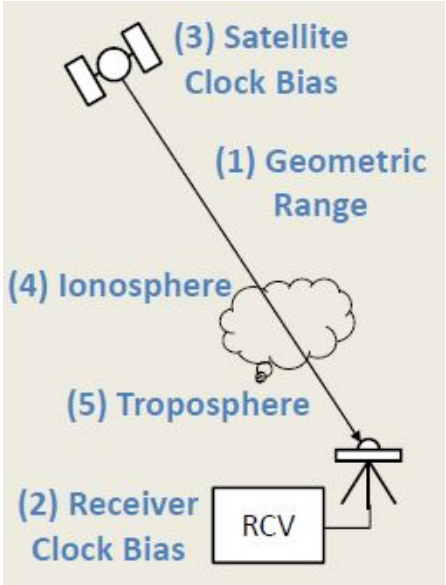

Differential GPS

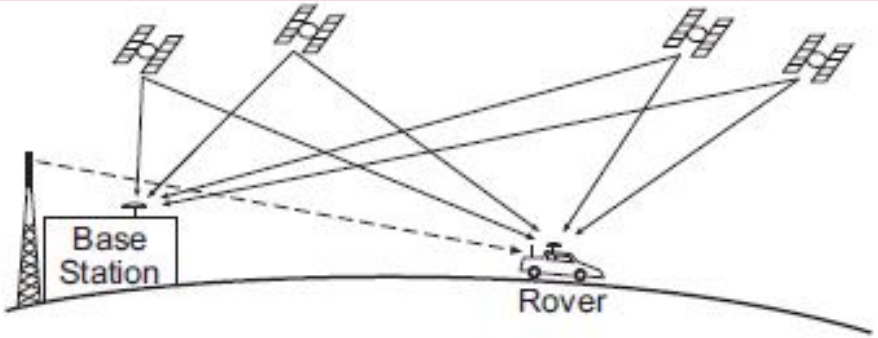

$$E_{cm}^{ib} = E_{cm}^{i}$$

RTK GPS background

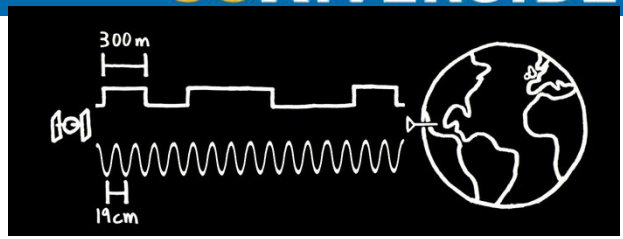

Figure from Swift Navigation

State: $\boldsymbol{x}(t) = [\boldsymbol{p}(t), \tau_r(t)] \epsilon\, R^4$

Code meas.: $\rho^i(t_k) = \boldsymbol{h}_k^i(\boldsymbol{x}(t_k)) + n_\rho^i(t_k),\ n_\rho^i \sim \mathcal{N}(0, {\sigma_\rho}^2)$

Phase meas.: $\varphi^i(t_k) = \boldsymbol{h}_k^i(\boldsymbol{x}(t_k)) + \lambda N^i(t_k) + n_\varphi^i(t_k),\ n_\varphi^i \sim \mathcal{N}(0, {\sigma_\varphi}^2)$

Real Time Kinematic (RTK):

$$\min_{\boldsymbol{p}(t_k)\in\mathbb{R}^3, \mathbf{N}\in\mathbb{Z}^m} \sum_i \left[\|h_k^i(\boldsymbol{p}(t_k)) - \rho^i(t_k)\|_{\sigma_\rho^2}^2 + \|h_k^i(\boldsymbol{p}(t_k)) + \lambda N^i - \varphi^i(t_k)\|_{\sigma_\varphi^2}^2 \right].$$

Challenges:

1. Requires 7+ satellites to ensure good constellation geometry
2. Outlier & incorrect integer (i.e., error) detection
3. Frequent loss-of-lock in urban environments, need reliable on-the-fly integer ambiguity solutions

RTK GPS/INS background

UC RIVERSIDE UNIVERSITY OF CALIFORNIA

State: $\boldsymbol{x}(t) = [\boldsymbol{p}^\intercal(t), \boldsymbol{v}^\intercal(t), \boldsymbol{q}^\intercal(t), \boldsymbol{b}_a^\intercal(t), \boldsymbol{b}_g^\intercal(t)]^\intercal \in \mathbb{R}^{n_s}, \quad n_s \geq 15$

Code meas.: $\rho^i(t_k) = \boldsymbol{h}_k^i(\boldsymbol{x}(t_k)) + n_\rho^i(t_k), \; n_\rho^i \sim \mathcal{N}(0, {\sigma_\rho}^2)$

Phase meas.: $\varphi^i(t_k) = \boldsymbol{h}_k^i(\boldsymbol{x}(t_k)) + \lambda N^i(t_k) + n_\varphi^i(t_k), \; n_\varphi^i \sim \mathcal{N}(0, {\sigma_\varphi}^2)$

Prior for the initial state: $\boldsymbol{x}(t_1) \sim \mathcal{N}(\boldsymbol{x}_1, \mathbf{P}_1),$

Rover kinematics: $\dot{\boldsymbol{x}}(t) = \boldsymbol{f}(\boldsymbol{x}(t), \boldsymbol{u}(t)),$

IMU meas.: $\tilde{\boldsymbol{u}}_a = \mathbf{f} + \boldsymbol{b}_a + \boldsymbol{n}_a,$

$\tilde{\boldsymbol{u}}_g = \boldsymbol{\omega} + \boldsymbol{b}_g + \boldsymbol{n}_g,$

Standard (Extended) Kalman Filter:

- Single epoch (K=1), linear, Gaussian
- Redundancy insufficient for required reliability

Bayesian Trajectory Estimation

UC RIVERSIDE UNIVERSITY OF CALIFORNIA

Constraints:

- IMU: $\mathbf{U}_k = \{\tilde{\boldsymbol{u}}(\tau_n), t_k \leq \tau_n \leq t_{k+1}\}$

$$\mathbf{U} = \{\mathbf{U}_k\}_{k=1}^{K-1}$$

$$\dot{\hat{\mathbf{x}}}(t) = \boldsymbol{f}(\hat{\mathbf{x}}(t), \tilde{\mathbf{u}}(t))$$

$$\hat{\boldsymbol{x}}(\tau_{k+1}) = \boldsymbol{\phi}\big(\hat{\boldsymbol{x}}(\tau_k), \tilde{\boldsymbol{u}}(\tau_k)\big)$$

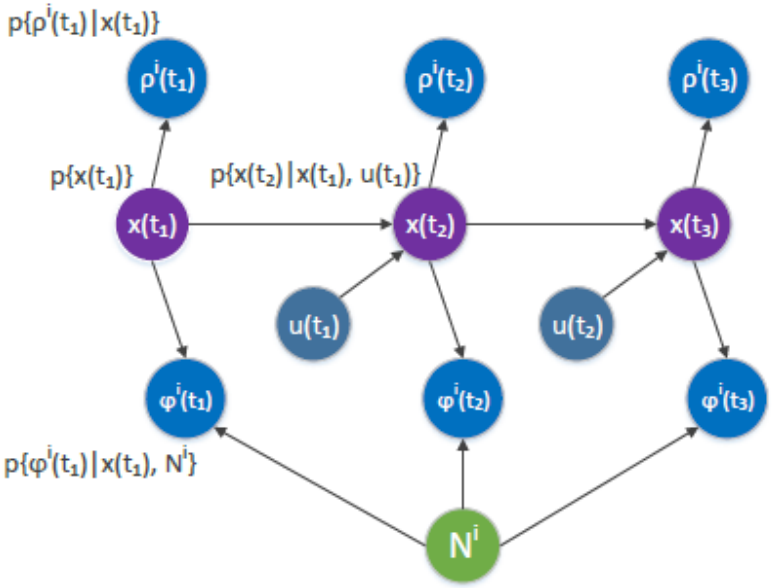

- Standard Measurements: **Y**

$$\rho^i(t_k) = h_k^i(\boldsymbol{x}(t_k)) + n_\rho^i(t_k)$$

- Measurements with Unknown Integer: **Z**

$$\varphi^i(t_k) = h_k^i(\boldsymbol{x}(t_k)) + \lambda N^i(t_k) + n_\varphi^i(t_k)$$

$$\max_{\mathbf{X}\in\mathbb{R}^{n_s K}, \mathbf{N}\in\mathbb{Z}^m} p(\boldsymbol{x}(t_1))p(\mathbf{X}_+|\boldsymbol{x}(t_1), \mathbf{U})p(\mathbf{Y}|\mathbf{X})p(\mathbf{Z}|\mathbf{X}, \mathbf{N})$$

where X is the trajectory over a K second window

Solved using computational methods developed in the SLAM literature, extended to accommodate integer unknowns.

Problem Statement

Given:

- an initial distribution for the state $\boldsymbol{s}(t_1) \sim \mathcal{N}(\boldsymbol{s}_1, \mathbf{P}_{s_1})$,
- IMU measurements $\mathbf{U} = \{\mathbf{U}_k\}_{k=1}^{K-1}$, where $\mathbf{U}_k = \{\tilde{\boldsymbol{u}}(\tau_n), t_k \leq \tau_n \leq t_{k+1}\}$,
- DGPS code and carrier phase measurements $\mathbf{Y} = \{\mathbf{Y}_k\}_{k=1}^{K}$, where $\mathbf{Y}_k = \{\rho^i(t_k)\}_{i=1}^{m_k} \bigcup \{\varphi^i(t_k)\}_{i=1}^{m}$.

Objective:

Estimate the optimal state trajectory $\mathbf{X} \triangleq [\boldsymbol{x}^\intercal(t_1), \ldots, \boldsymbol{x}^\intercal(t_K)]^\intercal \in \mathbb{R}^{Kn_s}$ and integers $\mathbf{N} \triangleq [N^1, \ldots, N^m]^\intercal \in \mathbb{Z}^m$ with the given sensor measurements $\mathbf{U}$, $\mathbf{Y}$ and the prior state density $p_{\boldsymbol{s}}(\boldsymbol{s}(t_1))$.

$$\max_{\mathbf{X} \in \mathbb{R}^{n_s K}, \mathbf{N} \in \mathbb{Z}^m} p(\boldsymbol{s}(t_1)) p(\mathbf{X}_+ | \boldsymbol{x}(t_1), \mathbf{U}) p(\mathbf{Y} | \mathbf{X}, \mathbf{N})$$

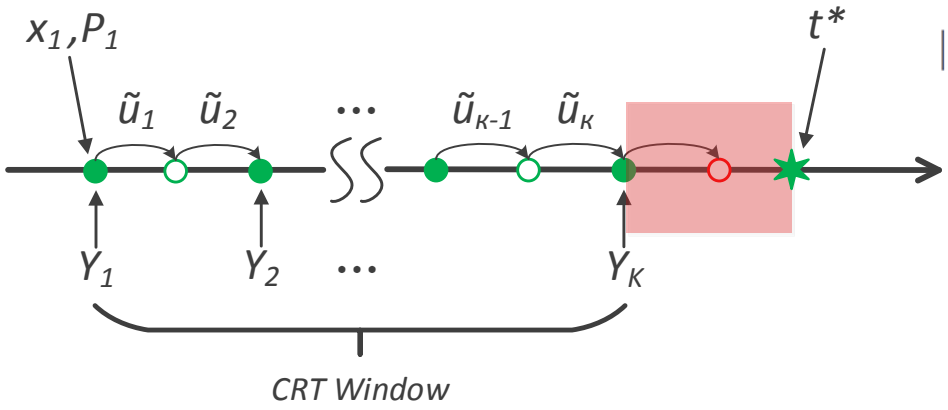

$$\begin{aligned}
\|\mathbf{v}(\mathbf{X}, \mathbf{N})\|_{\mathbf{W}}^2 &= \|\boldsymbol{s}(t_1) - \boldsymbol{s}_1\|_{\mathbf{P}_{s_1}}^2 \\
&+ \sum_k \|\boldsymbol{\phi}(\boldsymbol{x}(t_k), \mathbf{U}_k) - \boldsymbol{x}(t_{k+1})\|_{\mathbf{Q}_k}^2 \\
&+ \sum_k \sum_i \|h_k^i(\boldsymbol{x}(t_k)) - \rho^i(t_k)\|_{\sigma_\rho^2}^2 \\
&+ \sum_k \sum_i \|h_k^i(\boldsymbol{x}(t_k)) + \lambda N^i - \varphi^i(t_k)\|_{\sigma_\varphi^2}^2
\end{aligned}$$

Bayesian Trajectory Estimation

Available Constraints:

$$\rho(t) = R(x(t)) + \nu_\rho(t)$$

$$\phi(t) = R(x(t)) + \nu_\phi(t) + \lambda N$$

$$x(t) = x(t_0) + \int_{t_0}^{t} f\Big(x(\tau), u(\tau) + \omega(\tau) + b(\tau)\Big) d\tau$$

Measured: $\rho(t_i), \phi(t_i), u(\tau_k), i = 1, 2, \ldots, M$
Estimated: $x(\tau_k) \in \Re^{15}, N \in I^m \; k = 0, \ldots, 200M$

Notation:

- **U** – IMU data
- **Y** – GNSS pseudorange data
- **Z** – GNSS carrier phase data
- **X** – state trajectory

Physical ideas:

- $\nu_\rho(t)$ is accurate to a few meters
- $\nu_\phi(t)$ is accurate to centimeters
- $\omega(\tau)$ is very small per step, but accumulates due to integration

1. IMU Constrained Trajectory Estimate

$$\hat{\mathbf{X}} = \arg\max_{\mathbf{X}} \Big(p_{\delta \boldsymbol{x}_0}\big(\boldsymbol{x}(t_0) - \boldsymbol{x}_0\big) p_{\boldsymbol{\omega}_u}\big(\mathbf{X}_+ - \boldsymbol{\phi}(\mathbf{X}, \mathbf{U})\big) \Big)$$

2. Pseudorange Constrained Trajectory Estimate:

$$\hat{\mathbf{X}} = \arg\max_{\mathbf{X}} \Big(p_{\delta \boldsymbol{x}_0}\big(\boldsymbol{x}(t_0) - \boldsymbol{x}_0\big) p_{\boldsymbol{\omega}_u}\big(\mathbf{X}_+ - \boldsymbol{\phi}(\mathbf{X}, \mathbf{U})\big) p_{\boldsymbol{n}_\rho}\big(\mathbf{Y} - \boldsymbol{h}(\mathbf{X})\big) \Big)$$

3. Carrier Phase Constrained Trajectory Estimate:

$$\hat{\mathbf{X}}, \hat{\mathbf{N}} = \arg\max_{\mathbf{X},\, \mathbf{N}} \Big(p_{\delta \boldsymbol{x}_0}\big(\boldsymbol{x}(t_0) - \boldsymbol{x}_0\big) p_{\boldsymbol{\omega}_u}\big(\mathbf{X}_+ - \boldsymbol{\phi}(\mathbf{X}, \mathbf{U})\big) p_{\boldsymbol{n}_\rho}\big(\mathbf{Y} - \boldsymbol{h}(\mathbf{X})\big) p_{\boldsymbol{n}_\rho}\big(\mathbf{Z} - \boldsymbol{h}(\mathbf{X}, \mathbf{N})\big) \Big)$$

Prior

IMU Kinematic Integration

Carrier Phase

Pseudorange

Trajectory Estimation Process

- Joint Estimation: platform trajectory and landmarks
  - Bayesian: $\hat{\mathbf{X}} = \arg\max_{\mathbf{X}} \left(p_{\delta \boldsymbol{x}_0}(\boldsymbol{x}(t_0) - \boldsymbol{x}_0) p_{\boldsymbol{\omega}_u}(\mathbf{X}_+ - \boldsymbol{\phi}(\mathbf{X}, \mathbf{U})) p_{\boldsymbol{n}_z}(\mathbf{Z} - \boldsymbol{h}(\mathbf{X})) \right)$
  - Equiv: $\|\mathbf{v}\|^2_{\mathbf{W}} = \|\boldsymbol{x}(t_0) - \boldsymbol{x}_0\|_{\mathbf{P}_0} + \sum_k \|\boldsymbol{\phi}(\boldsymbol{x}(t_k), \mathbf{U}_k) - \boldsymbol{x}(t_{k+1})\|_{\mathbf{Q}_k} + \sum_i \|\boldsymbol{h}(\boldsymbol{x}(t_i)) - \tilde{\boldsymbol{z}}(t_i)\|_{\mathbf{R}_{z_i}}$
    1. Prior
    2. Integrated inertial measurements
    3. GPS: Code, Phase, Doppler
    4. Landmark parameters (not shown)

Large set of residual enables reliable outlier detection

$$\mathbf{J}^\top \mathbf{J} \delta \boldsymbol{x} = -\mathbf{J}^\top \boldsymbol{b}$$

Decompose **J = [A, B],** where **A** is full column rank.

$$\mathbf{J} = \left[\begin{array}{ccccc|c} \boldsymbol{\Sigma}_{\mathbf{P}_0} & \mathbf{0} & \dots & \mathbf{0} & \mathbf{0} & \mathbf{0} \\ \bar{\boldsymbol{\Phi}}_0 & -\boldsymbol{\Sigma}_{\mathbf{Q}_0} & \dots & \mathbf{0} & \mathbf{0} & \mathbf{0} \\ \vdots & \vdots & \dots & \vdots & \vdots & \vdots \\ \mathbf{0} & \mathbf{0} & \dots & \bar{\boldsymbol{\Phi}}_{K-1} & -\boldsymbol{\Sigma}_{\mathbf{Q}_{K-1}} & \mathbf{0} \\ \hline \mathbf{0} & \bar{\mathbf{H}}_1 & \dots & \mathbf{0} & \mathbf{0} & \mathbf{0} \\ \vdots & \vdots & \dots & \vdots & \vdots & \vdots \\ \mathbf{0} & \mathbf{0} & \dots & \mathbf{0} & \bar{\mathbf{H}}_K & \mathbf{0} \\ \hline \mathbf{0} & \bar{\mathbf{H}}_1 & \dots & \mathbf{0} & \mathbf{0} & \boldsymbol{\Sigma}_{\mathbf{R}_{z_N}} \\ \vdots & \vdots & \dots & \vdots & \vdots & \\ \mathbf{0} & \mathbf{0} & \dots & \mathbf{0} & \bar{\mathbf{H}}_K & \boldsymbol{\Sigma}_{\mathbf{R}_{z_N}} \end{array}\right] \quad \delta \boldsymbol{x} = \left[\begin{array}{c} \delta \mathbf{x}_0 \\ \delta \mathbf{x}_1 \\ \vdots \\ \delta \mathbf{x}_{K-1} \\ \delta \mathbf{x}_K \\ \hline N \end{array}\right] \quad \boldsymbol{b} \triangleq \boldsymbol{r}(\hat{\mathbf{X}}) = \left[\begin{array}{l} \boldsymbol{\Sigma}_{\mathbf{P}_0}(\hat{\boldsymbol{x}}(t_0) - \boldsymbol{x}_0) \\ \boldsymbol{\Sigma}_{\mathbf{Q}_0} \boldsymbol{a}_1 \\ \vdots \\ \boldsymbol{\Sigma}_{\mathbf{Q}_{K-1}} \boldsymbol{a}_K \\ \boldsymbol{\Sigma}_{\mathbf{R}_{y1}}(\boldsymbol{g}(\hat{\boldsymbol{x}}(t_1), \hat{\boldsymbol{x}}(t_0)) - \tilde{\boldsymbol{y}}(t_1)) \\ \vdots \\ \boldsymbol{\Sigma}_{\mathbf{R}_{y4}}(\boldsymbol{g}(\hat{\boldsymbol{x}}(t_4), \hat{\boldsymbol{x}}(t_0)) - \tilde{\boldsymbol{y}}(t_4)) \\ \boldsymbol{\Sigma}_{\mathbf{R}_{z_1}}(\boldsymbol{h}(\hat{\boldsymbol{x}}(t_1)) - \tilde{\boldsymbol{z}}(t_1)) \\ \vdots \\ \boldsymbol{\Sigma}_{\mathbf{R}_{z_N}}(\boldsymbol{h}(\hat{\boldsymbol{x}}(t_N)) - \tilde{\boldsymbol{z}}(t_N)) \end{array}\right]$$

Integer Estimation (by MILES)

Nonlinear constraint equations:

$$\begin{aligned}\rho(t) &= R(x(t)) + \nu_\rho(t)\\ \phi(t) &= R(x(t)) + \nu_\phi(t) + \lambda N\\ x(t) &= x(t_0) + \int_{t_0}^{t} f\Big(x(\tau), u(\tau) + \omega(\tau) + b(\tau)\Big) d\tau\end{aligned}$$

Measured: $\rho(t_i), \phi(t_i), u(\tau_k), i = 1, 2, \ldots, M$
Estimated: $x(\tau_k) \in \Re^{15}$, $N \in I^m$ $k = 0, \ldots, 200M$

Physical ideas:

- $\nu_\rho(t)$ is accurate to a few meters
- $\nu_\phi(t)$ is accurate to centimeters
- $\omega(\tau)$ is very small per step, but accumulates due to integration

Linearized residual equations:

$$\min_{z \in \Re^{15M},\ N \in I^m} \|y - Az - BN\|^2$$

MILS Decomposition:

$$\|y - Az - BN\|^2 = \|Q_A^\top y - Q_A^\top BN - R_A z\|^2 + \|Q_A^\top y - Q_A^\top BN\|^2$$

- For any N, there exist z to solve first term exactly

QR factors:

$$A = [Q_A,\ \bar{Q}_A] \begin{bmatrix} R_A \\ 0 \end{bmatrix}$$

- $[Q_A,\ \bar{Q}_A]$ orthogonal
- R_A nonsingular upper triangular

ILS Solution: $\min_{N \in I^m} \|Q_A^\top y - Q_A^\top BN\|^2$

- Involves search over integers within feasible ellipse
- Utilizes unimodual Z:

$$Z, Z^{-1} \in I^{m \times m}, |Z| = 1$$

- X.-W. Chang, T. Zhou, "MILES: MATLAB package for solving Mixed Integer LEast Squares problems," *GPS Solutions*, Springer-Verlag, 2007.
- P. De Jonge, C. Tiberius, "LAMBDA method for integer ambiguity estimation: implementation aspects," Delft Geodetic Computing Center LGR-Series, No. 12.

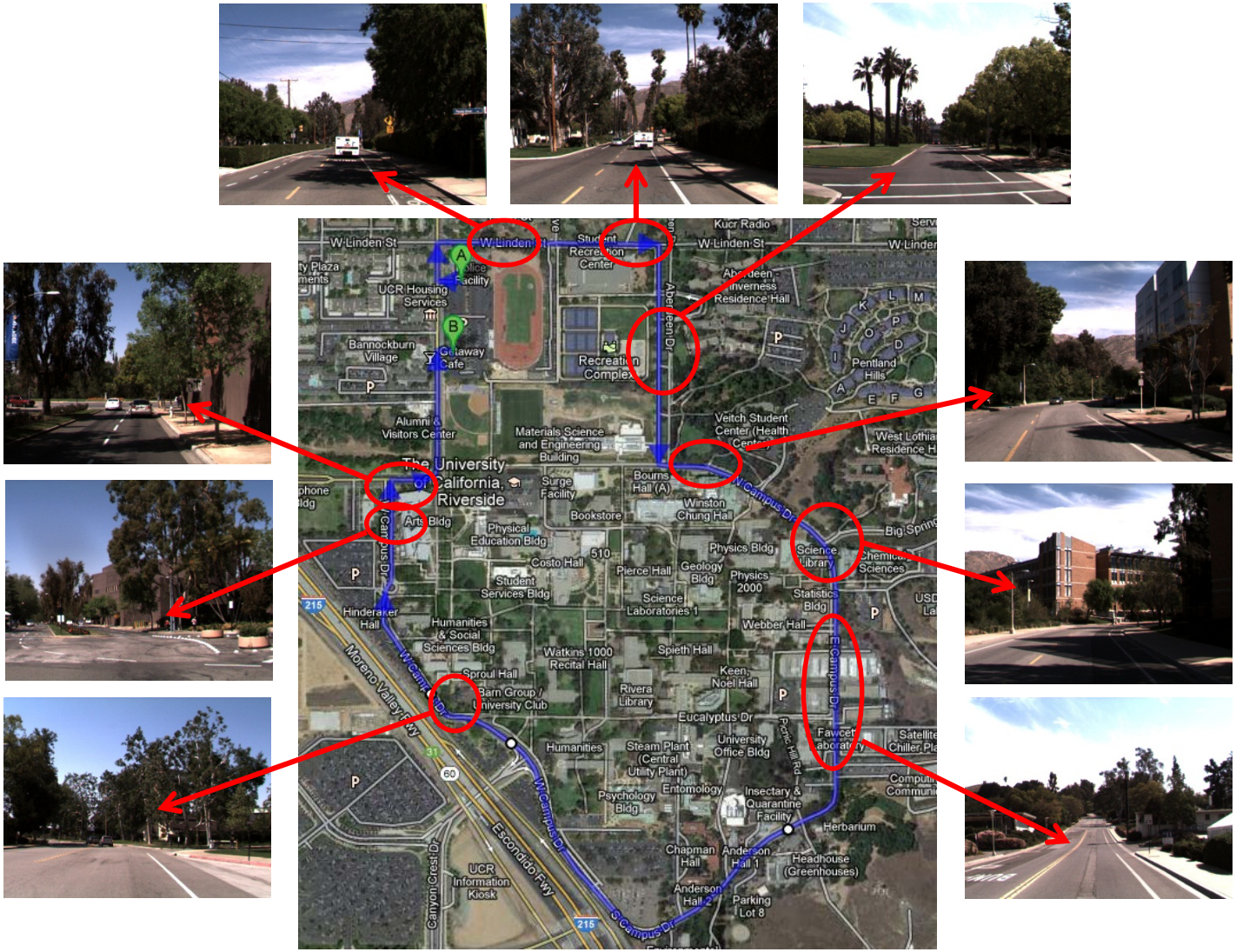

UCR Implementation Trajectory

- 3.6 km campus ring
- Significant tree cover
- Buildings and terrain shading

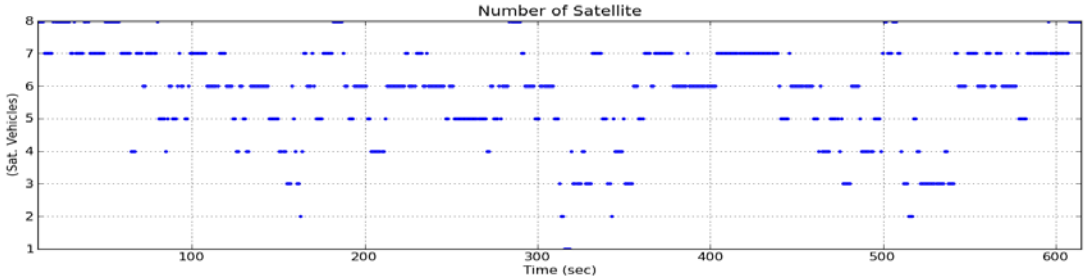

Trajectory Estimation Results

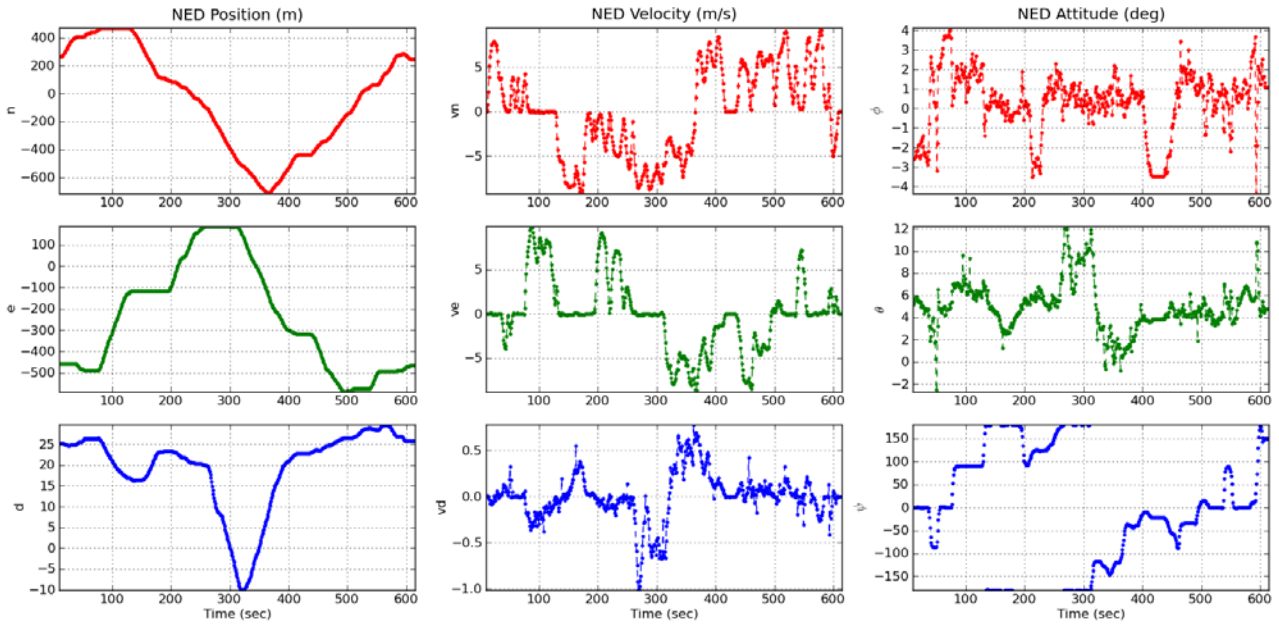

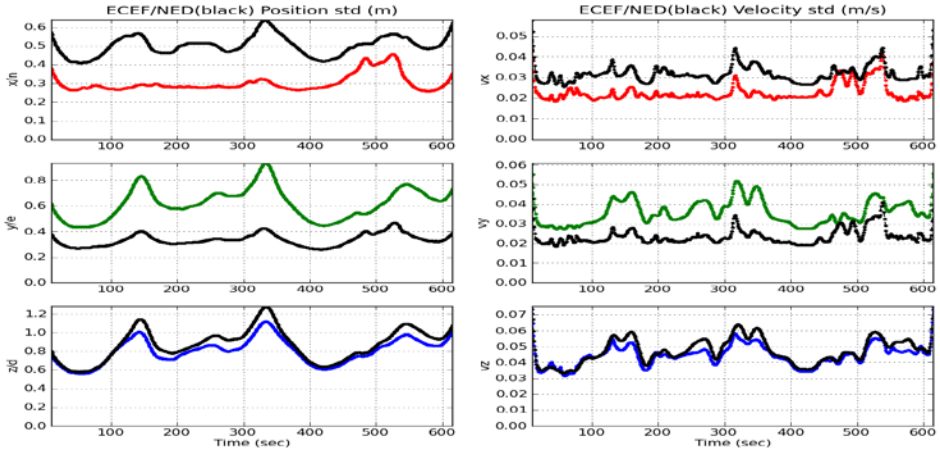

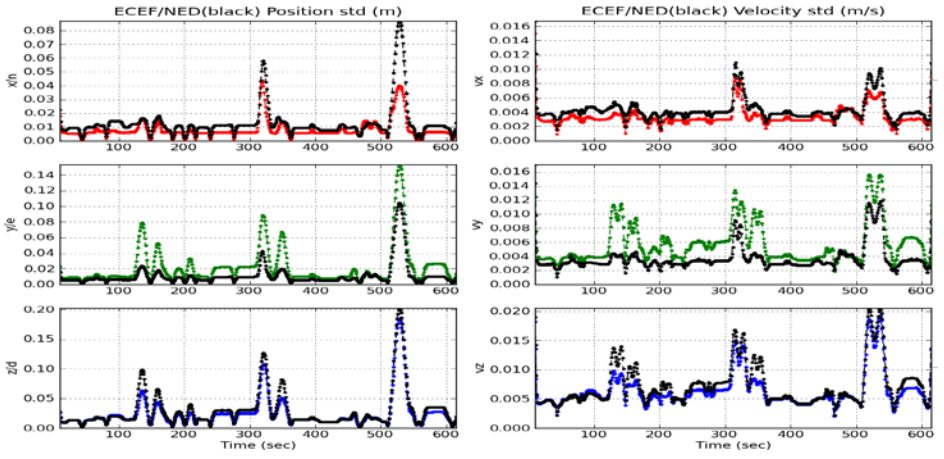

Pseudorange

Carrier Phase

Trajectory Estimation Results: Residuals

Process 1:

- Code, Doppler, IMU
- Bayesian Smoothing

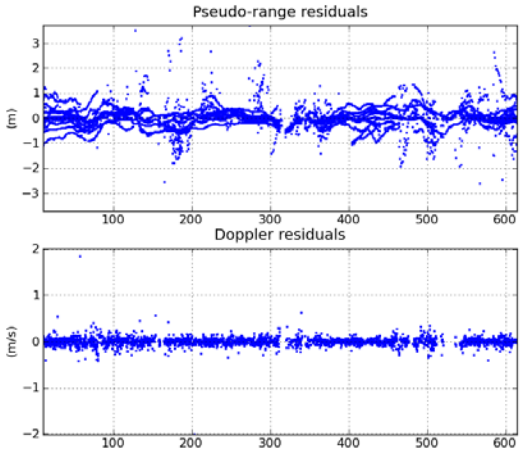

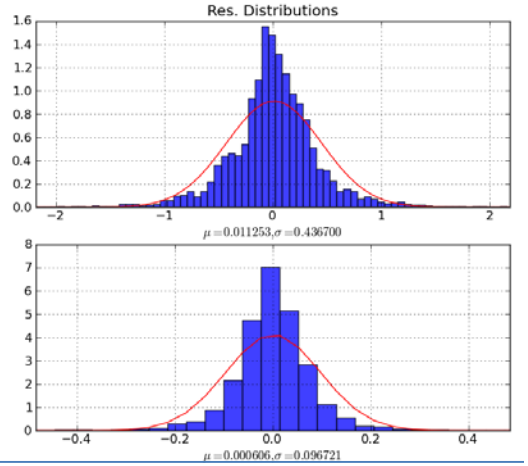

Process 2:

- Integer Estimation
- Bayesian Smoothing
  - Integer-resolved phase and IMU when available
  - Code, Doppler, IMU otherwise

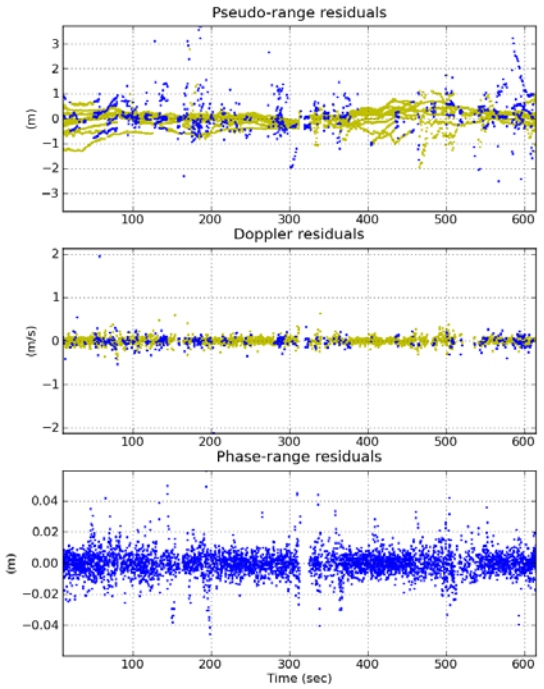

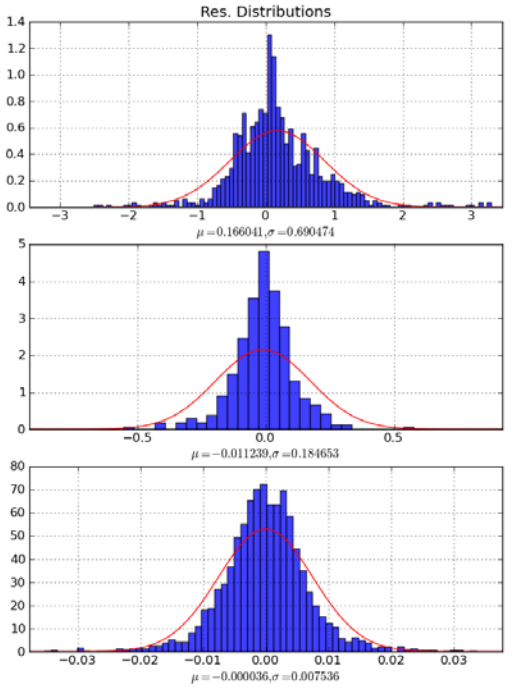

LIDAR Intensity Point Cloud…

Bing Map with TFHRC aerial image overlay

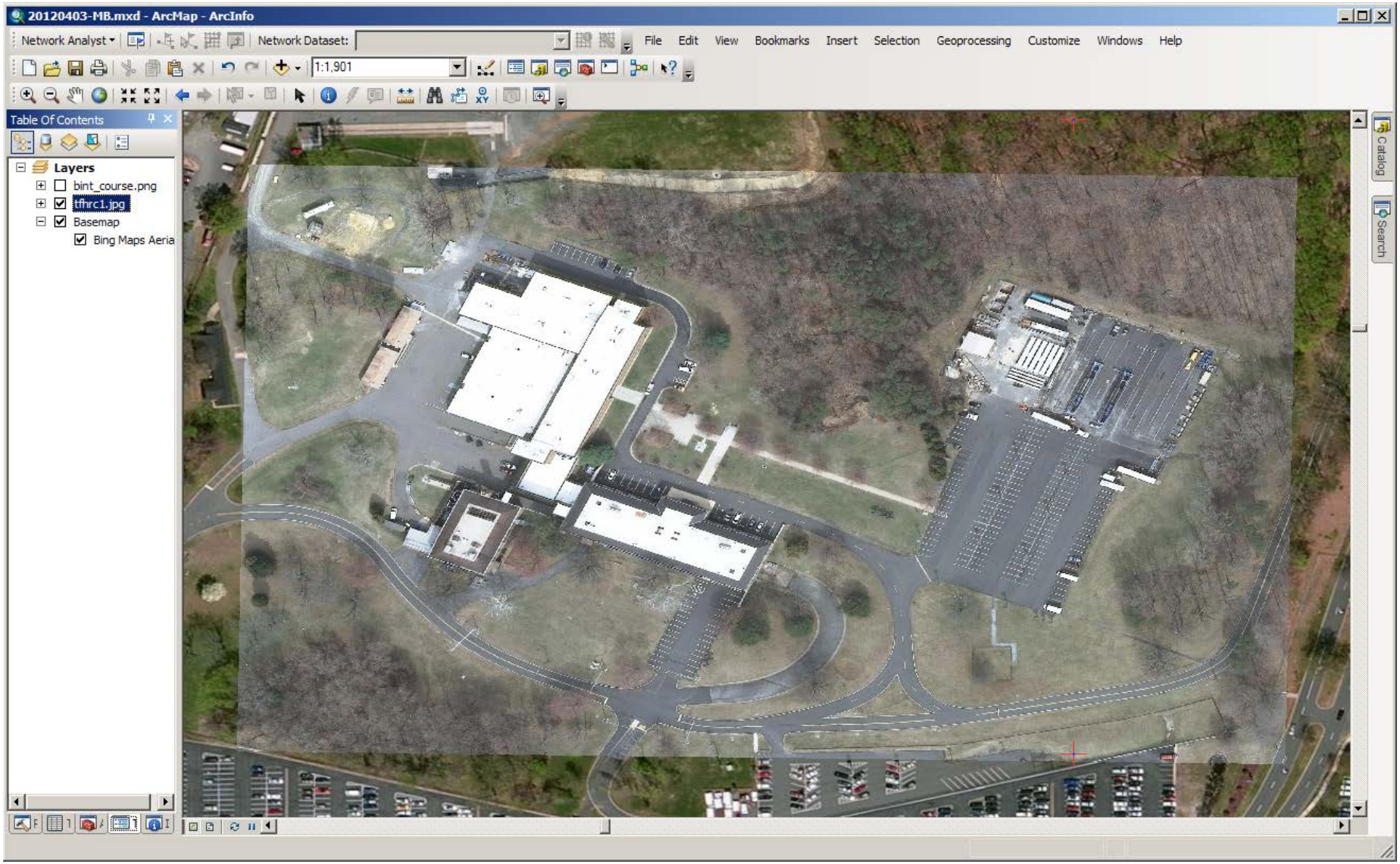

Georectified LIDAR-based intensity image

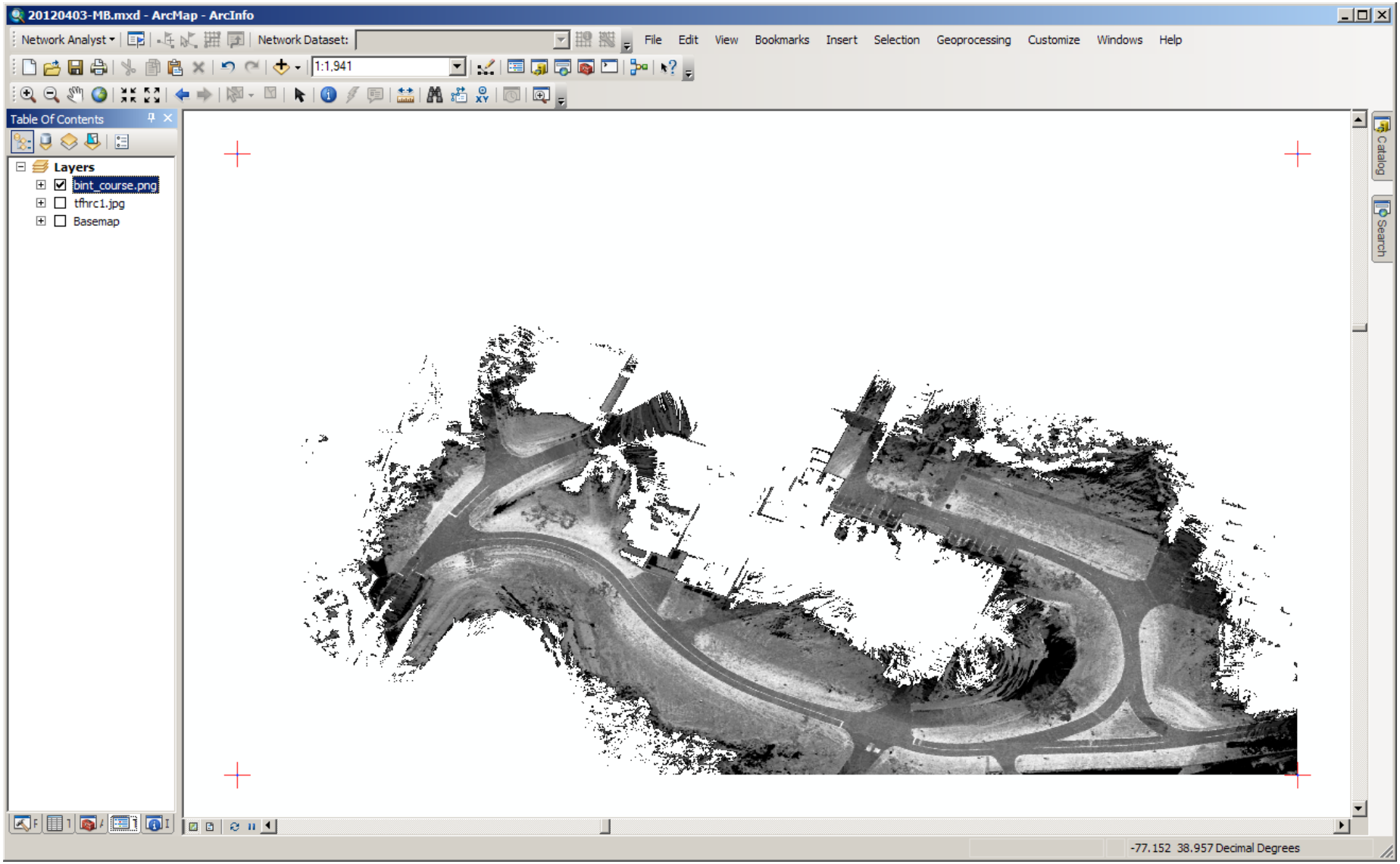

Bing Map, Aerial Image, LIDAR image overlay

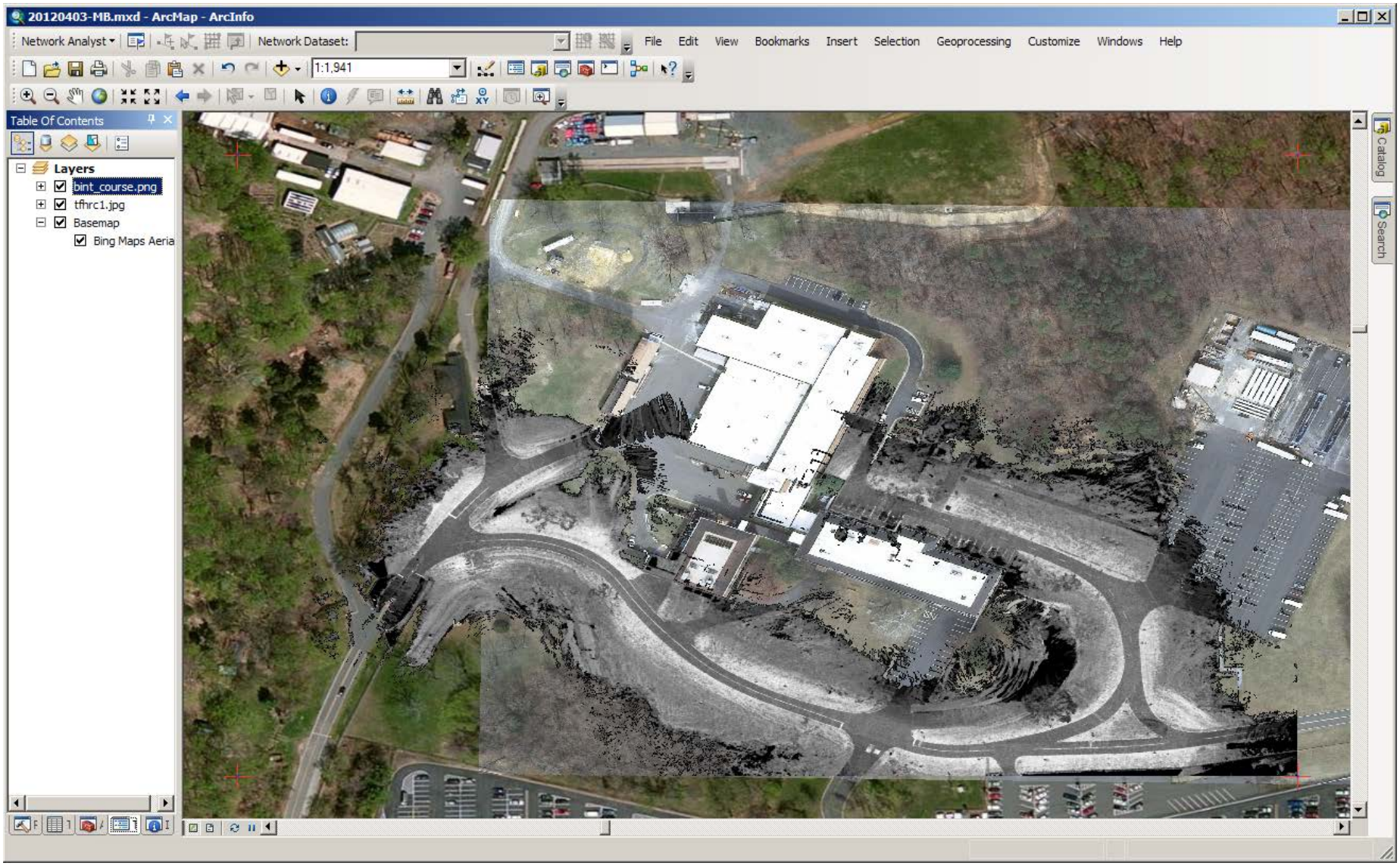

LIDAR Traffic Sign Extraction…

Detection & mapping:

- High intensity Lidar return, due to high reflectivity
- Cluster diameter of approximately one meter
- Initialization: Cluster defines plane with horizontal normal vector (minumum eigenvalue problem)
- Refinement: Bayesian nonlinear estimation problem

Each sign detected from multiple angles has an observable location.

Estimated Plane Position vs. Surveyed Plane Position

Sign Post #	Survey North (m)	Survey East (m)	Max Survey ECEF Std (m)	Computed North (m)	Computed East (m)	Abs. Horiz. Error (m)
1	-41.192	-87.313	0.042	-41.133	-87.345	0.067
2	-55.321	-62.332	0.126	-55.271	-62.328	0.050
3	-89.666	-36.001	0.159	-89.656	-36.112	0.111
4	-142.194	80.051	0.057	-142.244	80.054	0.050
5	-139.078	146.342	0.047	-139.101	146.358	0.028
6	-115.571	144.863	0.009	-115.658	144.923	0.106
7	-85.860	141.540	0.031	-85.882	141.543	0.022
8	-47.903	122.360	0.025	-47.952	122.415	0.073
9	-35.369	99.666	0.045	-35.381	99.686	0.023
10	-44.498	101.259	0.024	-44.433	101.281	0.068
11	-62.597	125.258	0.04	-62.555	125.306	0.063
12	-134.138	76.493	0.025	-134.073	76.519	0.069
13	-104.598	-4.185	0.061	-104.569	-4.152	0.044
16	-118.704	133.631	0.015	-118.618	133.724	0.126

Sub-decimeter accuracy is achieved.

Real-time Navigation

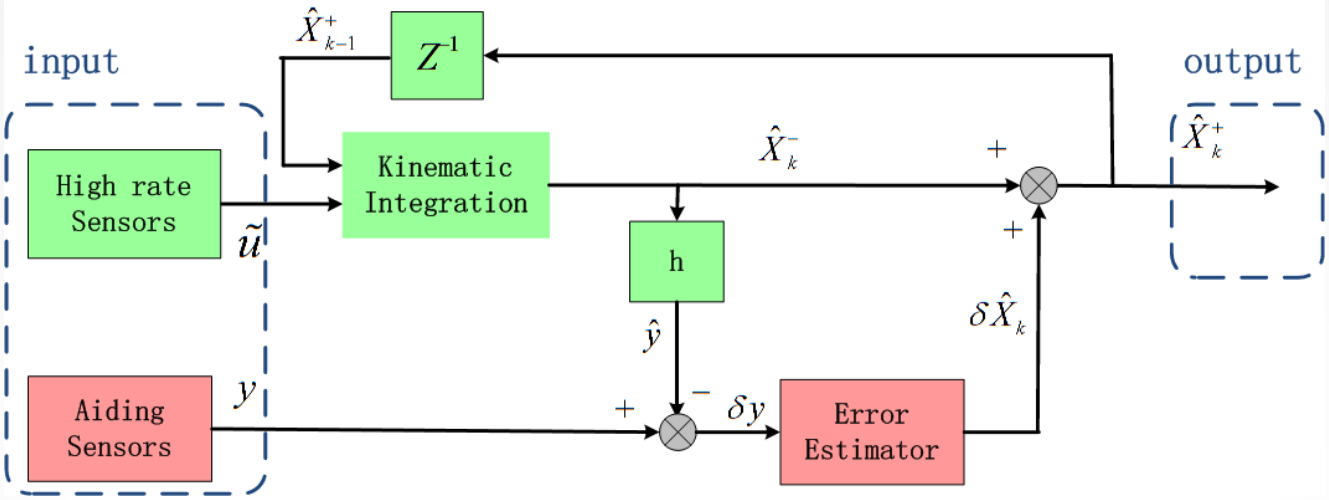

1. **High rate sensors**
   - Encoder or IMU
2. **Aiding measurements**
   - GPS, image features
3. **CRLB**

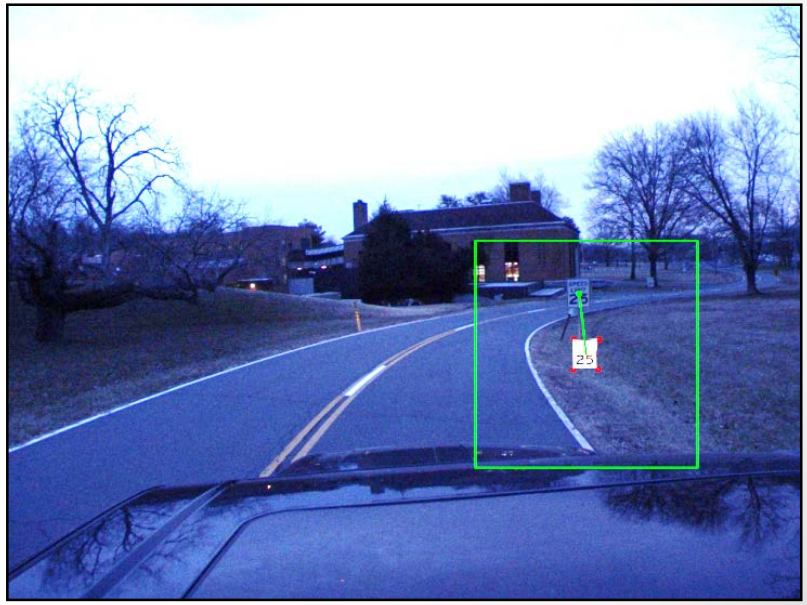

See J.A. Farrell, *Aided Navigation*, McGraw-Hill, 2008.

Application Graphical User Interface…

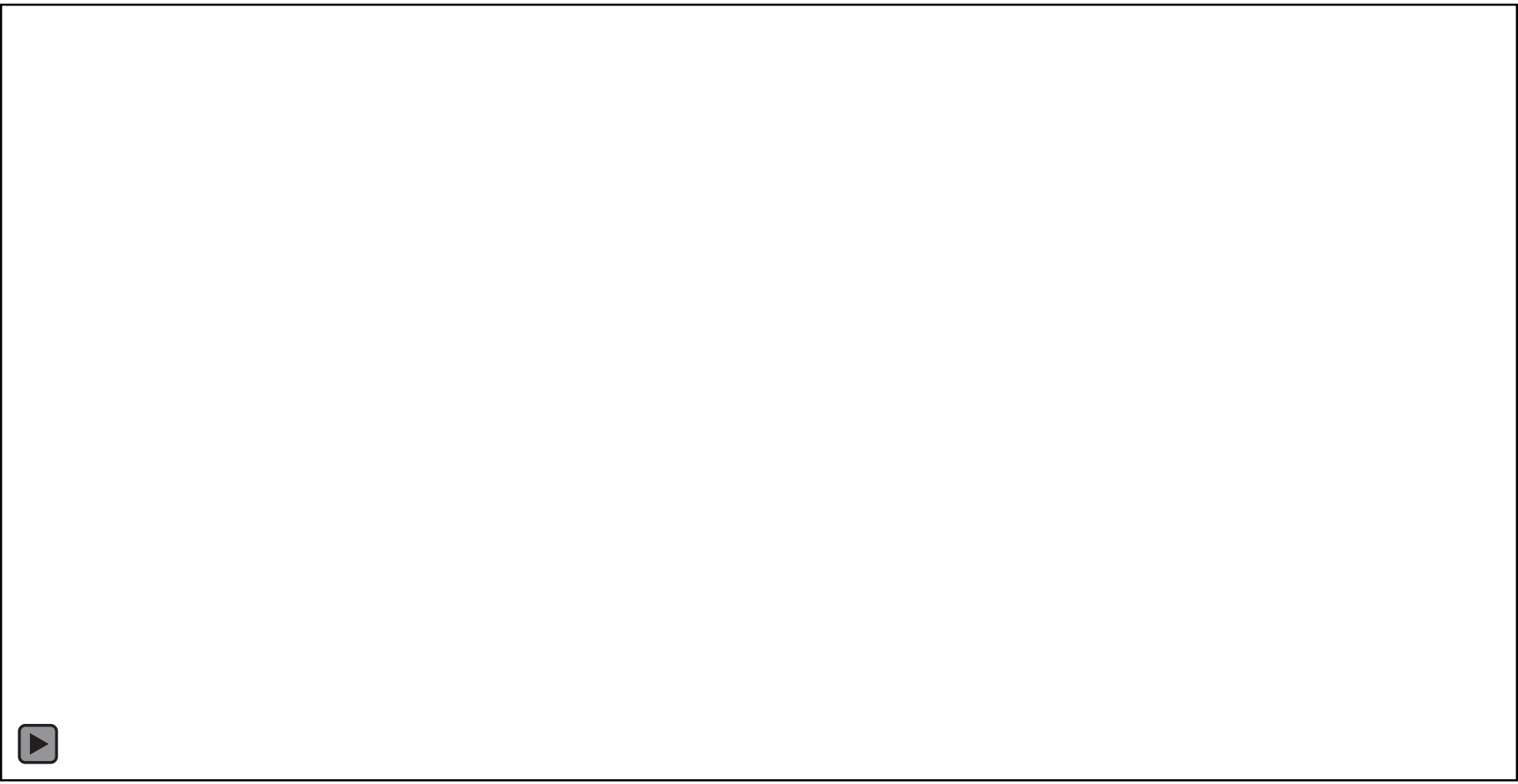

Real-Time Traffic Sign Recognition Process

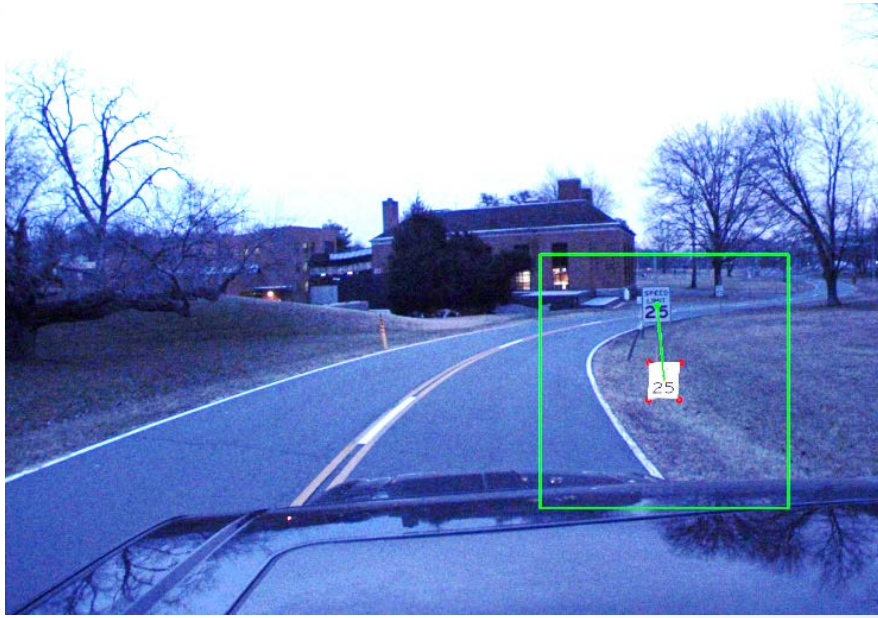

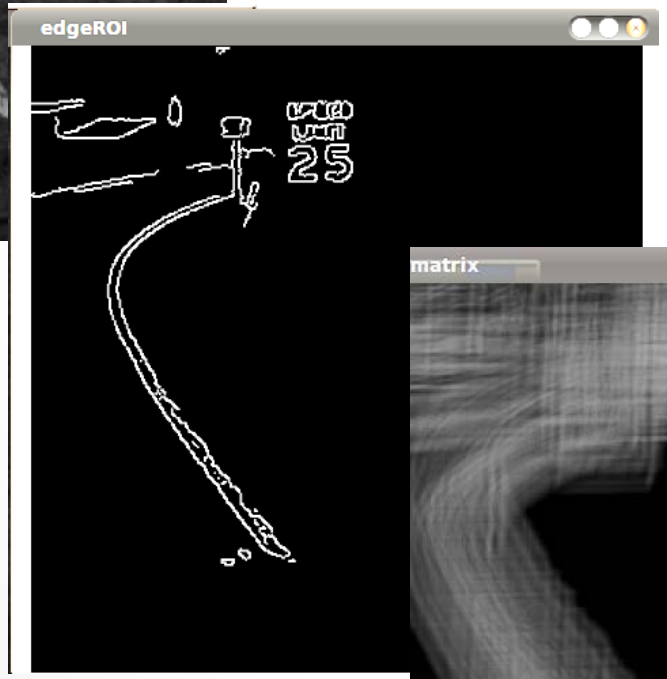

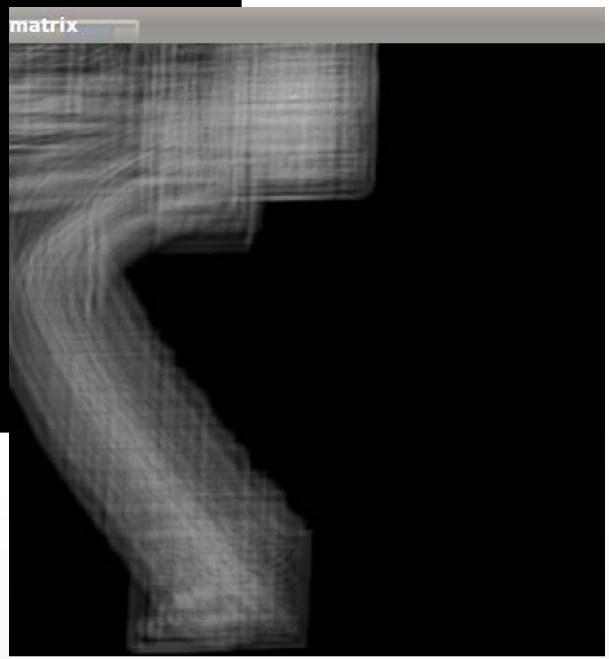

Sign Aiding …

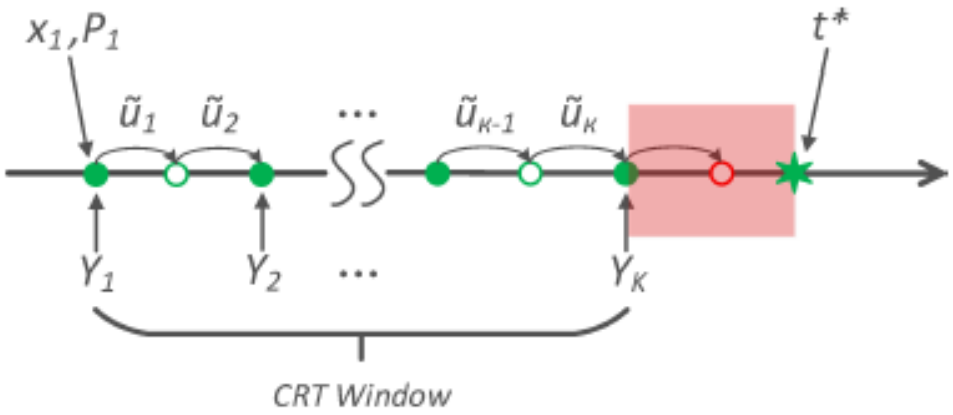

$$
\begin{aligned}
p(\mathbf{X}, \mathbf{N}, \mathbf{Y}, \mathbf{U}) &= p(\mathbf{X}, \mathbf{U}, \mathbf{N}) p(\mathbf{Y}|\mathbf{X}, \mathbf{U}, \mathbf{N}) \\
&= p(\mathbf{X}_+, \boldsymbol{x}(t_1), \mathbf{U}) p(\mathbf{Y}|\mathbf{X}, \mathbf{N}) \\
&= p(\boldsymbol{x}(t_1), \mathbf{U}) p(\mathbf{X}_+|\boldsymbol{x}(t_1), \mathbf{U}) p(\mathbf{Y}|\mathbf{X}, \mathbf{N}) \\
&= p(\boldsymbol{x}(t_1)) p(\mathbf{X}_+|\boldsymbol{x}(t_1), \mathbf{U}) p(\mathbf{Y}|\mathbf{X}, \mathbf{N}) \\
&= p(\boldsymbol{s}(t_1)) p(\mathbf{X}_+|\boldsymbol{x}(t_1), \mathbf{U}) p(\mathbf{Y}|\mathbf{X}, \mathbf{N}).
\end{aligned}
$$

$$
(\mathbf{X}^*, \mathbf{N}^*) = \underset{\mathbf{X} \in \mathbb{R}^{n_s K}, \mathbf{N} \in \mathbb{Z}^m}{\arg\min} \|r(\mathbf{X}, \mathbf{N})\|^2,
$$

where r is the vector:

$$
r(\mathbf{X}, \mathbf{N}) = \begin{bmatrix}
\Sigma_{\mathbf{P}_{s_1}} (s(t_1) - s_1) \\
\hdashline
\Sigma_{\mathbf{Q}_1} (\phi(x(t_1), \mathbf{U}_1) - x(t_2)) \\
\vdots \\
\Sigma_{\mathbf{Q}_{K-1}} (\phi(x(t_{K-1}), \mathbf{U}_{K-1}) - x(t_K)) \\
\hdashline
\sigma_\rho^{-1} \left(h_1^1(x(t_1)) - \rho^1(t_1)\right) \\
\vdots \\
\sigma_\rho^{-1} \left(h_K^m(x(t_K)) - \rho^m(t_K)\right) \\
\sigma_\varphi^{-1} \left(h_1^1(x(t_1)) + \lambda N^1 - \varphi^1(t_K)\right) \\
\vdots \\
\sigma_\varphi^{-1} \left(h_K^m(x(t_K)) + \lambda N^m - \varphi^m(t_K)\right)
\end{bmatrix}
$$

Multi-epoch sensor fusion:

Increasing the window size K

- Pro: Increased measurement redundancy
- Pro: Increased ability to detect and remove anomalies
- Con: Increases computational load

Commercial applications are cost, accuracy, and reliability sensitive. Decreased computational load enhances commercial feasibility.

$$
\boldsymbol{s}(t) = [\boldsymbol{v}^\intercal(t), \boldsymbol{q}^\intercal(t), \boldsymbol{b}_a^\intercal(t), \boldsymbol{b}_g^\intercal(t)]^\intercal \in \mathbb{R}^{(n_s - 3)}
$$

Contemplative Real-time Estimation (CRT)

$$\hat{\mathbf{X}} = \arg\max_{\mathbf{X}} \left(p_{\delta \mathbf{x}_0}(\mathbf{x}(t_0) - \mathbf{x}_0)\, p_{\omega_u}(\mathbf{X}_+ - \phi(\mathbf{X}, \mathbf{U}))\, p_{\mathbf{n}_\rho}(\mathbf{Y} - \mathbf{h}(\mathbf{X})) \right)$$

- Real-time computation
- Removal of faulty data within the CRT window
- Correction of linearization point errors
- Yaw & bias initialization

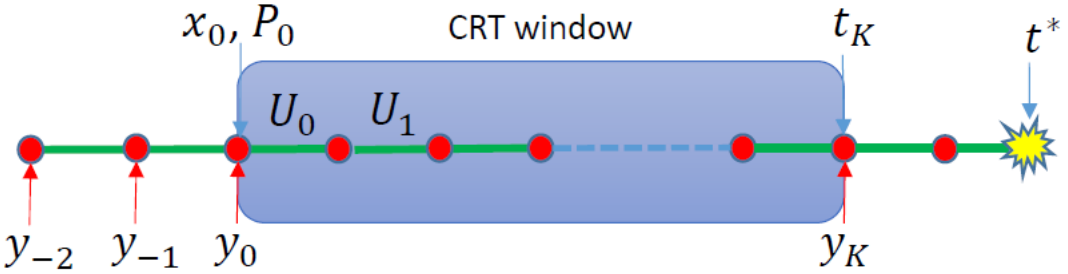

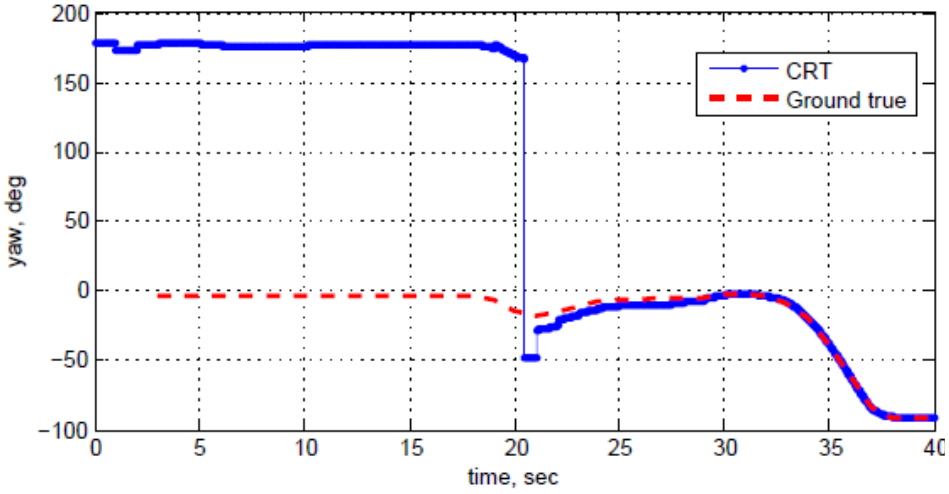

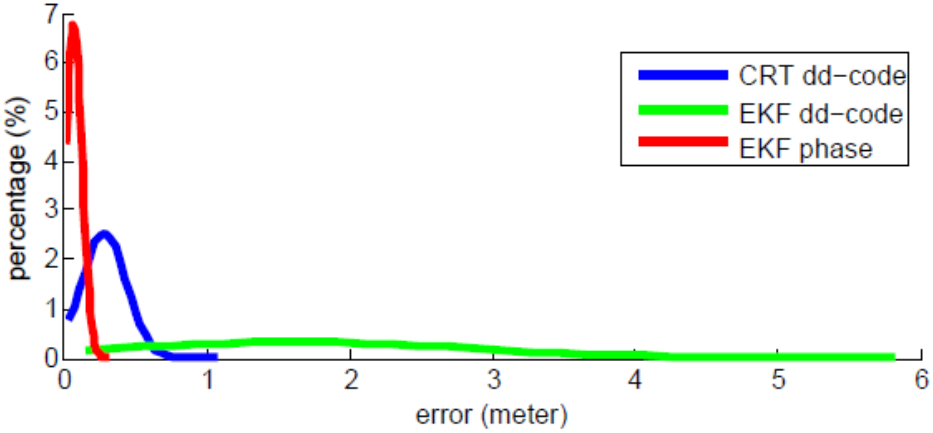

CRT Performance

Different algorithms. Exactly the same data (INS and L1 pseudorange).

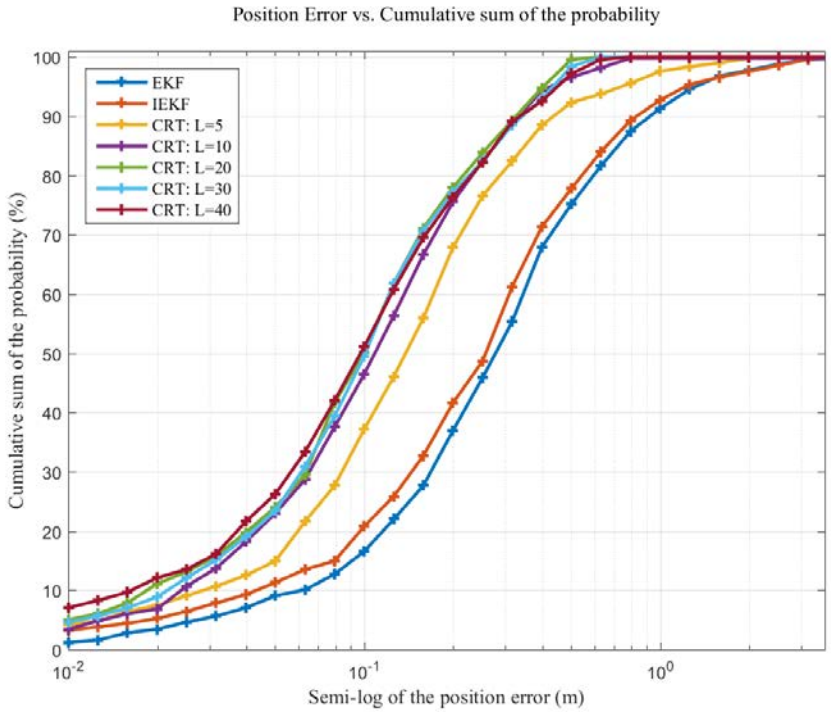

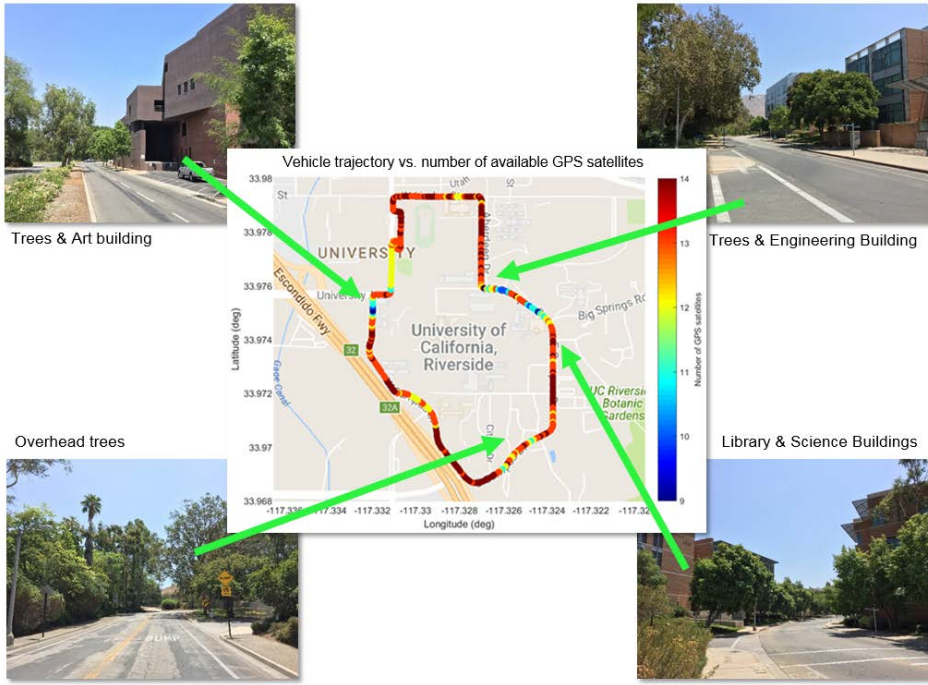

- 3d position error CDF
- Outliers removed via residual analysis
- CDF of other states show similar trends

- IMU: Epson M-G320, 250 Hz
- GPS: Ublox 6T (differential)
- CPU: Qualcomm Snapdragon 410c
- OS: Linux Debian 8
- Biases and yaw initialized at zero
- Duration: 495 seconds

CRT Performance

Different algorithms. Exactly the same data (INS and L1 pseudorange).

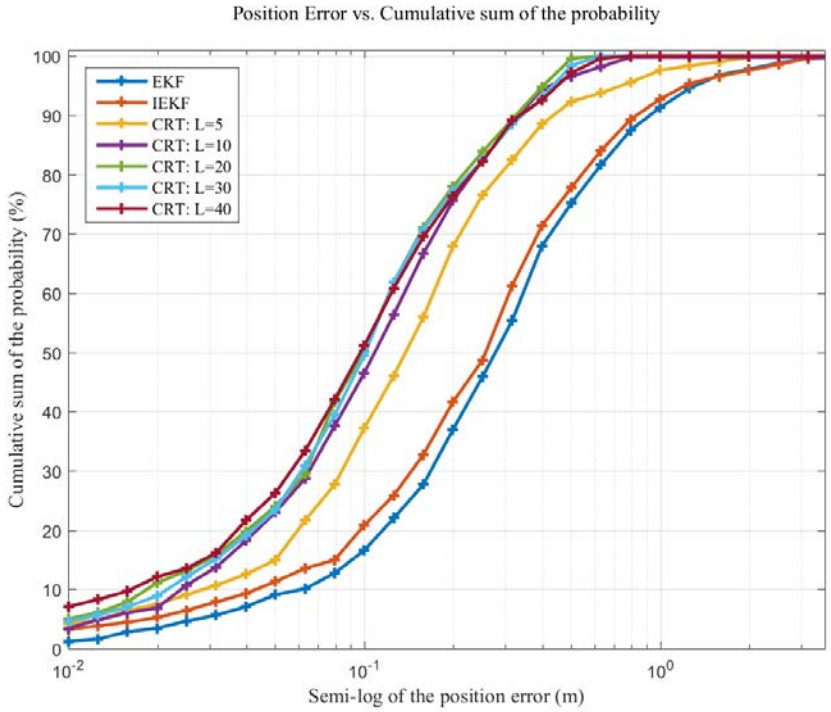

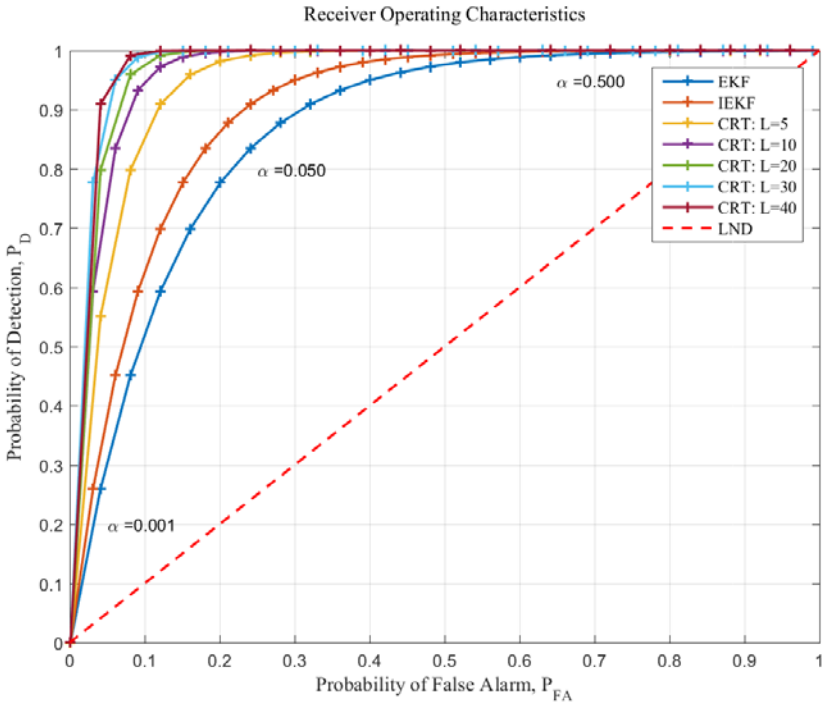

- 3d position error CDF
- Outliers removed via residual analysis
- CDF of other states show similar trends

- Receiver Operating Characteristics
- False alarms and Probability of detection evaluated relative to “ground truth”

Existing Bayesian Carrier Phase/IMU Approach

1) Obtain the *float solution* by neglecting the integral nature of the ambiguity $\mathbf{N}$

$$(\check{\mathbf{X}}, \check{\mathbf{N}}) = \underset{(\mathbf{X},\mathbf{N})\in\mathbb{R}^{n_s K+m}}{arg\,min} \|\boldsymbol{r}(\mathbf{X},\mathbf{N})\|^2.$$

with standard outlier rejection.

2) Starting from $(\check{\mathbf{X}}, \check{\mathbf{N}})$, solve the NMILS problem in eqn. (11) to obtain the optimal solution $(\mathbf{X}^*, \mathbf{N}^*)$:

$$(\mathbf{X}^*, \mathbf{N}^*) = \underset{\mathbf{X}\in\mathbb{R}^{n_s K},\mathbf{N}\in\mathbb{Z}^m}{arg\,min} \|\boldsymbol{r}(\mathbf{X},\mathbf{N})\|^2,$$

3) Check the validity of integer estimates with integer validation techniques.

X.W. Chang and T. Zhou. MILES: MATLAB Package for Solving Mixed Integer LEast Squares Problems. GPS Solution, 11(4):289-294, 2007.

Revised Step 2: Common Position Shift (CPS)

Common Position Shift Definition:

$$\mathbf{X}' = \mathbf{X} \oplus \Delta\boldsymbol{p} \triangleq [\boldsymbol{x}^\mathsf{T}(t_1) \oplus \Delta\boldsymbol{p}, \ldots, \boldsymbol{x}^\mathsf{T}(t_K) \oplus \Delta\boldsymbol{p}]^\mathsf{T}$$

Main Result: $\|\boldsymbol{r}(\mathbf{X}, \mathbf{N})\|^2 \doteq \|\boldsymbol{r}_a(\mathbf{X})\|^2 + \|\boldsymbol{r}_b(\Delta\boldsymbol{p}, \mathbf{N}|\mathbf{X})\|^2$

where

- Insensitive to CPS: $\|\boldsymbol{r}_a(\mathbf{X})\|^2 = \|\boldsymbol{r}_a(\mathbf{X} \oplus \Delta\boldsymbol{p})\|^2$
- Equality holds in the time-invariant, linear case.
- Error is bonded in time-varying, nonlinear case:

$$\boldsymbol{E}\{\|\boldsymbol{r}(\check{\mathbf{X}} \oplus \Delta\boldsymbol{p}^\star, \mathbf{N}^\star)\|^2\} \leq (1 + C_3)\boldsymbol{E}\{\|\boldsymbol{r}(\mathbf{X}^*, \mathbf{N}^*)\|^2\}$$

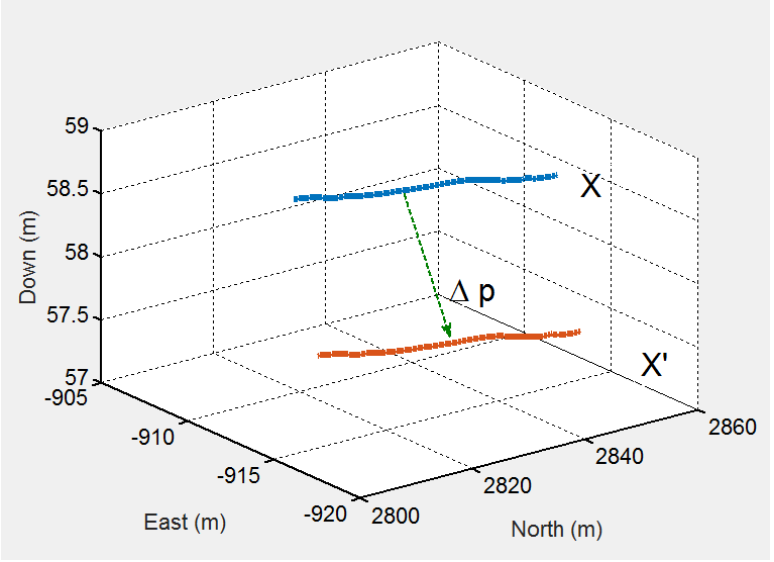

Float Solution:

$$(\check{\mathbf{X}}, \check{\mathbf{N}}) = \underset{(\mathbf{X},\mathbf{N}) \in \mathbb{R}^{n_s K + m}}{arg\,min} \|\boldsymbol{r}(\mathbf{X}, \mathbf{N})\|^2.$$

Integer-free Solution

$$\mathbf{X}^{\circledast} = \underset{\mathbf{X} \in \mathbb{R}^{n_s K}}{arg\,min} \|\boldsymbol{r}_a(\mathbf{X})\|^2.$$

Proposition 1. If the variable $\mathbf{N}$ is treated as a real vector, then for $\check{\mathbf{X}}$ and $\check{\mathbf{N}}$ as defined in eqn. (12)

$$\|\boldsymbol{r}(\check{\mathbf{X}}, \check{\mathbf{N}})\|^2 = \|\boldsymbol{r}_a(\mathbf{X}^{\circledast})\|^2$$

and $\mathbf{X}^{\circledast} = \check{\mathbf{X}}$.

New Algorithm.

1) Find either the float solution $\check{\mathbf{X}}$ or the integer-free solution $\mathbf{X}^{\circledast}$.
2) Find $(\Delta\boldsymbol{p}^\star, \mathbf{N}^\star)$ that is the optimal NMILS solution of

$$\min_{\Delta\boldsymbol{p} \in \mathbb{R}^3, \mathbf{N} \in \mathbb{Z}^m} \|\boldsymbol{r}_b(\Delta\boldsymbol{p}, \mathbf{N}|\check{\mathbf{X}})\|^2,$$

where $\check{\mathbf{X}}$ is fixed when evaluating $\|\boldsymbol{r}_b\|^2$.

3) Check the validity of the integer estimates.

The trajectory-integer CPS estimate is $(\check{\mathbf{X}} \oplus \Delta\boldsymbol{p}^\star, \mathbf{N}^\star)$.

$$C_3 = \frac{Km\left(4\sigma_\rho^{-2} + 3\sigma_\varphi^{-2}\right)[B_1(\Delta_f, \bar{v})]^2}{(2K-1)m - 3}$$

- For $K = 10$, $\Delta_f = 1.5$, $m = 7$, $\sigma_\rho = 1.0$ meters and $\sigma_\varphi = 0.020$: $C_3 = 0.04$
- For NMILS with residuals at the cm level; perturbations are expected to be less than $0.4mm$.

Computation Reduction

Table 1: Computation Comparison

Step	Process	Original Method	New Method
1)	Float solution	$\mathcal{O}((n_s K)^3) \times \mathfrak{I}_1$	$\mathcal{O}((n_s K)^3) \times \mathfrak{I}_1$
2a)	Integrate INS	$f K n_s \times \mathfrak{I}_2$	0
2b)	QR of A	$2M(n_s K)^2 \times \mathfrak{I}_2$	$2(2m)(3)^2 \times \mathfrak{I}_2$
2c)	QRZ of $\bar{\mathbf{Q}}_A^\intercal B$	$2(2Km)m^2 \times \mathfrak{I}_2$	$2(2m)m^2 \times \mathfrak{I}_2$
2d)	Integer Search	$(*) \times \mathfrak{I}_2$	$(*) \times \mathfrak{I}_2$
3)	Integer Valid.	Km	Km

TABLE II
EXAMPLE COMPARISON OF COMPUTATIONAL LOAD: $f = 200$, $K = 10$, $n_s = 16$, $N_s = 160$, $M = 297$ AND $m = 7$

Step	Direct MILS	CPS MILS
2a)	$3.20 \times 10^4 \times \mathfrak{I}_2$	0
2b)	$1.52 \times 10^7 \times \mathfrak{I}_2$	$2.52 \times 10^2 \times \mathfrak{I}_2$
2c)	$1.37 \times 10^4 \times \mathfrak{I}_2$	$1.37 \times 10^3 \times \mathfrak{I}_2$

$\mathfrak{I}_1$ - # NLS linearized iterations to find float solution
$\mathfrak{I}_2$ - # ILS linearized iterations
K - Measurement window length
m - Number of measurements per measurement time
n_s - Dimension of the state vector
f - IMU sample rate
M - Row dimension of the residual vector:

$$M \triangleq n_s K + 2mK - 3$$

Position Estimation Comparison

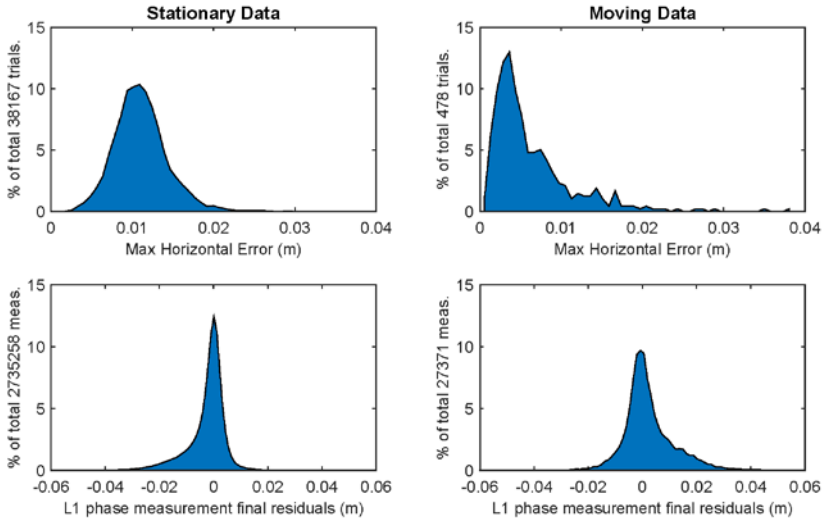

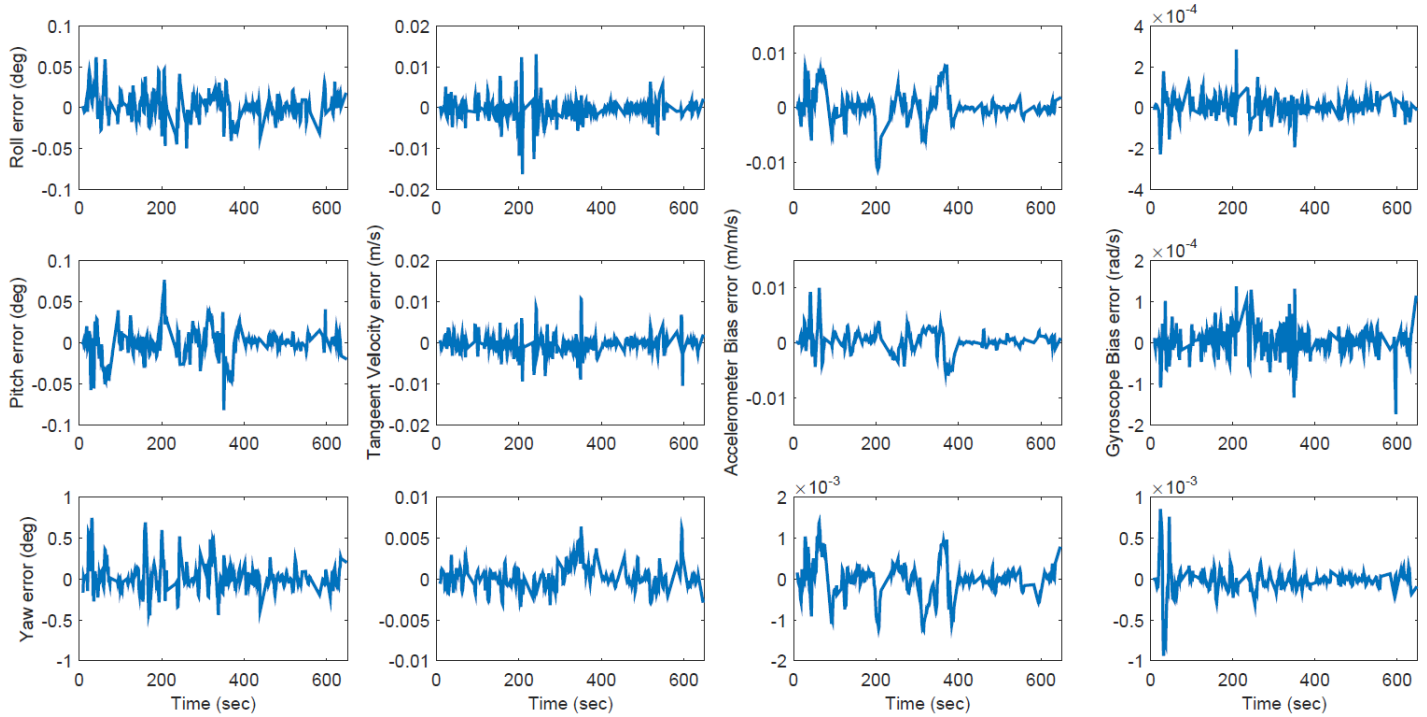

CPS, Error Bound, & Error

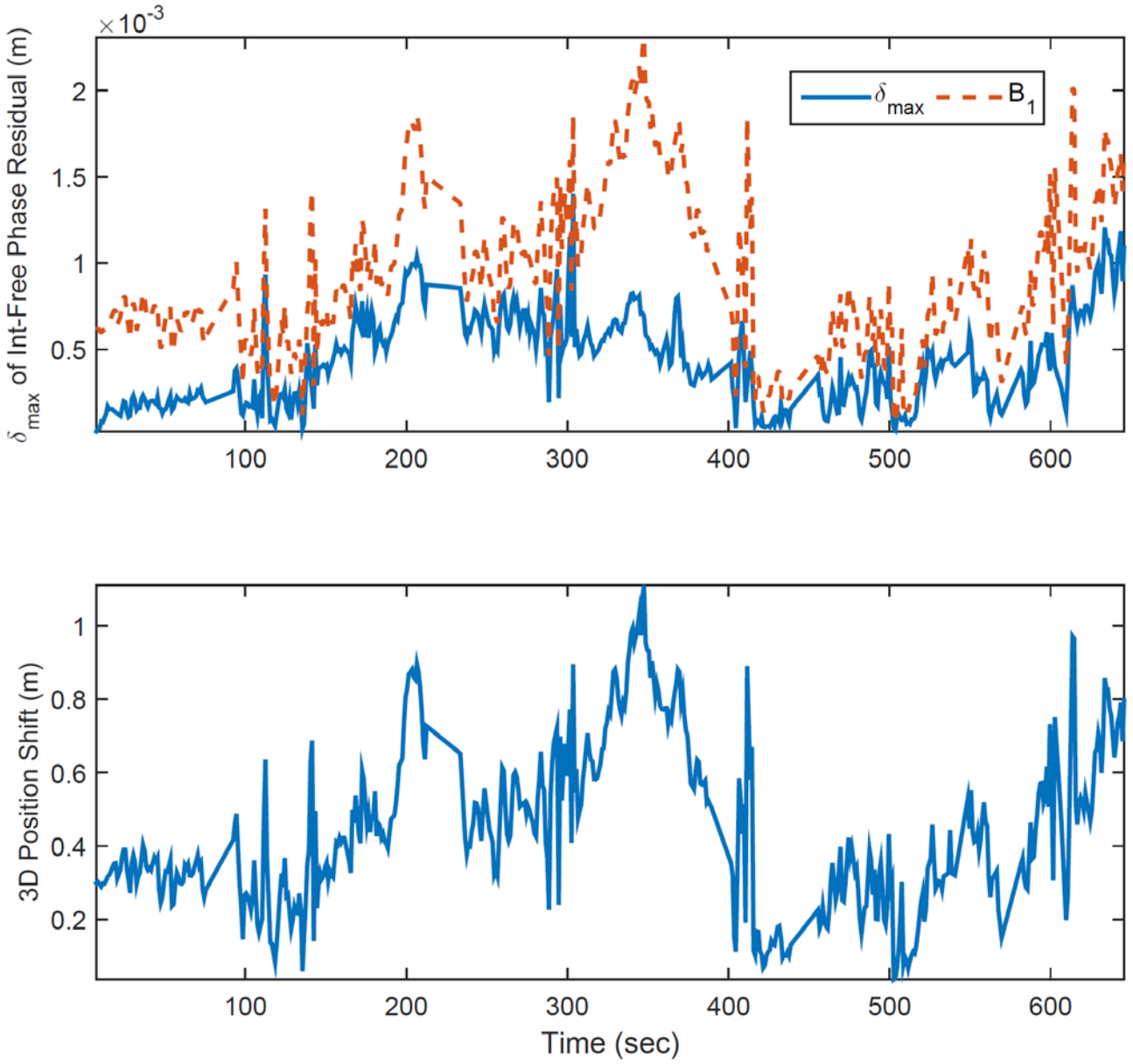

Aiding Sensor Categories

	Technology	Principle	Range Accuracy	Veh. Cost	Rdwy. Cost	Req'd Advances
	GPS	TOA	10 m	Low	Bases, comms	Modernization
	DGPS		1 m	Low	Bases, comms	Modernization
	CPDGPS		0.01 m	High	Bases, comms	Modernization
Terrestrial Radio Navigation	Pseudolites	TOA, TDOA	0.01 m	Med	High	> First generation
	-- Cell Phone	RSSI	km's	Low	Existing	
	-- Cell Phone	TOA, TDOA	100's m	Low	Existing	Physical layer timing
	-- TV - digital	TOA	10's m	??	Bases, comms	??
	-- Radio AM Analog	TOA	10's m	Low	Existing	??
	-- Radio FM Analog	TOA	??	Low	Existing	??
	-- Radio Digital	TOA	??	Low	Existing	??
	-- Packet Radios	TOA, TDOA	km's	Low	High	Physical layer timing
Feature Based	Vision	AOA		Low-Med	Feature Mapping	Feature Robustness
	Radar	AOA, RTOA	0.1 m	Low-Med	Feature Mapping	Feature Robustness
	Lidar	AOA, RTOA	0.01 m	High	Feature Mapping	Feature Robustness

GNSS: Proven with open skies. Challenging in urban environments.

TRN: Shows great promise as physical layer timing advances

FB: Assessed as viable *if precision roadway feature maps are available*. Research leading to reliable and accurate FB positioning demonstrations was a project focus.

Visible Light Communication
LED's as Active Features

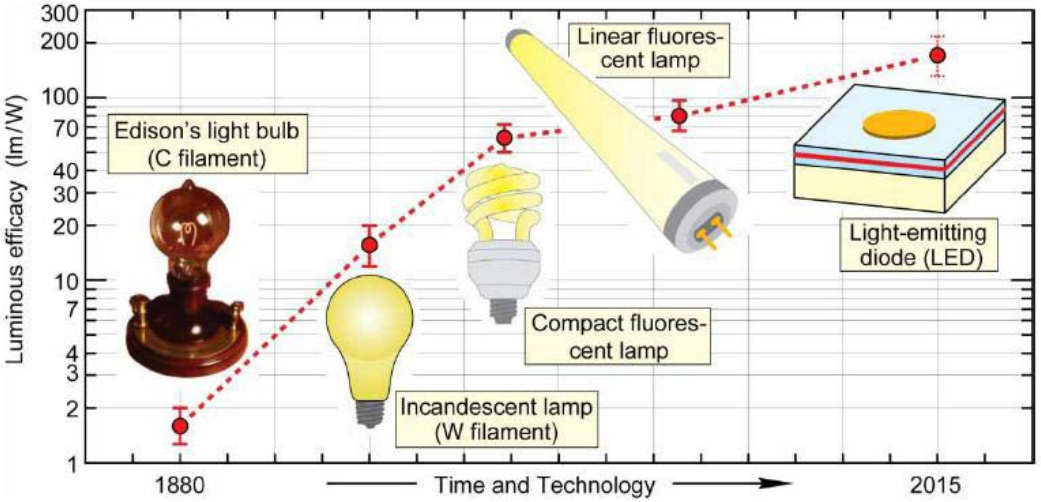

VLC based navigation

- LEDs are known features
  - Active and bright
  - Known shape & location
- Facilitate data association
  - Mahalonobis distance
  - Encoded IDs ensure correctness

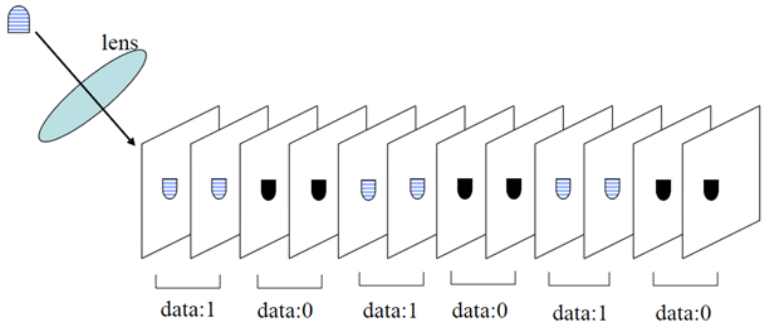

Solution approach: Joint
- LED path recovery
- Data sequence extraction

LED VLC Navigation Applications

- Outdoor Applications
  - Transportation
  - Aircraft taxiways
- Indoor Applications
  - Hospital patients & equipment
  - Retail & tourism assistant

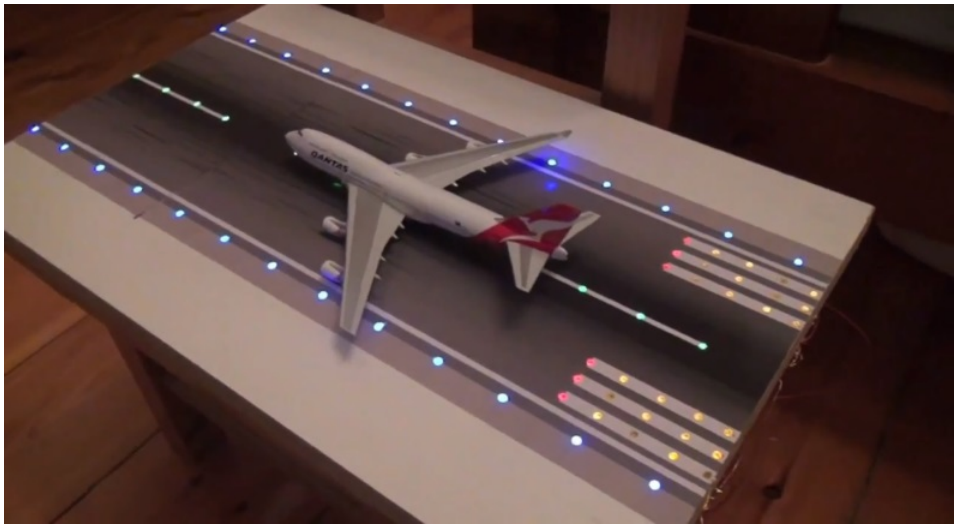

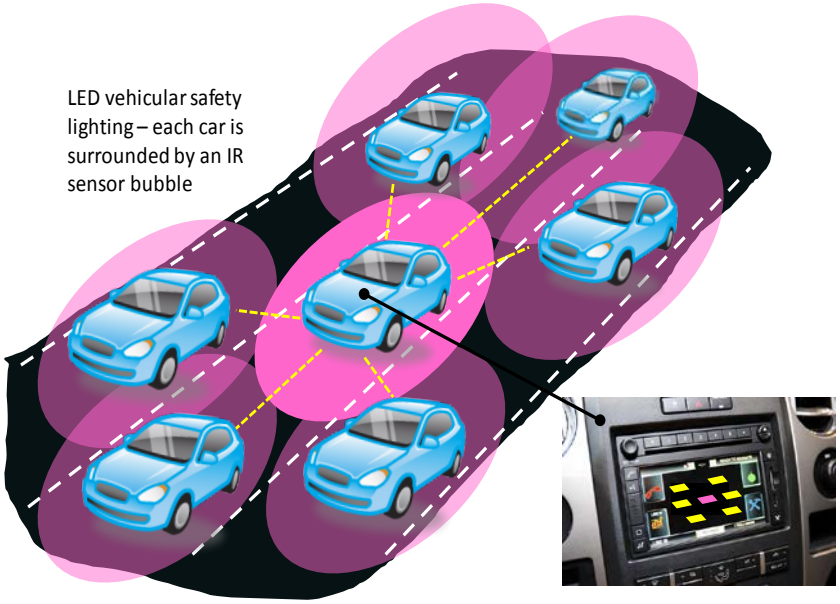

LED VLC Navigation Solution

Challenges:

- Multiple LED projections within FOV
- Noise and clutter
- Moving sensor causes moving LED projection onto array.
  - Is this bit a zero or am I looking at the wrong pixel?

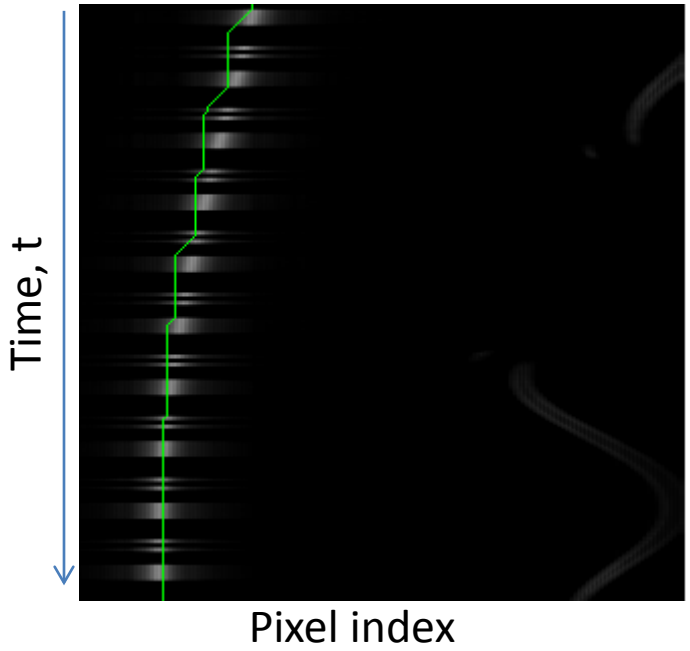

Q-best hypotheses and time window data extraction:

- Motion information can be used to match the measurements between frames
- Allows likelihood evaluation per candidate sequence
- Challenge is algorithm for finding most likely sequences

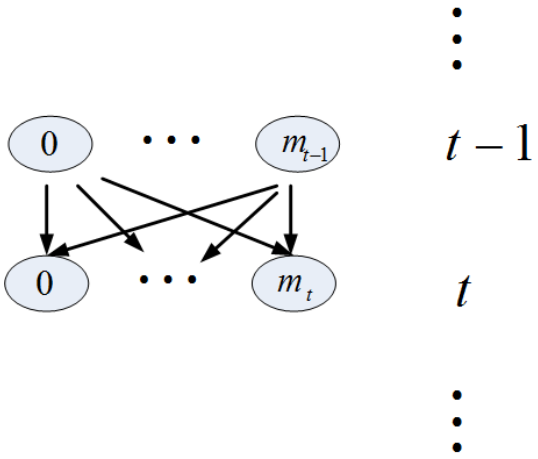

Finding & Storing Lanes and Edges

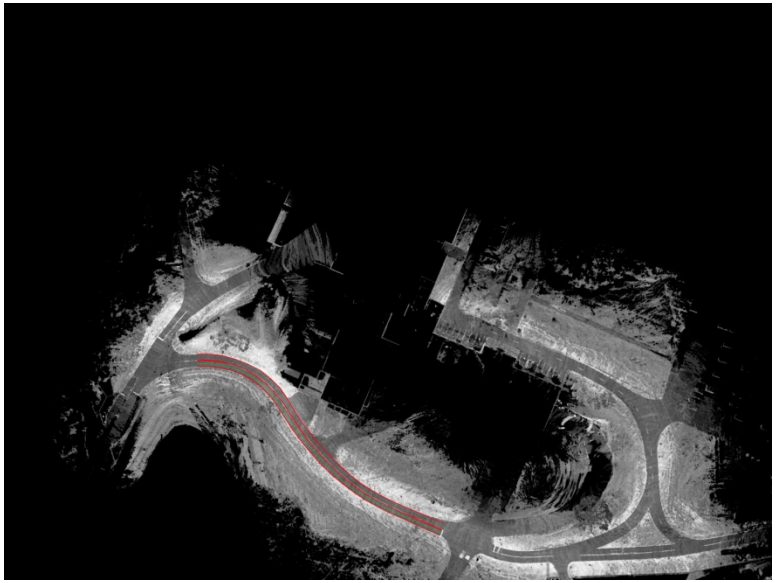

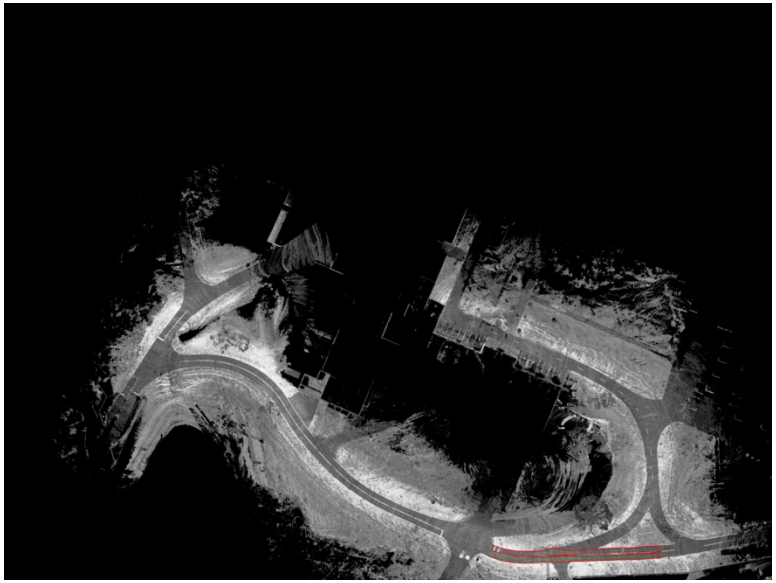

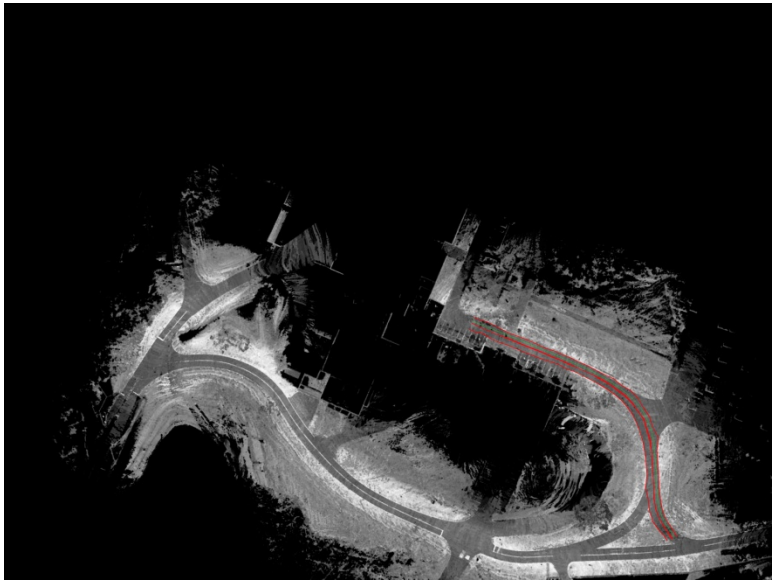

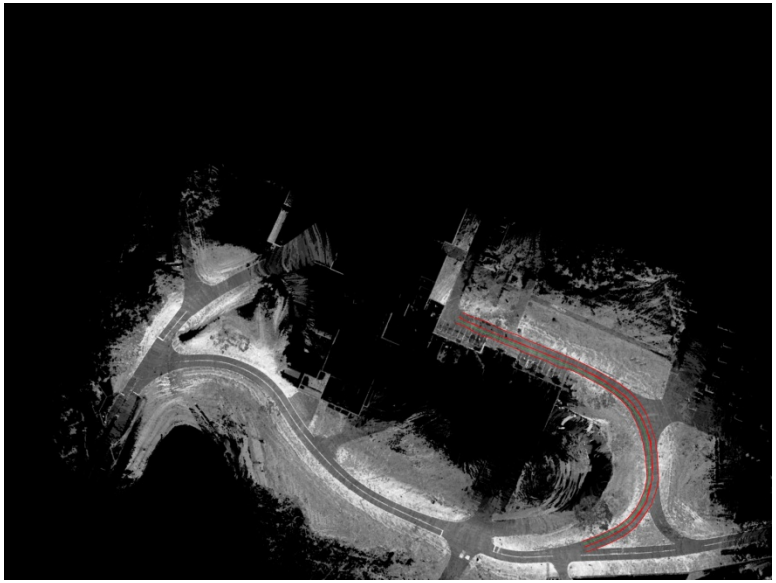

Curve Fitting: Sparse Optimization

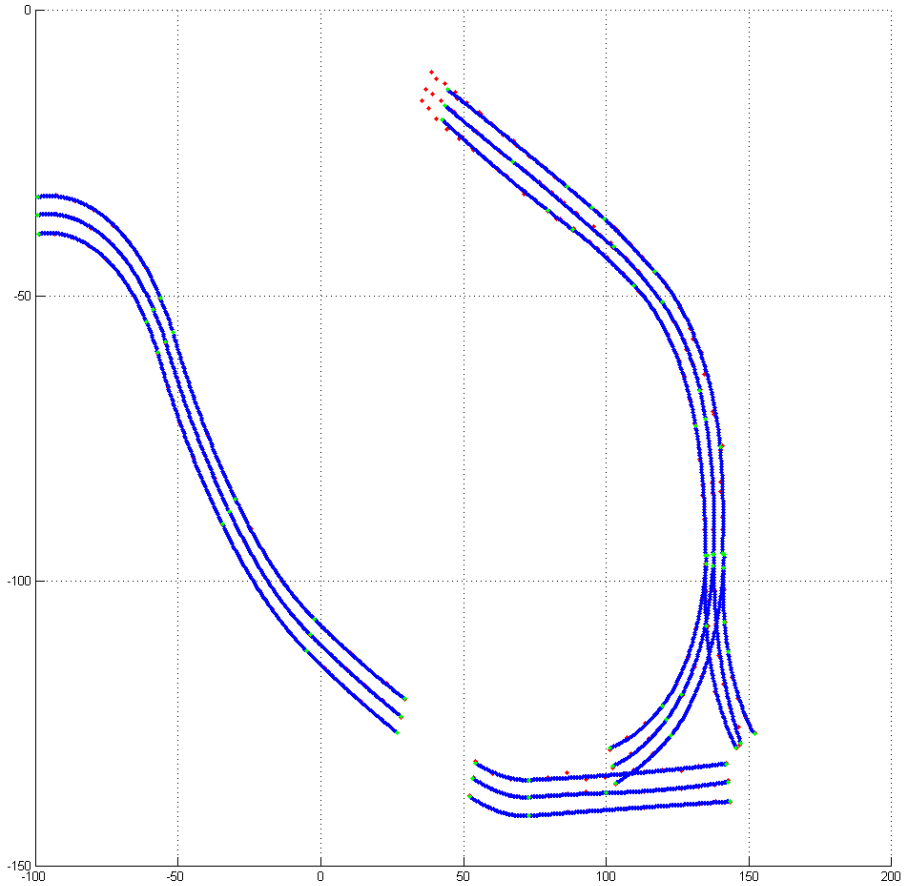

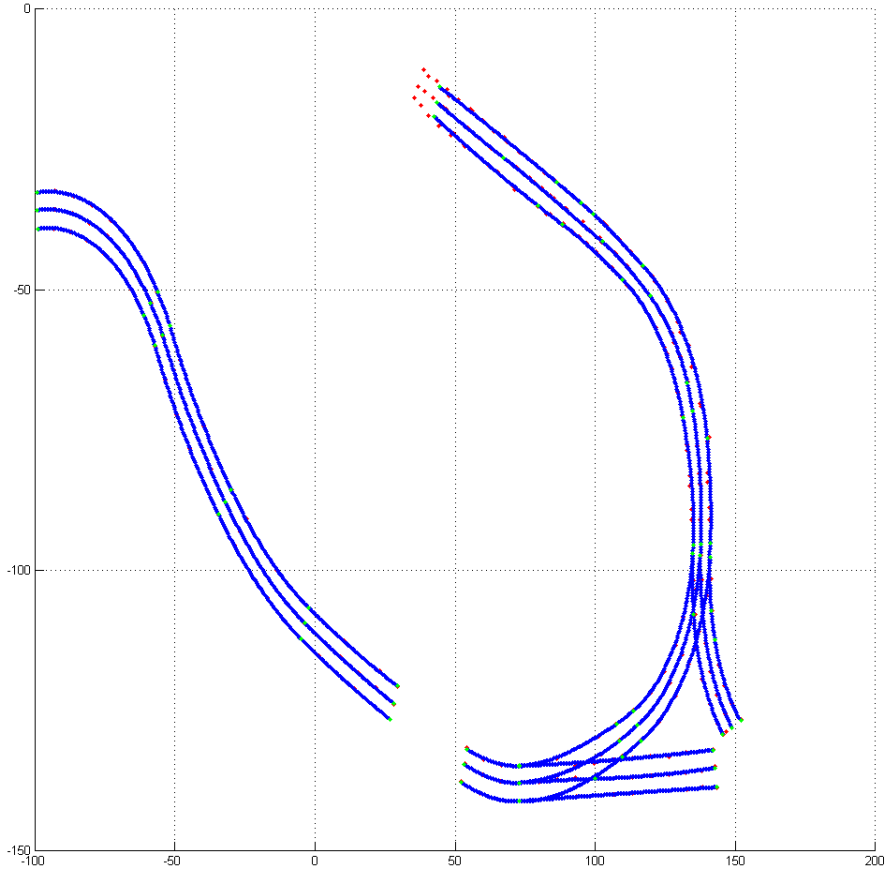

Given a set of position data $\mathcal{D} = \{N_k, E_k\}_{k=0}^{N}$ representative of a lane centerline, fit a piecewise C^2 curve, with piecewise constant curvature to the data.

Road Design and Spline Fitting

Given $\{P_i\}_{i=1}^{N}$, find the parameter vector $\mathbf{\Theta}$, such that the road curve $\gamma(s) = \mathbf{\Phi}^T(s)\mathbf{\Theta}$, where $\mathbf{\Phi}(s)$ is the basis vector.

Solution:

$$\begin{bmatrix} \gamma(s_1) \\ \vdots \\ \gamma(s_N) \end{bmatrix} = \begin{bmatrix} \mathbf{\Phi}^T(s_1) \\ \vdots \\ \mathbf{\Phi}^T(s_N) \end{bmatrix} \mathbf{\Theta}$$

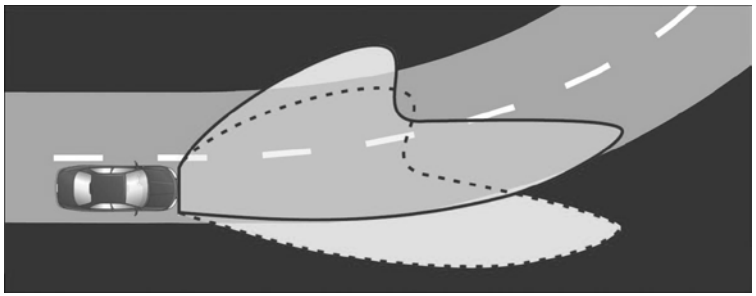

EDMap 2004 concluded that curvature computed from spline fitting was not appropriate for curve warning applications.

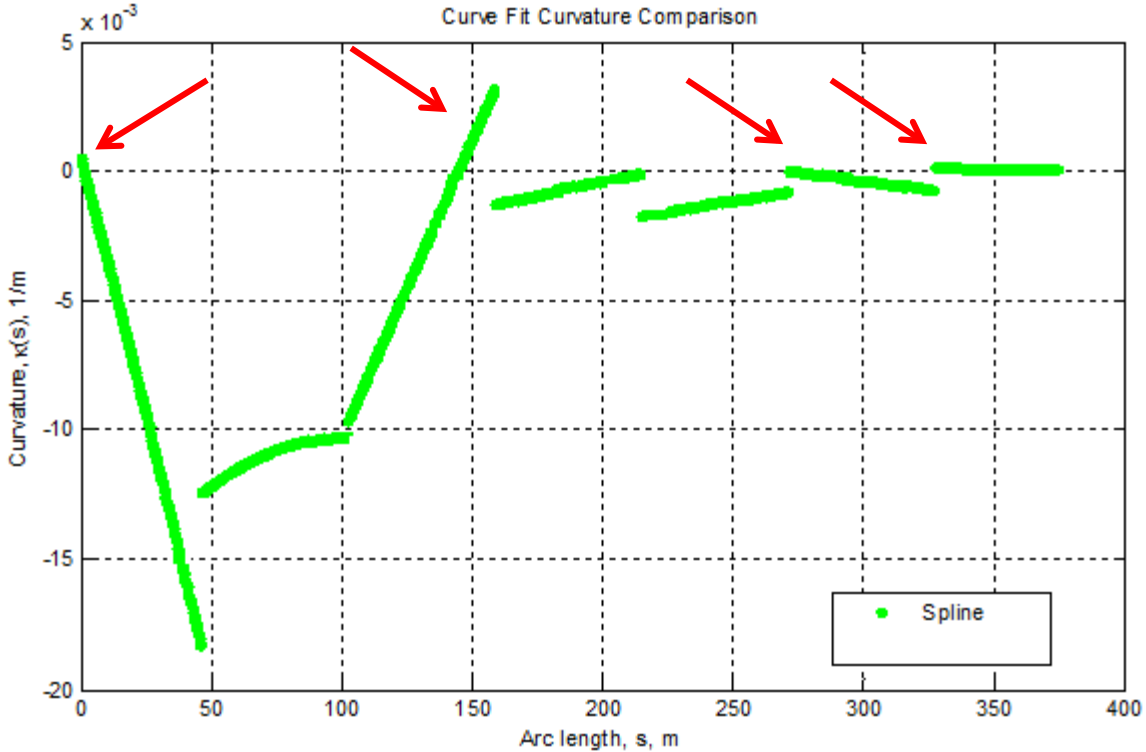

Road Design Constraints

Given a set of position data $\mathcal{D} = \{N_k, E_k\}_{k=0}^{N}$ representative of a lane centerline, fit a piecewise C^2 curve, with piecewise constant curvature to the data.

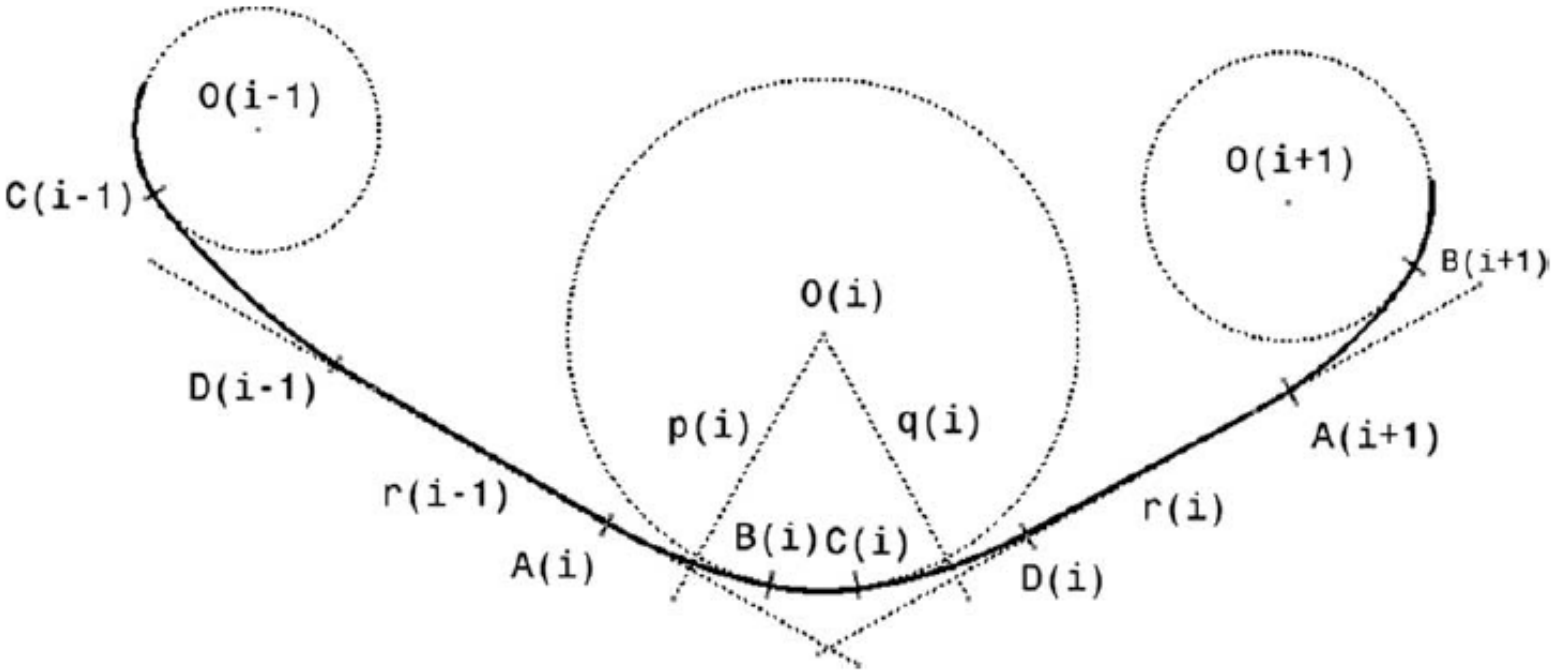

Curve Generation via Sparse Optimization

Given a set of position data $\mathcal{D} = \{N_k, E_k\}_{k=0}^{N}$ representative of a lane centerline, fit a piecewise C^2 curve, with piecewise constant curvature to the data.

$$\min_{x(0),\beta(k),\Delta s(k)} \sum \|y(k) - W(k)\|_2^2 + \lambda \|\mathbf{b}\|_0$$

$$s.t. \quad x(k+1) = f\left(x(k), \Delta s(k), \beta(k)\right)$$

$$-\Delta s(k) \leq 0, \; k = 0, ..., N-1$$

Kinematic function: *f*

$$\begin{aligned} p_x(k+1) &= p_x(k) + \Delta s(k) \cos\psi(k) \\ p_y(k+1) &= p_y(k) + \Delta s(k) \sin\psi(k) \\ \psi(k+1) &= \psi(k) + \kappa(k)\Delta s(k) \\ s(k+1) &= s(k) + \Delta s(k) \\ \kappa(k+1) &= \kappa(k) + \beta(k) \end{aligned}$$

$$y(k) = [p_x(k), p_y(k)]$$

$$\mathbf{b} = [\beta(0), ..., \beta(N-1)]$$

$$x(k) = [p_x, p_y, \psi, s, \kappa]_{(k)}$$

$$W(k) \in \mathcal{D} = \{N_k, E_k\}_{k=0}^{N}$$

S. Zhao, J. A. Farrell, "Optimization-based Road Curve Fitting," IEEE CDC and ECC, 5293-5298, 2011.

Curve Generation via Sparse Optimization

Given a set of position data $\mathcal{D} = \{N_k, E_k\}_{k=0}^{N}$ representative of a lane centerline, fit a piecewise C^2 curve, with piecewise constant curvature to the data.

$$\min_{x(0),\beta(k),\Delta s(k)} \sum \|y(k) - W(k)\|_2^2 + \lambda \|\mathbf{b}\|_0$$

$$s.t. \quad x(k+1) = f\left(x(k), \Delta s(k), \beta(k)\right)$$

$$-\Delta s(k) < 0, \; k = 0, ..., N-1$$

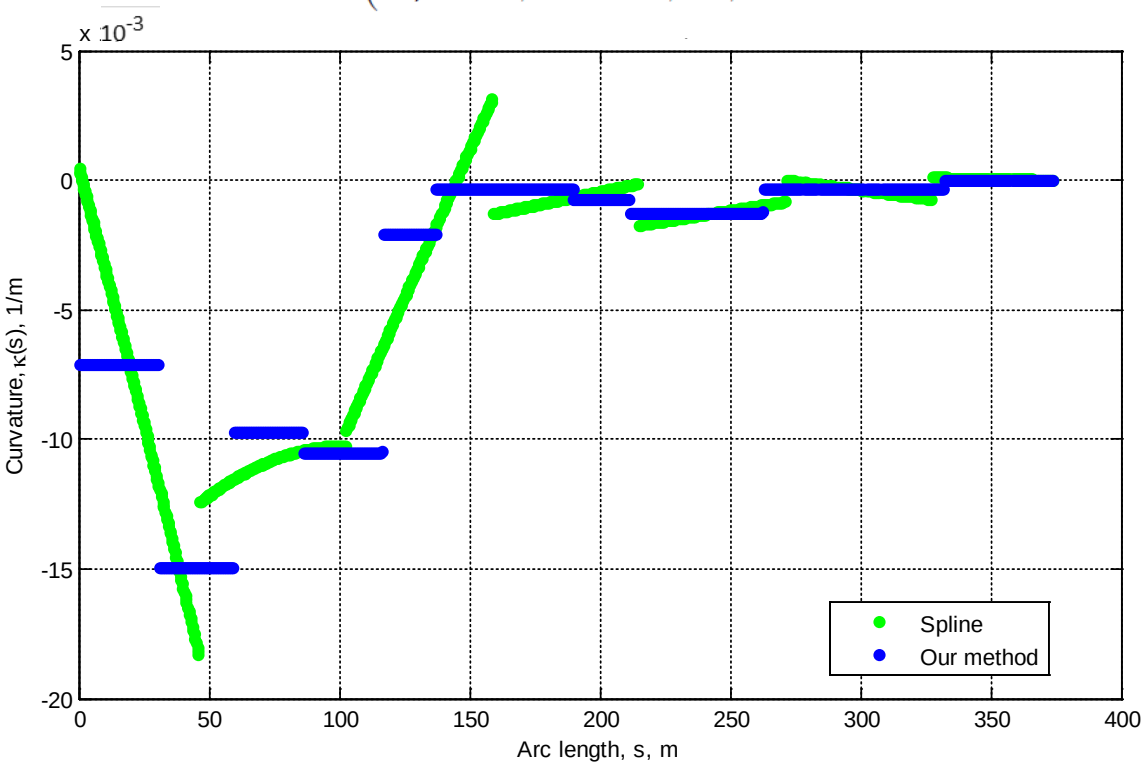

Literature: SLAM

- R. Smith, P. Cheesman, “On the representation of spa
1987
- H.F. Durrant-Whyte, “Uncertain geometry in robotics
- R.C. Smith, P. Cheeseman, "Estimating uncertain spa
Vehicles, I.J. Cox and G.T. Wilfon, Eds., Springer-Verla
- J.J. Leonard, H.F. Durrant-Whyte, "Simultaneous map
robot," IEEE/RSJ IROS, pp. 1442–1447, 1991.
- J.J. Leonard, H.F. Durrant-Whyte, “Mobile robot loca
June 1991.
- H. Durrant-Whyte, D. Rye, and E. Nebot, “Localisatio
Research , Springer Verlag, pp. 613–625, 1996.
- M. Csorba, “Simultaneous Localisation and Map Buil
- S. Thrun, D. Fox, and W. Burgard, “A probabilistic app
mobile robots,” Mach. Learning, 31, (1), pp. 29–53, 1
- M. W. M. Gamini Dissanayake, P. Newman, S. Clark, H
simultaneous localization and map building (SLAM) p
- R. Eustice, H. Singh, J. Leonard, M. Walter, and R. Bal
information filters,” Robotics: Science and Systems. MIT Press, 2005.
- H. F. Durrant-Whyte, T. Bailey, “Simultaneous Localization and Mapping: Part 1,” IEEE R&A Magazine, p.99 – 108, June 2006.
- R. M. Eustice, H. Singh, J. J. Leonard, “Exactly sparse delayed-state filters for view-based SLAM,” IEEE T.-Rob., 22 (6), pp. 1100 – 1114, 2006.
- F. Dellaert, M. Kaess, “Square Root SAM: Simultaneous Localization and Mapping via square root information smoothing,” Int. J. Rob. Res., pp. 1181 - 1203 , Dec. 2006.
- M. Kaess, A. Ranganathan, F. Dellaert, “iSAM: Incremental Smoothing and Mapping,” IEEE T.-Rob., 24 (6), pp. 1365 – 1378, 2008.
- K. Konolige; M. Agrawal, “FrameSLAM: From bundle adjustment to real-time visual mapping,” IEEE T.- Rob., 24 (5), pp. 1066 – 1077, 2008.

- Statistical relationships between geometric uncertainties

- Joint state and map estimation, huge state, huge (i.e., $O(L^2)$) computational load.
- No convergence proofs
- Approximate implementations

- Convergence results
- Importance of cross-correlations
- Understanding of the probabilistic problem structure

Literature: Receding/Moving Horizon Estimation

- A.H. Jazwinski, "Limited memory optimal filtering," IEEE TAC, 13 (5), pp. 558-563, 1968.
- K. R. Muske, J. B. Rawlings, J. H. Lee, "Receding horizon recursive state estimation," ACC, pp. 900-904, 1993.
- D. Q. Mayne, H. Michalska, "Adaptive receding horizon control for constrained nonlinear systems," IEEE CDC, pp. 1286-1291, December 1993.
- G. Zimmer, "State observation by on-line minimization," Int. J. Control, 60 (4), pp. 595-606, 1994.
- P. E. Moraal, J. W. Grizzle, "Observer design for nonlinear systems with discrete–time measurements," IEEE TAC, vol. 40, no. 3, pp. 395–404, 1995.
- D.G. Robertson, J. H. Lee, and J. B. Rawlings, "A moving horizon-based approach for least-squares estimation," AIChE Journal, 42 (8), pp. 2209-2224, August 1996.
- M. Alamir, "Optimization based non-linear observers revisited," Int. J. Control, 72 (13), pp. 1204-1217, 1999.
- D. Q. Mayne, J. B. Rawlings, C. V. Rao, and P. O. Scokaert, "Constrained model predictive control: Stability and optimality," Automatica, 36(6), pp. 789-814, 2000.
- C. V. Rao, J. B. Rawlings, "Constrained process monitoring: moving-horizon approach," AIChE Journal, 48 (1), pp. 97- 109, January 2002.
- C. V. Rao, J. B. Rawlings, D. Q. Mayne, "Constrained state estimation for nonlinear discrete-time systems: stability and moving horizon approximations," IEEE TAC, 48 (2), pp. 246-258, February 2003.
- E. L. Haseltine, J. B. Rawlings, "A critical evaluation of extended Kalman filtering and moving horizon estimation," Technical Report 202-03, March 12, 2003.
- A. Alessandri, M. Baglietto, G. Battistelli, V. Zavala, "Advances in moving horizon estimation for nonlinear systems," IEEE CDC, pp. 5681 - 5688, December 2010.
- D. A. Copp, J. P. Hespanha, "Nonlinear output-feedback model predictive control with moving horizon estimation," IEEE CDC, pp. 3511-3517, December 2014.

Comments & Conclusions

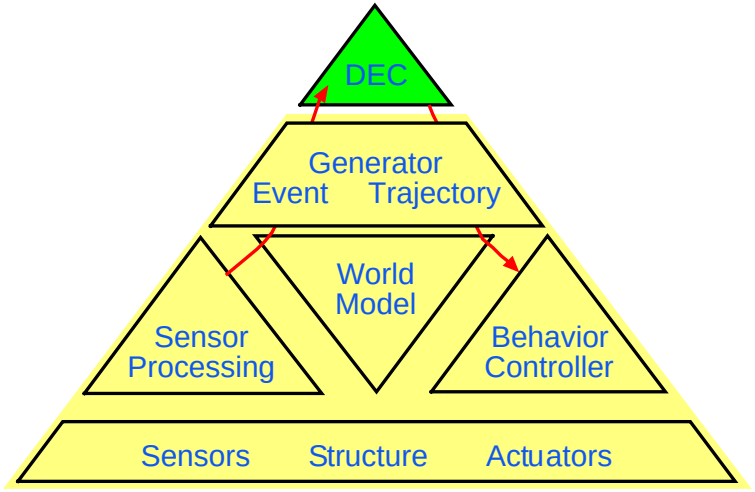

- **Vehicle autonomy is built upon:**
  - **Planning and Decision Making**
  - **World Models**
  - **Sensor Processing**
  - **State Estimation and Control**
- **Feasibility demonstrations abound**
- **Reliability enhancements are required to contain risk and build confidence**
  - **Multiple sensors provide a wealth of independent information**
  - **Information extraction, fusion, validity checking are critical**
  - **Systems, control, and instrumentation engineers and scientists have the knowledge and skills to achieve these advancements**

Acknowledgements

- Many of the photos used herein were taken by others or downloaded from the internet.
- This research project has been ongoing since 1994 with many collaborators contributing ideas: M. Barth, M. Billah, A. Chen, Y. Chen, J. Cheng, T. Givargis, M. Li, Y. Lu, A. Mourikis, H. Qiu, A. Ramanandan, F. Rahman, P. Roysdon, A. Vu, Q. Yang, Y. Yang, H. Zhang, S. Zhao, D. Zheng.
- Research sponsors: USA-DOT-FHWA, CA DOT, ARO, AFOSR, ONR, NSF.

Levels of Autonomous Vehicles (NHTSA 2013)

- **Level 1 –** Function-specific Automation: Automation of specific control functions, such as cruise control, lane guidance and automated parallel parking. Drivers are fully engaged and responsible for overall vehicle control (hands on the steering wheel and foot on the pedal at all times).
- **Level 2** - Combined Function Automation: Automation of multiple and integrated control functions, such as adaptive cruise control with lane centering. Drivers are responsible for monitoring the roadway and are expected to be available for control at all times, but under certain conditions can disengaged from vehicle operation (hands off the steering wheel and foot off pedal simultaneously).
- **Level 3** - Limited Self-Driving Automation: Drivers can cede all safety-critical functions under certain conditions and rely on the vehicle to monitor for changes in those conditions that will require transition back to driver control. Drivers are not expected to constantly monitor the roadway.
- **Level 4** - Full Self-Driving Automation: Vehicles can perform all driving functions and monitor roadway conditions for an entire trip, and so may operate with occupants who cannot drive and without human occupants.

Additional References

- X. W. Chang and T. Zhou. MILES: MATLAB Package for Solving Mixed Integer LEast Squares Problems. GPS Solution, 11(4):289-294, 2007.
- F. Dellaert. Factor Graphs and GTSAM: A Hands-on Introduction. Technical Report, Georgia Institute of Technology, 2012.
- J. A. Farrell. Aided Navigation: GPS with High Rate Sensors. McGraw Hill, 2008.
- P. Jonge and C. Tiberius. The LAMBDA Method for Integer Ambiguity Estimation: Implementation Aspects, TUDelft, 1996.
- M. Kaess, A. Ranganathan, and F. Dellaert. iSAM: Incremental Smoothing and Mapping, IEEE Trans. on Robotics, 24(6), 1365-1378, 2008.
- R. Kuemmerle, G. Grisetti, H. Strasdat, K. Konolige, and W. Burgard. g2o: a General Framework for Graph Optimization, Proc. ICRA, 3607 – 3613, 2011.
- M. Li and A. I. Mourikis. Optimization-based Estimator Design for Vision-aided Inertial Navigation, Proc. Robotics: Science and Systems, 2012.
- M. Li and A. I. Mourikis. High-Precision, Consistent {EKF}-based Visual-Inertial Odometry, Int. J. Robotics Research, 32(6), 690-711, 2013.
- S. Zhao, Y. Chen, and J. A. Farrell. High Precision 6DOF Vehicle Navigation in Urban Environments using a Low-cost Single-frequency GPS Receiver. Proc. IROS/PPNIV, 2014.
- S. Zhao, Y. Chen, H. Zhang, and J. A. Farrell. Differential GPS Aided Inertial Navigation: a Contemplative Real-time Approach. In the Proc. 19th IFAC World Congress, 2014.
- A. Vu, J. A. Farrell, M. Barth, “Centimeter-Accuracy Smoothed Vehicle Trajectory Estimation,” IEEE Intelligent Transportation Systems Magazine, In Press.
- A. Vu, J. A. Farrell, M. Barth, “Improved Vehicle Trajectory and State Estimation using Raw GPS and IMU Data Smoothing”, *IEEE Intelligent Vehicle Symposium*, Madrid Spain, June 2012.